NUREG/CR-3710
ANL-84-16

NUREG/CR-3710
ANL-84-16

LABORATORY STUDIES OF A BREACHED NUCLEAR WASTE REPOSITORY IN BASALT

by

M. G. Seitz, D. L. Bowers,
T. J. Gerding, and G. F. Vandegrift

ARGONNE NATIONAL LABORATORY, ARGONNE, ILLINOIS
Operated by THE UNIVERSITY OF CHICAGO

Prepared for the Office of Nuclear Regulatory Research
U. S. NUCLEAR REGULATORY COMMISSION
under Interagency Agreement DOE 40-550-75

Argonne National Laboratory, with facilities in the states of Illinois and Idaho, is owned by the United States government, and operated by The University of Chicago under the provisions of a contract with the Department of Energy.

NUREG/CR-3710
ANL-84-16
(Distribution
Code: AN)

ARGONNE NATIONAL LABORATORY
9700 South Cass Avenue
Argonne, Illinois 60439

LABORATORY STUDIES OF BREACHED NUCLEAR WASTE REPOSITORY IN BASALT

by

M. G. Seitz, D. L. Bowers,
T. J. Gerding, and G. F. Vandegrift

Chemical Technology Division

September 1984

Prepared for the
Division of Radiation Programs and Earth Sciences
Office of Nuclear Regulatory Research
U. S. Nuclear Regulatory Commission
Washington, D. C. 20555
under Interagency Agreement DOE 40-550-75

NRC FIN No. A2230

ABSTRACT

Experiments are described that combine backfill, radioactive waste, and basalt rock in a single flowing groundwater stream in a manner analogous to a hydraulic breach of a waste repository. The experiments were used to study chemical interactions that would occur if repository components were breached by flowing water.

The result of most significance to issues of repository performance was that uranium, neptunium, and plutonium were found to move more rapidly through repository components that were altered to represent aging than through fresh materials. In contrast, cesium moved slower through altered repository materials, as had been deduced from previous work using batch adsorption tests.

Two other parameters studied experimentally, the metal alloy used in the apparatus and an ionizing radiation field imposed on the experimental apparatus, had little or no measurable effect on radioactive element transport by flowing water.

Inasmuch as the alteration of the repository materials represents aging in an actual repository, we conclude that changes with age will detrimentally affect the ability of a repository to isolate uranium, neptunium, and plutonium. Because these elements have long-lived radioactive isotopes in nuclear waste, the degradation with time is a major issue regarding the performance of a nuclear waste repository in basalt.

NRC FIN No. A2230

Title: Laboratory Analog of Waste Leaching and Migration

CONTENTS

CONTENTS

FIGURES

FIGURES

TABLES

TABLES

TABLES

TABLES

ACKNOWLEDGMENTS

Much of the work reported was performed by personnel at Argonne National Laboratory other than the authors. A. M. Essling, E. A. Huff, and F. L. Williams of the Analytical Chemistry Laboratory performed the analyses of stable elements in solution. M. J. Steindler reviewed the ongoing work and contributed to the technical content of the program.

The program was greatly assisted by the enthusiasm of, and the results of work by, students K. L. Branham, J. P. Dymczyk, P. D. Hyde, C. K. Wilbur, and R. Wogelius, who contributed to the successful completion of the project through Student Research Participation Programs at Argonne. The results of their efforts are a significant part of the whole program presented in this report.

The authors would like to acknowledge and publicly thank Rex Couture and John Bates, both members of the Fuel Cycle Section, Chemical Technology Division, for the valuable laboratory services they performed for this program and for the sharing of their expertise during informal discussions with the authors.

We would also like to acknowledge the support we have received from the U.S. Nuclear Regulatory Commission, especially the individual attention and support of the NRC Project Managers, Kyo Kim and Don Alexander.

The secretarial work was directed by L. J. Jensen, who was ably assisted by R. T. Kiel. R. B. Keener edited the manuscript. The authors thank these people for their contributions and the many others of the Chemical Technology Division, headed by L. Burris, who contributed to the success of this program.

We also thank M. J. Smith of the Basalt Waste Isolation Program, who graciously supplied us with rock samples and kept us informed of progress in designing waste packages.

LABORATORY STUDIES OF A BREACHED NUCLEAR WASTE REPOSITORY IN BASALT*

by

. G. Seitz, D. L. Bowers,
T. J. Gerding, and G. F. Vandegrift

EXECUTIVE SUMMARY

Disposal of radioactive waste in geologic formations may offer a practical method of permanently isolating the waste from the biosphere. For such disposal, solidified nuclear waste is surrounded by multiple barriers such as a metal canister, backfill, and the formation rock itself, which can isolate the waste from the biosphere even if the barriers are breached by flowing water.

A comprehensive description of the performance of the repository requires consideration of many chemical species that can dissolve, complex, exchange, sorb, or precipitate while traversing each of the breached barriers. The reactions involving the chemical species are kinetically controlled and, thus, depend on the geometry of groundwater flow. The reactions occur in the radiation and thermal fields that are centered on the waste itself. Moreover, the reactions controlling the behavior of radioelements may be different for different repository ages. Because the performance of a repository even after thousands of years is important for the safe disposal of the nuclear waste, the comprehensive description of repository performance must include long-term performance.

Much experimental work to evaluate the potential for dispersal of radioactivity has focused on a single process such as the leaching of solid nuclear waste or the adsorption of radioactivity by rock. Another approach is to measure fundamental parameters such as thermodynamic properties of solids and solutions, knowing that these parameters can be shown to be related ultimately to the dispersal of radioactivity.

This experimental program was undertaken to improve our ability to predict radioelement behavior in the complex system of a nuclear waste repository. In particular, the experimental program was intended to identify the important processes not revealed in simple tests that could lead to substantial dispersal of radioelements from a repository.

In contrast to the approaches of dissection and analyses, therefore, the approach we used in this work linked solid radioactive waste, repository backfill, and repository host rock in a flowing groundwater stream in a manner analogous to the way they might be linked in a breach of a repository. The experiments employed a flow system of well-defined geometry containing well-characterized materials in which radioelement migration was measured directly.

---

*Work supported by the U.S. Nuclear Regulatory Commission under Contract FIN A-2230.

To establish our ability to predict radioelement migration, these measurements were compared to predictions obtained from results of simpler experiments and from calculations of computer-based models. In this manner, the results of this experimental program were used with results of other experimental and analytical approaches to identify the processes important to migration in complex systems involving groundwater flow.

Relationships between the results reported here and behavior expected in an actual repository can be complex. Specifically, no single scaling factor can relate all the experimental results to repository behavior. However, measured parameters such as radioelement concentrations, distances of radioelement migration, and groundwater compositional changes can readily be projected to those expected in a repository that experiences conditions comparable to those studied experimentally.

Experiments were performed to examine the effects of repository aging and the effects of a gamma radiation field on radioelement migration. In addition, two metal alloys proposed for construction of waste canisters were examined to observe how they might affect radioelement migration.

Materials

The rock used in this work was taken from the Pomona basalt flow in the vicinity of the Near Surface Test Facility at the Hanford, Washington, site. The Pomona flow is part of the Saddle Mountains basalt formation of the Columbia River Plateau; the Pomona flow is a high-magnesium (~7.0 wt % MgO) tholeiite and occurs at a depth of 250 m at the proposed repository location.

Rock cores, 6.83 cm in diameter by 14.60 cm long, were cut from the interior of basalt blocks and were split along their lengths using a hydraulic press. Other interior portions of the basalt block were crushed to be used with bentonite or alone to examine the interaction of the basalt with groundwater solution.

Wyoming bentonite was mixed with crushed basalt to serve as backfill in this experimental program. The bentonite is the source clay, SWy-1, of the Clay Mineral Society consisting primarily of sodium smectite with minor amounts of albite, quartz, mica, calcite, amorphous silica, aluminum oxide, and iron oxides.

Radioactive waste glass was prepared with uranium and eight other radioelements to have the composition of PNL 76-68 borosilicate glass loaded with 33 wt % nuclear waste. The actinide elements plutonium, neptunium, and uranium were added at the concentrations expected in fresh waste glass because these elements would not decrease substantially in concentration over the 1000-yr periods considered in this project. In contrast, low levels of radioactive cesium and strontium were added to the glass to account for the decay of the short-lived isotopes of these elements that would occur in 1000 years.

The simulated groundwater solution used in these experiments was prepared to the composition of groundwater from well DC-6, Grande Ronde Formation, which was sampled primarily from 200 m below the Umtanum unit on the Hanford, Washington site.

The solution contained 720 mg/L dissolved solids, with sodium the major cation and chloride and sulfate the major anions. The solution was sparged with nitrogen and capped under nitrogen gas to prevent adsorption of carbon dioxide or oxygen gases.

Some of the radioactive waste glass, basalt, and bentonite was altered hydrothermally to produce materials similar to those expected in an old repository. Two samples of radioactive waste glass were altered in steam and air at 340°C for 17 days, a treatment that produced a hydrated yellow-green layer over the surface of the glass.

Basalt cores and bentonite were altered in liquid groundwater solution with air at a temperature of 320°C for either 30 days or 60 days. One basalt core was altered in liquid groundwater with argon gas replacing air. Crushed basalt rock was altered in liquid groundwater with air at 350°C.

The altered basalt exhibited surface coatings of minerals produced in the alteration. Most dominant were a silica mineral, identified as quartz, and a magnesium-iron alumino-silicate, identified as stevensite (initially thought to be anthophyllite), that formed rapidly at elevated temperatures and persisted in contact with groundwater at 90°C. Scapolite, several zeolites, and minor amounts of sericite were also formed at elevated temperatures during alteration.

The mineralogy of the altered bentonite, as revealed by X-ray diffraction, was comparable to that of original bentonite. All altered materials were stored at room temperature in humidified chambers prior to their use in the experiments.

Apparatus used in this project was constructed of two alloys proposed as canister material for nuclear waste. Hastelloy C-276 and Monel-400 are both nickel-based alloys, but the Hastelloy contains molybdenum, chromium, and tungsten, whereas the Monel contains copper, iron, manganese, carbon, and silica as the other major constituents.

Experiments

Experiments in this program were done primarily by pumping groundwater solution over or through the repository materials and observing the chemical reactions and transport of elements by analyzing the solutions and materials sampled along the flow stream. In these experiments, termed analog experiments, water was pumped sequentially through a mixture of bentonite and basalt, over a tablet of radioactive waste glass, through another mixture of bentonite and basalt, then through a fissure in a core of basalt. The materials were contained in three vessels connected by tubing and valves from which groundwater solution could be sampled.

The apparatus was maintained at a temperature of 90°C and water was pumped at the nominal flow rate of 0.5 mL/h. At this nominal flow rate, water passed through the first two vessels containing radioactive waste glasses, bentonite, and crushed basalt at the linear velocity of 30 m/yr. The water passed through the fissure of the rock core at the velocity of 250 m/yr. The Darcy velocity for the water passing through the core was 1 m/yr. The velocities were selected for experimental purposes and may be

higher than the ambient velocities presently at the proposed repository site. The velocities are not inconsistent, however, with velocities expected under some repository conditions.

Experiments were started without radioactive glass and allowed to run until the composition of the groundwater solution exiting the apparatus was no longer changing in composition (~30 days). At this time, radioactive glass was added to the stream and flow continued for another 60 to 120 days, during which time solutions were collected continuously at the outlet of the experiment and intermittently at the outlet of the first or second vessel.

Pressures and temperatures throughout the experimental period were recorded on strip charts or by data acquisition equipment. At the termination of the experiment, the apparatus was disassembled and samples of bentonite, waste glass, and rock were taken for analyses.

Six analog experiments were conducted. Experiments were run using different experimental setups to verify the reproducibility of results and any dependence of the results on the materials of construction. One experiment was run in a gamma radiation field to examine the effects of radiolysis on radioelement migration. Three experiments were run with altered bentonite and basalt, with and without altered radioactive glass, to examine what effects aging of a waste repository might have on radioelement migration.

In addition to these analog experiments, additional simpler experiments were run to examine specific phenomena, such as the flow of groundwater through mixtures of bentonite and basalt or the reaction of groundwater with basalt, that were important to running the analog experiments or to interpreting the results of the analog experiments.

Results and Conclusions

Results of the program are a series of observations made upon pumping groundwater solution through the various components of a repository and upon analyzing the materials and solutions resulting from the experiments.

Perhaps the most significant observation resulting from running the experiments regarded the behavior of bentonite in flowing groundwater solution. Unaltered bentonite placed in the flow stream inhibited the flow of water by clogging tubing and the fissure of the rock core. However, bentonite that entered the flow stream as it expanded out of small tubes affected the flow of water very little, but did slowly accumulate on the fissure of the rock core. In contrast to the unaltered bentonite, altered bentonite was added directly to the groundwater stream without inhibiting flow.

The most significant chemical effects observed in the series of experiments conducted in this work were the greatly enhanced dissolution of plutonium, neptunium, and uranium from hydrated waste and the more rapid movement of these leached species through bentonite and basalt that were hydrothermally altered to simulate aging of the repository materials.

These effects are exemplified in the results given in the following table, which show the concentrations of plutonium, neptunium, and uranium in solutions that entered and exited the rock fissure of various experiments.

Radioelement concentrations in groundwater solutions before and after passing through the basalt core fissure in three experiments

Experiment and Conditions	Solution Concentrations[a] Inlet of Rock Core	Outlet of Rock Core	Percent Transmission
Experiment 1			
Unaltered Radioactive Glass			
Unaltered Basalt Fissure			
Plutonium	1.3	$\leq$0.02	$\leq$2
Neptunium	15	0.08	$\sim$0.5
Uranium	149	40	27
Experiment 6			
Unaltered Radioactive Glass			
Altered Basalt Fissure			
Plutonium	3.0	0.5	17
Neptunium	2.4	0.8	33
Uranium	50	22	44
Experiment 4			
Altered Radioactive Glass			
Altered Basalt Fissure			
Plutonium	89	41	46
Neptunium	109	67	61
Uranium	2560	1660	65

[a]Concentrations are 10^{-11} mol/L for plutonium and 10^{-9} mol/L for neptunium and uranium.

As observed in the data from experiment 1, the unaltered fissure of basalt binds almost all the plutonium and neptunium, not allowing these elements to pass any farther downstream. Most of the uranium is retained by the rock core, although 27% is allowed to pass downstream. Similar data exist from experiments 2 and 3, which were also performed using unaltered fissured cores. Radiographic maps of the core surfaces show that almost all the neptunium is bound on the first one-third of the fissure surfaces in these three experiments.

In contrast, results from experiment 6 show that significant portions of the plutonium and neptunium (17% and 33% respectively) passed through the hydrothermally altered fissure of basalt. Similarly, the amount of uranium transmitted through the altered fissure also increased, although not as markedly as for plutonium and neptunium.

Results from experiment 4 show the enhanced leaching of plutonium, neptunium, and uranium from the altered waste glass and the relatively unimpeded flow of these radioelements through the fissure compared with results for the unaltered basalt fissure (experiment 1). Experiment 5, performed with radioactive glass and fissured rock that were more altered than in experiment 4, gave results similar to those seen in experiment 4, except that leached

concentrations of the actinides were higher and greater fractions of the radioelements were transmitted through the basalt.

The results suggest that alteration of the radioactive glass and basalt rock that may occur upon aging of a waste repository could enhance the leachability of plutonium, neptunium, and uranium and allow these leached radioelements to be transmitted more readily through fissures of the host rock.

In a similar manner, barium and europium were found in this work to move more rapidly downstream through altered rock than through fresh materials. In contrast to the behavior of these elements, cesium was found in this work to move more slowly through hydrothermally altered basalt than through the unaltered basalt. This result is consistent with results of batch tests that show a greater sorption of cesium onto altered materials than onto fresh materials. Therefore, cesium would be expected to be immobilized to a greater extent in an aged repository than in a fresh repository.

No leach data from flow tests exist in available literature on altered glasses that could be compared with the enhanced leaching of plutonium, neptunium, and uranium seen in this work. In addition, no data are available concerning the sorption of any of the actinide elements, plutonium, neptunium, or uranium, on altered basalt surfaces that could be compared with the results reported here. In spite of this lack of data, the commonly held idea is that the ability to retain radioelements will increase as the repository ages due to the increased rock surface area and increased ion exchange capacity of altered materials. But the observations of enhanced transmission of radioelements through altered basalt seen in this work contradict this idea. Inasmuch as the alterations represent changes that may occur upon aging of the repository, the ability of a repository to isolate many radioactive elements is concluded from this work to degrade with time due to aging of the repository system. Therefore, the modification of repository behavior with age is a major concern regarding performance of the repository.

In an experiment performed in a radiation field of 1×10^5 rad/h, the dissolution of plutonium from radioactive waste glass was found to be enhanced and the dissolution of neptunium depressed by ionizing radiation. The species leached in a radiation field interacted with bentonite and basalt measurably the same as species leached in the absence of radiation. This result suggests that no radioelement species produced by radiolysis migrates differently than species formed in the absence of radiation. Except for the enhanced leaching of plutonium, which may be important to performance in some contexts, the effect of ionizing radiation does not appear to influence radioelement migration in a way detrimental to repository performance.

Seen in analyses of solutions from these experiments were substantial changes in the composition of groundwater upon contact with basalt. The groundwater solution decreases 15% in sodium and increased fivefold or more in calcium and potassium with changes persisting over the course of the experiments. These modified solutions have characteristics (pH, element concentrations, etc.) unlike the groundwater presently existing at the repository site, although such characteristics would be expected after exposure of the existing groundwater to fresh surfaces of basalt created upon excavating and backfilling the repository.

In contrast to the changes in groundwater composition seen on contact with freshly fissured basalt, much less change in composition of the groundwater

solution was seen from contact with the altered basalt, a result that suggests that the surfaces of the altered basalt are similar, chemically, to the old weathered surfaces of the basalt presently in contact with water sampled from drill hole DC-6.

Relatively little change in composition of the groundwater solution was observed upon contact with bentonite or radioactive glass. The changes caused by leaching of the radioactive glass are consistent in a general way with leach data from borosilicate glasses obtained in flowing tests.

Migration of the radioactive elements was found in this work not to be measurably changed by the use of either of the alloys, Hastelloy C-276 or Monel-400, as a material of construction for the apparatus. Because these alloys differ substantially in composition, the results indicate that neither alloy affected the chemical properties of dissolved radioelements.

Recommendations

The unanticipated behavior seen in these experiments is that neptunium, uranium, and plutonium moved more rapidly through hydrothermally altered basalt than through freshly fractured basalt. The elements barium and europium also showed this behavior. This behavior for plutonium, neptunium, and uranium can be understood in terms of reduction of the radioelements at the basalt surface. The behavior, however, is contrary to that predicted from the generally accepted theory that sorption of radioelements increases with the extent of alteration of basalt, behavior found in this program to be valid only for cesium. The stronger binding of cesium is likely due to the increased surface area and cation exchange capacity of the altered basalt. However, the extrapolation of this behavior of cesium to other radioelements, specifically those that are sensitive to reduction, such as plutonium, neptunium, and uranium, is not valid.

The major recommendation from this work is that descriptions of the performance of a repository in basalt should include the enhanced mobility of plutonium, neptunium, and uranium that can now be expected with age. Moreover, greater attention needs to be given, in general, to the consequence of aging of a waste repository.

An additional recommendation is that assumptions used to predict radioelement migration should be checked experimentally. Experiments that measure radioelement movement, such as those described here, give results that can be compared directly with those predicted in models of radioelement migration. The experimental approach is flexible and can be used to investigate many repository configurations in both saturated and unsaturated rock.

Experiments performed in this project were designed to incorporate conditions expected in an actual repository in basalt. Even though they are relevant to repository performance, many of the results obtained in this program had no counterpart in the results of simpler experiments, such as leach tests or sorption tests, to which they could be compared. These tests need to be performed under conditions of relevance to expected repository conditions and should include features such as water flow, elevated temperatures, and altered waste forms in leach tests, and actinide elements and altered rock in sorption tests.

1. INTRODUCTION

Disposal of radioactive waste in geologic formations may offer a practical method of permanently isolating the waste from the biosphere. For such disposal, solidified nuclear waste is surrounded by multiple barriers such as a metal canister and backfill, which isolate the radioactive waste. The flow of groundwater that would be allowed by the disruption of these barriers is considered as the most credible mechanism that may jeopardize the required performance of a waste repository. But even if groundwater infiltrates the barriers, dissolves radioactive elements in the solid waste, and eventually transports the radioactivity into fissures and pores of the surrounding rock, the radioelements can react with the rock and again become immobile. Thus, the geologic formation itself can be a barrier to the movement of the radioelements. Both manmade barriers and the geologic formation could thereby prevent the dispersal of radioactivity into the biosphere.

1.1 KNOWLEDGE OF RADIOELEMENT DISPERSAL

The interactions of radioactive elements with all these barriers are not simple. In a comprehensive description of the performance of the repository, there is a variety of solution and sorbed species that participate in the chemical processes of dissolution, complexation, ion exchange, sorption, and precipitation. Reactions involving the chemical species are kinetically controlled and, thus, depend on groundwater flow rate. The reactions occur in the radiation and thermal fields that are centered on the waste itself. Moreover, the prominent reactions change as the repository ages. Because the performance of a repository even after thousands of years is important for the safe disposal of the nuclear waste (U.S. Nuclear Regulatory Commission 1983), the understanding of the long-term performance of the repository is also needed.

Much experimental work to evaluate the potential for dispersal of radioactivity has focused on a single process such as the leaching of solid nuclear waste or the adsorption of radioactivity by rock. Each process studied is very complex and can preoccupy many investigators. Another approach is to measure fundamental parameters such as thermodynamic properties of solids and solutions, knowing that these parameters can be shown to be related ultimately to the dispersal of radioactivity.

In contrast to these approaches of dissection and analyses, experiments have been run that combined various components in environments that might be expected in a waste repository. Because the flow of groundwater is the most credible mechanism to jeopardize the performance of a waste repository, an attractive approach has been to use flowing groundwater to link components in experiments. Some studies have combined solid radioactive waste and repository host rock in flowing groundwater (Avagadro 1980; Seitz 1979a,b,c, 1980). The work was done with naturally fractured samples of impermeable rock (Seitz 1981a), as well as with permeable rock. The movement of radioelements was measured directly in some of these experiments with the results of interactions on radioelement movement clearly apparent. For example, the concentrations of a radioelement leached from the waste form were seen to affect directly the movement of that radioelement through rock (Seitz 1981b).

Studies have been performed of rock-water interactions in recirculating groundwaters subjected to a thermal gradient (Charles 1983). These techniques, originally developed to study alteration in recirculating hydrothermal systems, are applicable to the general understanding of alteration in the thermal gradients that would surround a waste repository. Other studies using flowing water have been limited to the leaching of waste glass (Coles 1982; Strachen 1982) in distilled water or in bicarbonate solutions moving at differing flow rates.

In another approach to laboratory studies, materials were combined in autoclaves and subjected to elevated temperatures to cause them to react (Bischoff 1978; McCarthy 1978; Savage 1982; Scheetz 1980; Shade 1980, 1982). Radioelement transport was not observed directly in these experiments. Instead, solution compositions and solid reaction products were monitored with time and temperature to gain an understanding of the progression of reaction products in a closed repository environment. These studies have focused on changes in major element compositions with the work on radioelements being limited to uranium (Shade 1982). In other studies of this type, compatibility of repository components such as metals for canisters and groundwaters have been investigated using an autoclave (Bradley 1983). Many of the approaches mentioned in this section as applied to testing waste package design have been reviewed by the Nuclear Regulatory Commission (Soo 1983a,b).

1.2 APPROACH USED IN THIS RESEARCH

The approach we have used in this research is an extension of the experiments that linked solid radioactive waste and repository host rock using flowing groundwater. In the work described here, backfill, solid radioactive waste, and repository host rock are coupled in a flowing groundwater stream in a manner analogous to the way they might be linked in a breach of a waste repository (Seitz 1981a,b; Vandegrift 1983). Using this approach, we have the advantage of being able to measure radioelement migration in this complex system directly. Chemical phenomena that affect migration are identified by comparing the experimental results with predictions from single-component tests and from models. The phenomena leading to significant mobilization or retention of radioactive elements, once identified, can then be incorporated into the considerations of repository performance.

The experimental program examined a waste repository in basalt. Bentonite mixed with basalt was the backfill and borosilicate glass containing seven radioelements was the nuclear waste form.

1.3 SCOPE OF RESEARCH

The experimental program is intended to identify the important processes that cause substantial dispersal of radioelements in flowing groundwater under some of the conditions that could be expected in a repository for nuclear waste. The experimental design is of a simple, well defined system in which radioelement migration is measured directly. To identify the processes important to migration, these measurements are compared to predictions of radioelement migration obtained from results of simpler experiments and from calculations of computer-based models. Also, these measurements can be used to help design field tests of significance to issues of repository performance.

Hence, the results of this experimental program are intended to be used with other experimental and analytical approaches to gain understanding of radioelement migration.

Relationships between the results reported here and behavior expected in an actual repository can be complex. Specifically, no single scaling factor is intended to relate experimental results to repository behavior because a single correlation between experiment and repository parameters does not apply to all phenomena. However, measured parameters such as radioelement concentrations, distances of radioelement migration, and groundwater compositional changes can readily be projected to values expected in a repository that is subject to conditions comparable to those studied experimentally.

1.4 ISSUES ADDRESSED BY THIS RESEARCH

This work addressed the need to understand the interactions between repository components that could affect repository performance with respect to licensing issues. This laboratory study of interactions was undertaken to identify those of importance to repository performance. By corollary, the study could also show that certain interactions are not important to radioelement migration and their relevance to repository performance could be relegated to low importance.

Specific issues addressed by the research are:

(1) Do different metal alloys that are proposed for canisters of nuclear waste affect radioelement migration and, hence, potential repository performance?

(2) Does radiolysis of groundwater solutions affect radioelement migration and, hence, potential repository performance?

(3) Does alteration of repository components, such as is expected upon aging of a repository, degrade repository performance or does it improve repository performance as commonly stated?

(4) What concepts and measurements (solubility products, leach rates, adsorption ratios, etc.) are sufficient to describe radioelement migration in systems with flowing groundwater?

(5) Are experimental programs that are undertaken to support repository development properly designed to address the subject of repository performance in the near and long terms?

General issues addressed in this work are:

(1) Do laboratory studies economically contribute to our general understanding of repository performance?

(2) Can we identify the interactions between repository components of most importance to repository performance under the conditions of the experiments? By corollary, can we demonstrate that some interactions are not important to issues of repository performance?

(3) Can we independently evaluate, using laboratory studies, commonly followed practices of repository design with regard to issues of repository performance?

In addition to addressing these issues, another goal of the work was to establish sets of data on radioelement migration collected under accurately measured conditions of temperature, water flow, water composition, etc. These data could be used to test computer codes of radioelement migration. This last goal of the work could be realized independently of whether or not the research uncovered new insight to the treatment of radioelement dispersal from a repository breached by flowing groundwater.

2. DESCRIPTION OF EXPERIMENTS

Two types of experiments were performed to accomplish the goals of the program. In the first type, water was pumped over radioactive waste glass and through backfill and fissured rock. These experiments were termed analog experiments. The second type of experiment was to study specific processes identified in analog experiments to be important to radioelement migration. These experiments were termed auxiliary experiments. The planning for the program and experimental results as they were obtained are described in a series of quarterly reports (Steindler 1982a,b,c,d,e, 1983a,b, 1984a,b,c).

2.1 ANALOG EXPERIMENTS

A schematic of the apparatus for the analog experiments is shown in Fig. 2.1. In an experiment, groundwater solution was pumped at a nominal rate of 0.5 mL/h through the system so that it passed through the first vessel, which contained basalt chips, bentonite, and the nuclear waste form; then through the second vessel, which contained more bentonite and basalt chips; and then through a narrow basalt fissure in the third vessel. The combination of bentonite and basalt chips constituted the backfill that would surround the waste in an actual repository. The apparatus was maintained at a temperature of 90°C for all experiments. The same groundwater solution was used in all experiments.

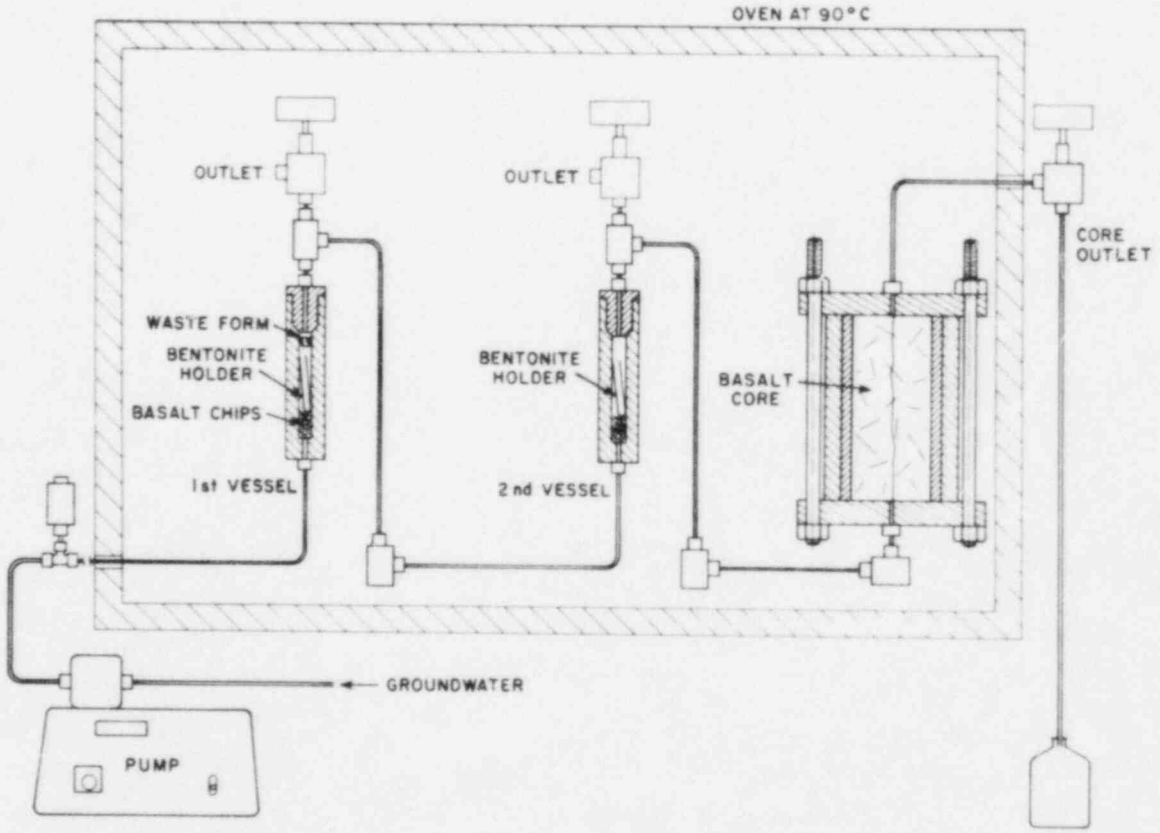

Fig. 2.1. Analog experimental apparatus

Solutions were collected continuously at the outlet of the core over the five-month duration of an experiment, and intermittent sampling was made at the outlets of the first and second vessels. These solutions were analyzed for stable and radioactive constituents. After termination of an experiment, the apparatus was disassembled and materials were analyzed radiochemically to determine the distribution of radioactive constituents that were leached from the waste form.

There were six analog experiments during the course of this program. Two analog experiments were run to test whether constructing the apparatus from either Hastelloy C-276 or Monel-400 would affect the results. A third experiment was performed in a gamma-radiation field to examine if radiolysis of stable or radioactive elements would lead to different leaching and migration characteristics of the radioelements. The remaining three experiments were performed with hydrothermally altered materials to examine whether alteration, such as could occur upon aging of the repository components, would substantially modify the migration of the radioelements. These experiments are listed in Table 2.1.

Table 2.1. Analog experiments conducted in the program

Analog Experiment Number	Simulated Repository Conditions and Experimental Variables
1	Recently constructed repository using Hastelloy C-276 alloy with as-manufactured waste glass and backfill, and recently fissured basalt.
2	Recently constructed repository using Monel-400 alloy (experiment was to establish the reproducibility of the results of experiment 1).
3	Recently constructed repository subjected to a gamma radiation field of $\sim 1 \times 10^5$ rad/h.
4	Old repository with long-term breach of waste package.
5	Old repository with long-term breach of waste package and extensively altered waste glass, backfill, and host rock.
6[a]	Old repository with the waste package recently breached (unaltered waste glass).

[a] In experiment 6, only the basalt and backfill were altered hydrothermally before the experiment. The waste glass was not altered hydrothermally as would be expected in a repository if the waste canister were breached after it had cooled thermally.

2.2 AUXILIARY EXPERIMENTS

The operation of the auxiliary experiments cannot be described simply because a variety of experimental designs was employed. Auxiliary experiments were performed with various components of the analog experiments. In some cases, the auxiliary experiments were performed using transparent glass vessels so that the interactions of fluid and materials could be observed directly. Such tests were used to design holders for bentonite to prevent it from clogging the flow stream. In other cases, auxiliary experiments were performed using Hastelloy or stainless steel vessels to eliminate contact of the fluid with glass apparatus. These auxiliary experiments were performed to examine the effects that bentonite and basalt had on the composition of water used in the experiments. In additional experiments, water containing suspended bentonite was passed through filters of various pore sizes and analyzed to determine the effects of filtering on the measured composition of the fluid. Results of these auxiliary experiments are reported together with results of the analog experiments in Section 3.

2.3 MATERIALS

Materials used in the experiments are representative of those that might be used or otherwise occur in a repository constructed in basalt. Borosilicate glass containing radioactive elements is one possible waste form that will be used to dispose of radioactive waste, and it was used as the waste form in these studies. Also used in the experiments was a mixture of bentonite and crushed basalt to serve as the backfill, as is currently being considered for a repository in basalt.

Cores of basalt from the Hanford site were also used in the experiments as the host rock of such a repository. An aqueous solution similar in composition of major constituents to groundwater sampled at the Hanford site was used as the groundwater fluid in these experiments (Apps 1979; Gephart 1979).

The preparation and characterization of these materials are described in this section. The radioactive waste glass is characterized in greater detail than are other materials because it was prepared specifically for this program and is, therefore, unique. Although characterization of the bentonite and basalt was conducted in this work, these materials have also been characterized by others, and references are made to their results.

2.3.1 Waste Glass Preparation and Characterization

2.3.1.1 Introduction

The glass wafers used in the series of analog experiments were prepared by adding eight radioactive elements to nonradioactive PNL 76-68 glass having the composition of stable elements expected in glass loaded with 33 wt % nuclear waste. Trace levels of radioactive cesium and strontium were added to the glass, rather than the high concentrations expected in fresh waste, to account for the decay of the short-lived isotopes of these elements that would occur in 1000 years. In contrast, the actinide elements, uranium, neptunium, and plutonium, were added at the concentrations that could be expected in fresh waste glass, because these elements would not decrease substantially in

concentration over the 1000-year period considered in this study. The radioactive glass was made considering uranium, neptunium, and plutonium to be present in the nuclear waste at concentrations of 8.6, 1.0, and 0.2 wt %, respectively.

Radioisotopes of americium, cerium, and europium were added to the glass to trace behavior of rare earth elements. In addition, europium has chemical properties in aqueous solutions below 150°C very similar to americium; thus, we would get an indication of the behavior of americium before using the more time-consuming separation techniques required for analyses of americium.

Briefly, the glass wafers were prepared by (1) mixing the nonradioactive PNL 76-68 glass with the radioactive components, (2) melting and casting the mixture, (3) annealing the glass ingot, (4) cutting the radioactive glass into wafers, and (5) cleaning the individual wafers. Details are given in Section 2.3.1.2.

Characterization of the waste glass described here serves two purposes. First, a technical description of the waste glass makes it possible to compare more knowledgeably the results of this program with results of other programs. Second, characterization established the extent of inhomogeneity of the wafers used in this program for a better understanding of results from different experiments.

To characterize the glass wafers, both destructive and nondestructive methods were employed. These methods included: (1) gamma-ray spectroscopy, (2) alpha radiography, (3) gamma radiography, (4) microprobe analysis, (5) X-ray diffraction analysis, (6) optical-microscopic examination, (7) MCC-1 type leach testing, (8) X-ray photoemission analysis, and (9) destructive dissolution. The details and results of each method are discussed in Section 2.3.1.3.

2.3.1.2 Glass Preparation

Uranium was added to nonradioactive PNL 76-68 glass having the average composition shown in Table 2.2. This glass has the composition of waste glass loaded with 33 wt % nuclear waste, but excluding the actinide elements. To form a glass containing 2.9 wt % uranium, 36.3 g of uranium nitrate ($UO_2(NO_3)_2 \cdot 6H_2O$) was mixed with 500 g of the nonradioactive glass. The mixture was heated for about six hours at 1050°C in air, then poured into water to fracture the glass for further processing. The glass was remelted to increase its homogeneity and poured into water a second time. Five samples of the glass (lot 2) were prepared for X-ray diffraction analyses. Upon normal exposure to X-rays, no crystallinity was detected in any of the samples. Overnight exposure of three samples to X-rays revealed diffraction lines of the spinel group attributed to Fe_2O_3 (maghemite) or $FeCr_2O_4$ (chromite). The mineral in the glass is estimated to have been present at less than 5 wt %.

Radioelement-bearing glass was prepared by melting the uranium-loaded glass with radioactive compounds. For the radioactive glass, 40 g of uranium-loaded glass served as the base to which was added a solution containing ^{137}Cs (0.65 μCi), ^{85}Sr (100 μCi), ^{141}Ce (1640 μCi), and ^{152}Eu (2000 μCi), along with solutions containing ^{241}Am (500 μCi), ^{239}Pu (1400 μCi), ^{237}Np (80 μCi),

Table 2.2. Compositions of nonradioactive PNL 76-68 waste glass from analyses of three bars of lot 2 glass[a]

Constituent	Analyses (wt %)			
	Bar 104E	Bar 160	Bar 22E	Avg
Al_2O_3	0.65	0.65	0.59	0.63
B_2O_3	9.12	9.03	8.82	9.32
BaO	0.55	0.54	0.52	0.54
CaO	2.17	2.14	2.34	2.22
CdO	0.04	0.05	0.05	0.05
CeO_2	0.73	0.71	0.90	0.78
Cr_2O_3	0.47	0.47	0.46	0.47
Cs_2O	1.15	1.13	1.13	1.14
Dy_2O_3	0.007	0.006	0.007	0.007
Eu_2O_3	0.006	0.005	0.005	0.005
Fe_2O_3	9.71	9.47	9.39	9.52
Gd_2O_3	0.02	0.02	0.02	0.02
K_2O	0.3	0.3	0.2	0.3
La_2O_3	4.52	4.41	4.06	4.33
MgO	0.14	0.13	0.14	0.14
MnO_2	0.07	0.06	0.06	0.06
MoO_3	2.01	1.96	1.92	1.96
Na_2O	11.3	11.1	11.5	11.3
Nd_2O_3	1.52	1.50	1.38	1.47
NiO	0.22	0.24	0.21	0.23
P_2O_5	0.54	0.71	0.74	0.66
SiO_2	41.1	40.5	40.6	40.7
SrO	0.43	0.43	0.41	0.42
TiO_2	3.08	3.02	3.02	3.04
ZnO	4.80	4.78	4.71	4.76
ZrO_2	1.78	1.73	1.87	1.79

[a]Analyses by J. Mendel, Battelle Pacific Northwest Laboratories, Richland, WA.

and ^{133}Ba (45 μCi). The quantities of radioelements, their original chemical forms, and their radiodecay characteristics are given in Table 2.3. The total volume of liquids that contained the radioelements was less than 10 mL.

Table 2.3. Radioactive isotopes added to the PNL 76-68 waste glass and their radiation properties

Radioactive Isotope	Half-Life	Decay Mode	Primary γ or α Radiation, keV (photons or alphas/100 decays)	Quantity per 40-g Batch[a]	Original Chemical Form of the Isotope
Alkali					
^{137}Cs	30.2 yr	β^-	γ: 661.7(8.50)	0.65 μCi	CsCl
Alkaline Earths					
^{85}Sr	64.7 d	EC	γ: 514.0(99.3)	100 μCi	$SrCl_2$
^{133}Ba	10.7 yr	EC	γ: 356.0(62), 81.0(31.7), 302.8(18.1), 383.8(9.0), 276.4(7.0)	45 μCi	$BaCl_2$
Rare Earths					
^{141}Ce	32.5 d	β^-	γ: 145.4(48.4)	1640 μCi	$CeCl_4$
^{152}Eu	14 yr	73% EC (β^+)	γ: 1408.0(21.3), 121.8(29.1), 344.3(27.2)	2000 μCi	$EuCl_3$
		27% β^-	γ: 964(14.8), 1112.1(13.8), 778.9(13.2)		
Actinides					
^{241}Am	432 yr	α	α: 5486(85.2), 5443(12.8)	500 μCi	$Am(NO_3)_3$
		γ	γ: 60(36)		
^{239}Pu	24,131 yr	α	α: 5155(73), 5143(15.1), 5105(11.5)	23 mg (0.06 wt %), 1400 μCi	$Pu(NO_3)_6$
^{237}Np	2.14×10^6 yr	α	α: 4817(1.5), 4803(1.6), 4788(51), 4770(19), 4765(17), 4664(1.6), 4639(4.6)	115 mg (0.3 wt %), 80 μCi	$Np(NO_3)_4$
		γ	γ: 86(13)		

[a]Quantity on 19 November 1981.

The solutions were added to the glass contained in a 95% platinum-5% gold crucible, and the contents were thoroughly mixed. Prior to heating the mixture, the liquids were allowed to evaporate at room temperature for 20 hours. The loaded crucible was put into a graphite secondary crucible and then into the Brew furnace, where it was heated in an argon atmosphere of 7.9×10^4 Pa (600 mm Hg) at 1050°C for six hours. The power to the furnace was then shut off, and the furnace was cooled to less than 100°C in 30 minutes. After cooling, the sample was removed from the Brew furnace and the 40-g glass ingot was separated from the primary crucible.

The glass ingot was tranferred to another platinum crucible (inside an Al_2O_3 secondary crucible) for annealing. The glass was heated to 500°C, held there for one hour, then cooled slowly for five hours until the temperature was below 150°C, at which point power to the furnace was turned off.

After the heat treatment, the annealed glass was sectioned into 24 pieces (0.4-g slabs, each about 11 × 9.3 × 1.2 mm). All but one of the samples were cut from the interior of the glass ingot. Distilled water was used as the cutting lubricant for a low-speed Isomet saw (Model 11-1180). The cuts were made at a linear speed of about 5000 cm/min, using a 10-cm-diameter circular blade with low-concentration diamond abrasive and a blade thickness of 0.3 mm. The cutting scheme is depicted in Fig. 2.2. The cut pieces were washed in ethanol in small beakers in an ultrasonic bath, then put into clean, labeled polypropylene bottles for storage until use. Five samples were used in the program; the other pieces were used for characterization.

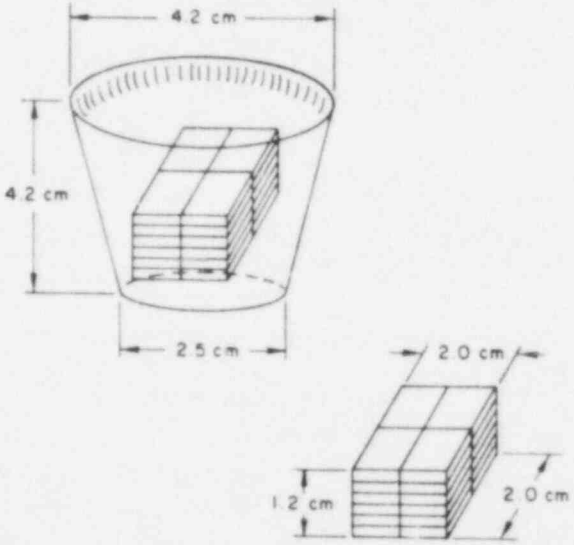

Fig. 2.2. Cutting scheme used to obtain radioactive waste-glass wafers for the experimental program

2.3.1.3 Characterization of Glass Sample Homogeneity

Gamma-Ray Spectroscopy

The gamma-ray spectra of fourteen wafers of the radioactive waste glass were measured. From these spectra, seven isotopes were monitored by measuring the areas of 11 peaks. The amounts of ^{137}Cs (661.7 keV) in all samples were too small to measure and are not considered further. Table 2.4 is a compilation of the radioisotopes that were monitored and the gamma-counting parameters associated with them.

The gamma-ray spectra were recorded and analyzed on a Camberra Series 80 multichannel analyzer equipped with a Ge(Li) detector. Each glass sample was

Table 2.4. Counting parameters for isotopes in the radioactive glass prepared in this program

Isotope	Peak Gamma Energy (keV)	Region of Interest (keV)	Photons / 100 Decays	Peak Area to Total Count Rate in Region of Interest (%)	Relative Count Rate to that of ^{241}Am	Half-Life Correction	Average Precision of Peak Area Measurements (%)
^{241}Am	59.5	56.0-62.5	36	43	1	No	0.6
^{237}Np	86.5	83.7-89.0	13	9	0.15	No	3.5
^{133}Ba	80.9	78.4-83.1	32	11	0.16	No	3.1
	356.0	352.4-359.5	62	36	0.16	No	2.1
^{141}Ce	145.5	140.3-149.7	48	73	4.2	Yes (32.5 d)	0.2
^{152}Eu	121.8	116.7-126.1	29	78	8.8	No	0.1
	344.3	337.1-350.7	27	81	2.9	No	0.2
	1112.1	1107.0-1116.4	14	81	0.35	No	0.6
	1408.0	1401.4-1414.4	21	96	0.42	No	0.4
^{85}Sr	514.1	509.7-518.0	99	43	0.18	Yes (64.7 d)	1.7

counted for 10,000 s of instrumentation live time or until channel 199 (the peak of the ^{152}Eu 122-keV peak) contained 1,000,000 counts. Each sample was placed 16 cm above the bottom of the shelf tray. At this distance, the instrument had a dead time for these samples of about 10%. Two glass samples (No. 9 and No. 11) were placed and counted on shelf 40 (about 40 cm from the bottom of the tray) to verify that geometric differences in the samples were not affecting relative count rate.

Table 2.5 shows the weight and dimensions of each sample analyzed. Table 2.6 compares the relative radioisotope activities in each sample. Both tables list the glass samples in the order of their overall gamma radioactivity. From this ordering, two conclusions are made:

(1) With the glass wafers separated into two categories--one group with average activities of the fission product isotopes less than the average values of all wafers and the other group with average activities greater than the average values--the division is correlated with the long-side dimension of the glass samples. As seen in Table 2.5, all samples in the first group have a length between 0.419 and 0.425 in.; all samples in the second group have a length between 0.466 and 0.485 in.

(2) The two actinide radioisotopes that were measured (^{241}Am and ^{237}Np) do not have as large a spread of activity as do the fission products, and the differences in activity do not correlate with those of the fission-product radioelements.

Table 2.5. Weights and dimensions of radioactive glass wafers analyzed by gamma counting

Sample No.[a]	Dimension (0.001 in.)			Weight (g)
	x	y	z	
11	425	361	50	0.3559
10	430	368	49	0.3545
6	419	362	52	0.3856
3	423	360	49	0.3578
1	421	361	50	0.3451
14	435	370	64	0.4391
2	428	360	51	0.3578
13	429	372	53	0.4444
4	481	357	52	0.4055
5	466	361	56	0.3877
7	475	361	51	0.4147
8	467	360	51	0.3886
9	471	357	48	0.3750
12	485	378	53	0.4169

[a]Arranged in order of increasing concentration of fission-product radioisotope concentration.

Table 2.6. A comparison of the relative activities for each radioisotope[a] in the radioactive glass wafers

Sample No.	Activities, Relative to the Averages for Each Isotope						
	^{241}Am	^{237}Np	^{141}Ce	^{85}Sr	^{133}Ba	^{152}Eu	Overall Fission Products[b]
11	0.988	1.03	0.849	0.863	0.876	0.846	0.858
10	0.928	ND[c]	0.889	0.958	0.906	0.887	0.910
6	1.006	ND	0.920	0.931	0.922	0.928	0.925
3	1.009	ND	0.926	0.950	0.930	0.932	0.934
1	1.035	ND	0.929	0.941	0.950	0.938	0.940
14	0.859	ND	0.956	0.955	0.920	0.958	0.947
2	0.912	ND	0.956	0.956	0.953	0.954	0.953
13	1.012	0.98	0.935	0.935	1.013	0.937	0.958
4	1.047	ND	1.065	1.038	1.034	1.064	1.050
5	1.056	ND	1.106	1.068	1.051	1.094	1.080
7	1.026	ND	1.113	1.085	1.046	1.101	1.080
8	1.051	ND	1.112	1.088	1.070	1.117	1.097
9	1.067	1.06	1.114	1.083	1.099	1.118	1.104
12	0.997	0.93	1.136	1.143	1.220	1.125	1.156

[a]The average activities were 144.3 cps/g for americium, 221.5 cps/g for neptunium, 1779 cps/g for cerium, 44.62 cps/g for strontium, 21.5 cps/g for barium, and 396.0 cps/g (344-keV peak) for europium.

[b]Isotopes are ^{141}Ce, ^{85}Sr, ^{133}Ba, and ^{152}Eu.

[c]Not determined.

The variations of radioelements in various glass wafers appear to be due to incomplete mixing of the radioelements and glass during preparation. (The difference in the long dimension for the two types of samples corresponds to glass wafers being cut from different sides of the glass monolith; see Sec. 2.3.1.2.) To make results of all analog experiments consistent, the glass wafers used in the six experiments were all picked from the series of wafers with the shorter x dimensions (Table 2.5).

Alpha Radiography

Eleven of the glass wafers cut from the single radioactive glass ingot were examined by alpha radiography. Each of the wafers was placed on an alpha-sensitive plastic (Kodak LR 115, type II) for 30 minutes. The exposed sheets were etched in about 6.0N NaOH solution at about 60°C for 10 minutes. This etching removed damaged plastic along the paths of the alpha particles, leaving cylindrical tracks. The tracks were viewed using an optical microscope to determine the microscopic distribution of alpha-emitting radionuclides near the surface of the wafers.

The alpha-emitting isotopes in the glass are ^{241}Am, ^{239}Pu, and ^{237}Np. The activities of these isotopes are in the proportion, 0.35:1.00:0.05, respectively, with all alpha particles having comparable energies. Therefore, on the alpha radiographs, it is primarily plutonium that is recorded, with 25% of the radiographic image due to americium and about 3% due to neptunium.

Ten percent or more of the alpha activity located in spots within the glass would have been detected if the spots were spaced no closer together than 10 μm. No evidence of this or any other inhomogeneity was apparent by observation with an optical microscope. Each glass was uniform in composition, as judged by the alpha-track radiographs.

The visible alpha tracks within known areas were counted at eight locations on each of the individual alpha radiographs. The numbers of tracks at the eight locations on each plastic sheet for the 11 wafers are listed in Table 2.7. The track densities due primarily to plutonium correlate very well with the gamma activities of the americium in these samples. This suggests that the plutonium mixed into the glass similarly to americium.

The average track density for the 11 plastic films is $1.57 \times 10^6/cm^2$, and is consistent with the amount expected by the addition of 4.4×10^9 dpm alpha activity to 40 g of glass, as shown by the following calculation. A $1\text{-}cm^2$ slab of the glass, 20 μm thick, is calculated to have an alpha activity of 6.1×10^5 dpm. In this calculation, a density of 2.8 g/cm^3 for the glass was used. Inasmuch as 20 μm is the approximate path length of alpha particles in glass, about one-quarter of the alpha particles emitted in the 20-μm-thick slab could intersect plastic placed adjacent to the slab. Therefore, in a 30-minute exposure of the plastic, 4.60×10^6 alpha particles would intersect each square centimeter of the plastic sheet.

The alpha track registration and counting efficiency is therefore 35%. This efficiency is expected. It is less than 100% because of such factors as: (1) alpha particles are not registered over the full length of their paths, (2) the surface of the plastic is removed by etching, (3) tracks are insufficiently developed by etching, and (4) the analyst does not count all sizes of tracks.

Table 2.7. Numbers of alpha tracks counted on etched plastic sheets[a]

Location Number	Glass Wafer Number										
	1	2	3	4	5	6	7	8	9	10	11
1	55	34	34	45	46	52	58	59	47	52	48
2	48	36	47	47	48	57	59	54	60	51	47
3	47	42	48	36	51	50	53	47	71	37	48
4	49	31	56	47	42	55	68	40	64	50	49
5	47	38	33	47	51	52	51	50	59	53	49
6	53	34	45	53	41	54	53	55	52	46	44
7	49	45	48	44	47	47	57	51	54	54	51
8	47	37	37	58	43	53	57	61	62	32	48
Avg	49.4	37.1	43.5	47.1	46.1	52.5	57.0	52.1	58.6	46.9	48.0

[a]Each number corresponds to the number of tracks counted in an area of 3.125×10^{-5} cm^2.

Gamma Radiography

Distributions of beta- and gamma-emitting isotopes were radiographed in the individual wafers of glass, using high-sensitivity Polaroid film. The film was exposed bare and through sheets of plastic and paper of various thicknesses to stop alpha particles and low-energy beta particles. The result was uniformly exposed film under the entire area of each wafer. Therefore, no inhomogeneity, on a microscopic scale (~50-μm scale), of the beta- and gamma-emitting radioisotopes was evident from these radiographs. These exposures could reveal microscopic inhomogeneities of gamma-emitting radionuclides such as those reported elsewhere (Mysen 1975).

The inhomogeneities of gamma-active radioisotopes that were detected by gamma counting (using electronic instruments) would not be apparent from these radiographs.

Microprobe Analyses

A sample of glass cut from the large radioactive glass ingot was subjected to analyses by microprobe. This sample extended from the edge of the glass ingot to about 1 cm into its interior. The chemical inhomogeneity of this sample would, therefore, be expected to be greater than that of any of the interior slabs used in the laboratory analog program.

The sample was mounted in epoxy resin, ground, then polished with diamond paste and coated with carbon. The mount was placed in an electron beam, and fluorescent X-rays were analyzed for energy and intensities. The X-ray intensities, for scans of the electron beam across the sample, are shown in Figs. 2.3 and 2.4 for energies corresponding to the X-rays characteristic of the elements specified.

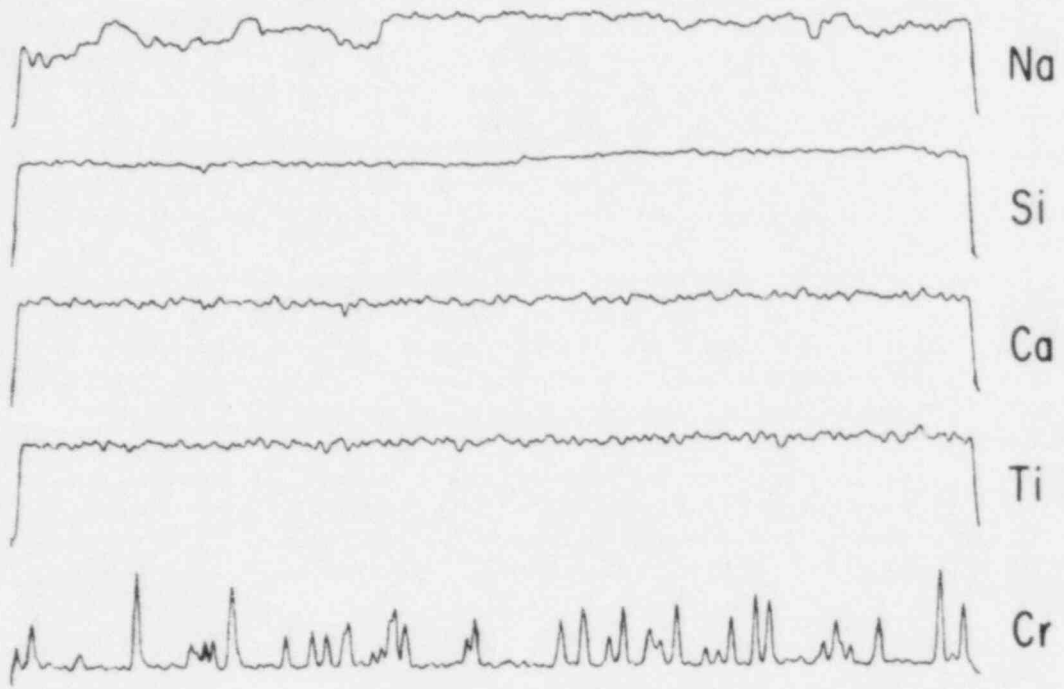

Fig. 2.3. X-ray intensities of Na, Si, Ca, Ti, and Cr from the edge (left) to 0.78 cm (right) into the radioactive glass ingot

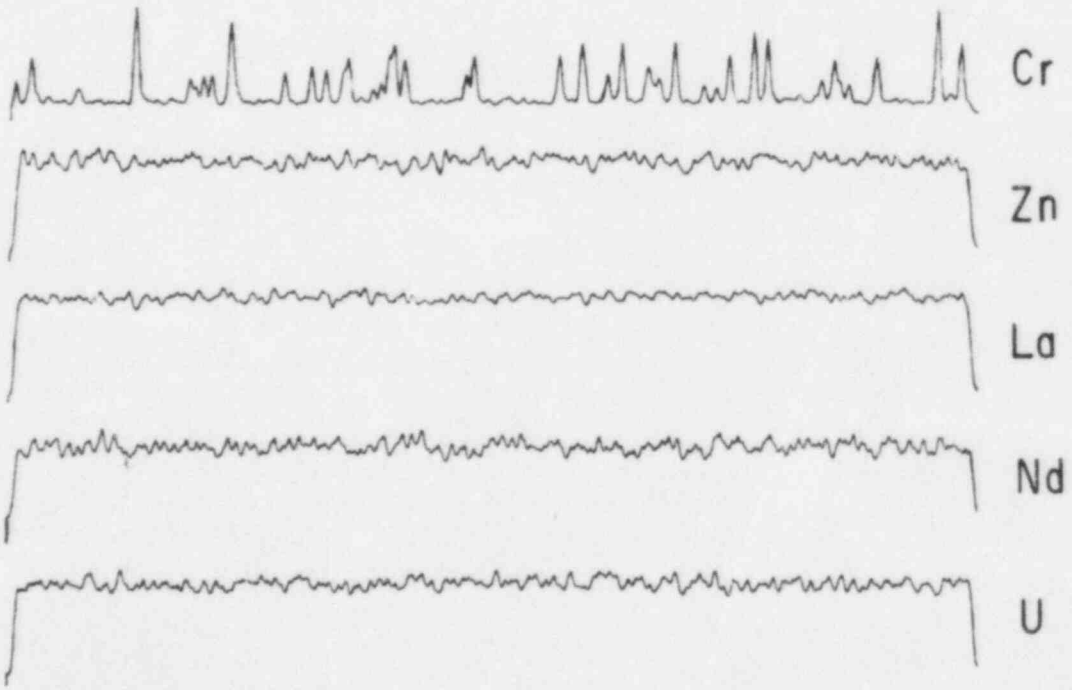

Fig. 2.4. X-ray intensities of Cr, Zn, La, Nd, and U from the edge (left) to 0.78 cm (right) into the radioactive glass ingot

The constant average intensities of X-rays at most energies indicate a uniform average composition from the edge to the interior of the glass ingot. At the edge of the glass ingot, there was a decrease in average intensity of X-rays corresponding to sodium, which indicated a loss of sodium from the region. The sharp changes in X-ray intensities, noted particularly for chromium, are due to small crystals embedded in the glass matrix. These crystals were analyzed in more detail by positioning the electron beam on the crystals and on the glass separately.

Figures 2.5 and 2.6 are energy spectra of a crystal and the glass matrix, respectively. The crystals are small and give spectra with X-ray contributions from the glass. Nonetheless, the spectra are indicative of the composition of the crystal. Based on these spectra, the crystals are enriched in chromium and iron and depleted in sodium, calcium, and silicon relative to the glass matrix. The spectra indicate the crystals to be chromite, the spinel $FeCr_2O_4$, which is consistent with X-ray diffraction analyses of the nonradioactive glass and with the general knowledge that spinels crystallize from this borosilicate waste glass on cooling.

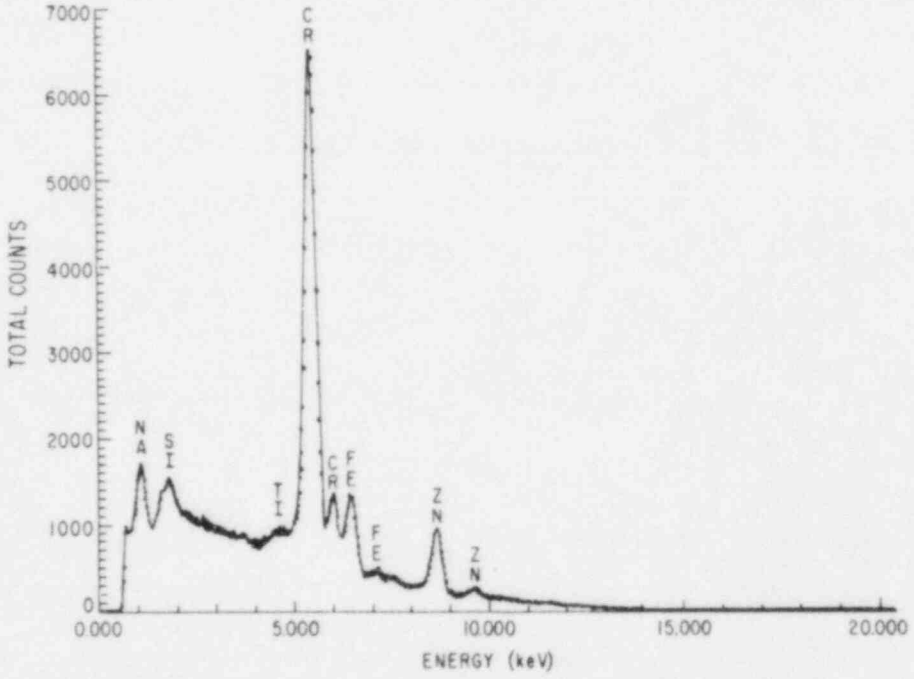

Fig. 2.5. Energy spectrum of X-rays from an electron beam centered on a ~5-μm-sized crystal identified as chromite in the radioactive glass

X-Ray Diffraction Analyses

Spinel was detected by X-ray diffraction in the nonradioactive glass used to make the borosilicate waste glass. To determine the amount of crystalline phase, X-ray diffraction patterns of two standards prepared in the laboratory

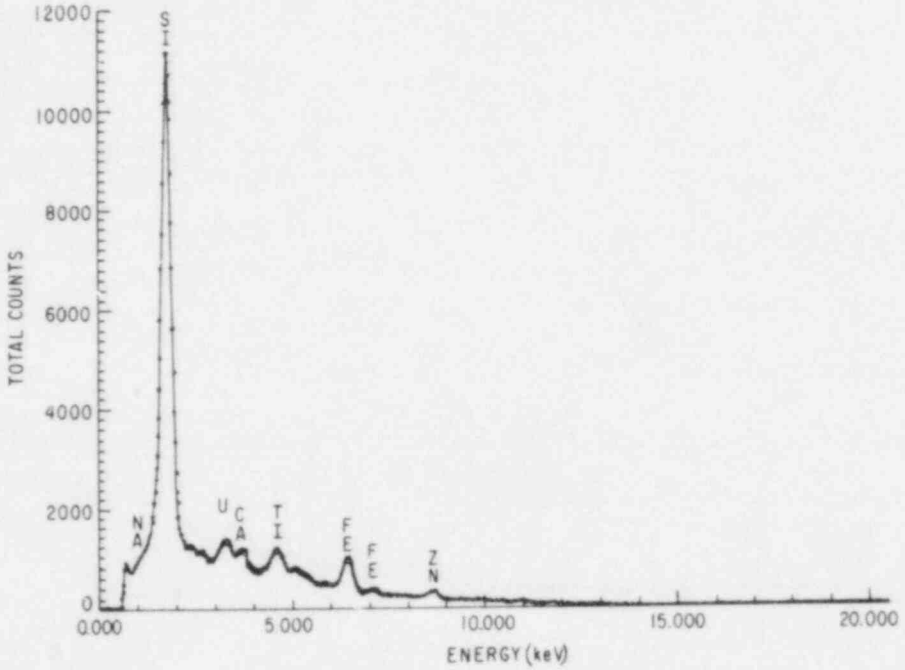

Fig. 2.6. Energy spectrum of X-rays from an electron beam on the radioactive waste glass without crystals

were compared with the pattern of the nonradioactive glass. Magnetite was used as the standard reference mineral because it has about the same crystal structure, chemical composition, and X-ray intensity lines as chromite--the spinel phase suggested by the microprobe analyses. The magnetite has other crystallographic features that are similar to the chromite. The crystallographic characteristics of the two spinels are given in Table 2.8.

Optical Microscopy

The extent of crystallization of the waste glass was determined by R. A. Couture, Argonne National Laboratory, by means of optical microscopic examination. Two rectangular slabs of the glass, designated as samples 501 and 504 (Steindler 1982a) and containing high and low fission product activities, were examined.

The mounts were opaque to light due to the thickness of the glass (about 1 mm) and its substantial opacity. Therefore, all observations were made in reflected light. In addition to glass, five phases were observed and are described in Table 2.9.

The amounts of the crystalline phases in each of the samples were estimated by point counting using a grid with 100 intersections. The results are given in Table 2.10.

Table 2.8 Physical and chemical properties of magnetite and chromite

Property	Mineral	
	Magnetite	Chromite
X-Ray Intensity Lines (Å) (3 strongest)	2.53 1.49 2.97	2.52 1.60 1.46
Chemical Composition	Fe_3O_4	$FeCr_2O_4$
Lattice Constant	8.397	8.336
Mineral Group	Spinel	Spinel
Crystal System Structure	Cubic Isometric	Cubic Isometric

Based on these observations, we conclude that only about 1% of the glass is crystalline, with the chromite being the dominant mineral phase. Identification of the phase as chromite is based on its high reflectivity and equant crystal morphology seen in the optical microscope and on its high iron and chromium concentrations identified by microprobe analyses. The identification is consistent with the X-ray mineral identification of a spinel group in the glass used to make this radioactive glass.

MCC-1 Type Leaching

Wafers of the radioactive glass prepared for the laboratory analog program were tested for their behavior under static MCC-1 conditions. The test matrix included 13 samples measured, with duplication, over periods of 3 to 91 days. The results of this study (Steindler 1982a,b,c) show leaching behavior as is expected for radioactive glass for both fission products and actinide elements.

X-Ray Photoemission Spectroscopy

Analyses of glass surfaces before and after leaching in water have been performed using X-ray photoemission spectroscopy. Figure 2.7 shows the full scan (1000 eV) of the glass before it was leached. Some of the elements are labeled next to the peaks they produce. Particularly noted are peaks to give the silicon to zinc ratio, the sodium intensity, and the intensities around the iron doublets at 700 eV.

Figure 2.8 shows the region where the actinide 4f doublets are located, with clearly visible uranium and neptunium peaks. The titanium 2p doublet is used as a reference to determine the valence state of the uranium (it is +6 in this sample).

Table 2.9. Identification of phases in the radioactive glass

Phase	Identification	Description
1	Spinel-type phase, identified as chromite	Occurs in anhedral grains (triangular, hexagonal, square sections) ~10-mm dia. Isotropic, dark orange-red by transmitted light (from internal reflections), medium reflectivity, gray. Occurs more commonly in aggregates of anhedral or subhedral grains, on the order of 0.7-μm dia. Harder than glass.
2	Metal: palladium, or possibly ruthenium	Spherical grains, typically 2.5-μm dia. Isotropic, high reflectivity. Softer than glass. Only one crystal was seen in the 20 scans of sample 501, giving a modal analysis of 1×10^{-4}%.
3	Polishing pits	Irregular shape, elongated. Possibly, plucked grains of phase 4. Appear dark green, suggesting glass is green by transmitted light. Typically 25 μm long.
4	Possibly RuO_2	Transparent, anisotropic. Occurs as single crystals or recrystallized grains, some of which are pseudomorphs. Color not discernible by reflected light. The crystals are typically 2-5 μm. Their distribution is not uniform.
5	Bubbles	- - -

Figure 2.9 shows the spectrum from the leached sample. Due to leaching, the zinc has enriched considerably on the surface relative to silicon. The surface (within a 30-Å layer) is made up mostly of Zn-Si oxides with small amounts of Ti, Fe, Ru, and Rh. Figure 2.10 shows the actinide region, where only weak Ru and Ti peaks can be observed, in contrast to the unleached sample (Fig. 2.8), which shows uranium and neptunium peaks.

Destructive Dissolution

The concentrations of ^{237}Np, ^{239}Pu, and ^{241}Am in the radioactive borosilicate glass serving as the nuclear waste solid were determined by radiochemical techniques. A 24.5-mg sample of one of the wafers was dissolved in

Table 2.10. Modal analyses of phases in two rectangles of the radioactive glass

Phase Type	Amount of Phase in Sample (%)	
	501	504
1	1.0 ± 0.2	0.7 ± 0.1
2	0 $(1 \times 10^{-4})^a$	0
3	0.02 ± 0.02	0.05 ± 0.03
4	0.02 ± 0.02 $(0.002 \pm 0.001)^a$	0.02 ± 0.02
5	0.18 ± 0.06	0

[a]Measurement made by estimating the area of the particle(s) of that phase against the entire area searched by the microscope grid.

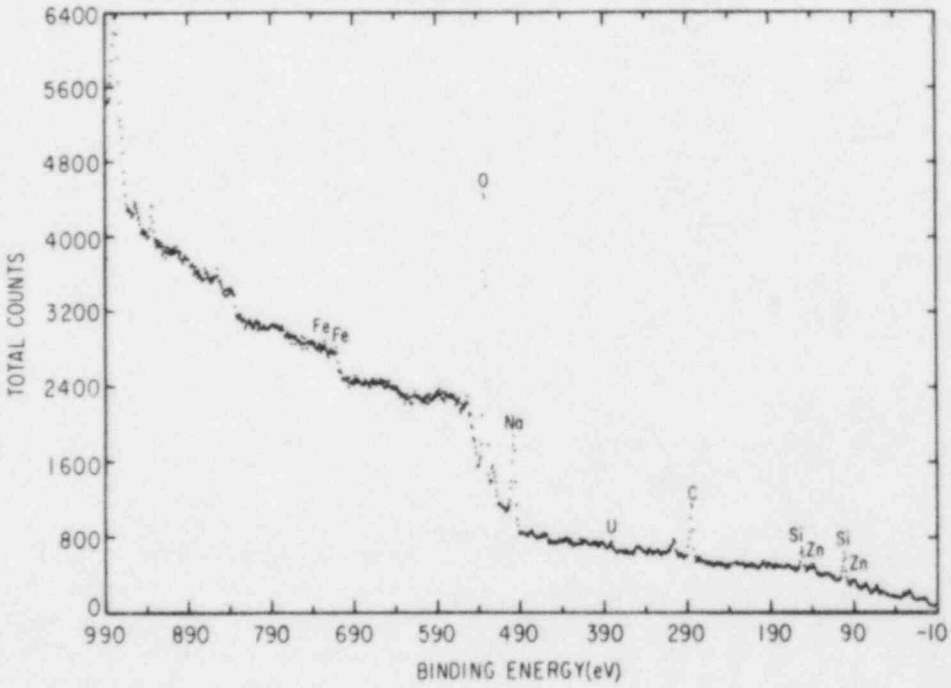

Fig. 2.7. Full X-ray photoemission spectroscopy spectrum of the radioactive glass before leaching

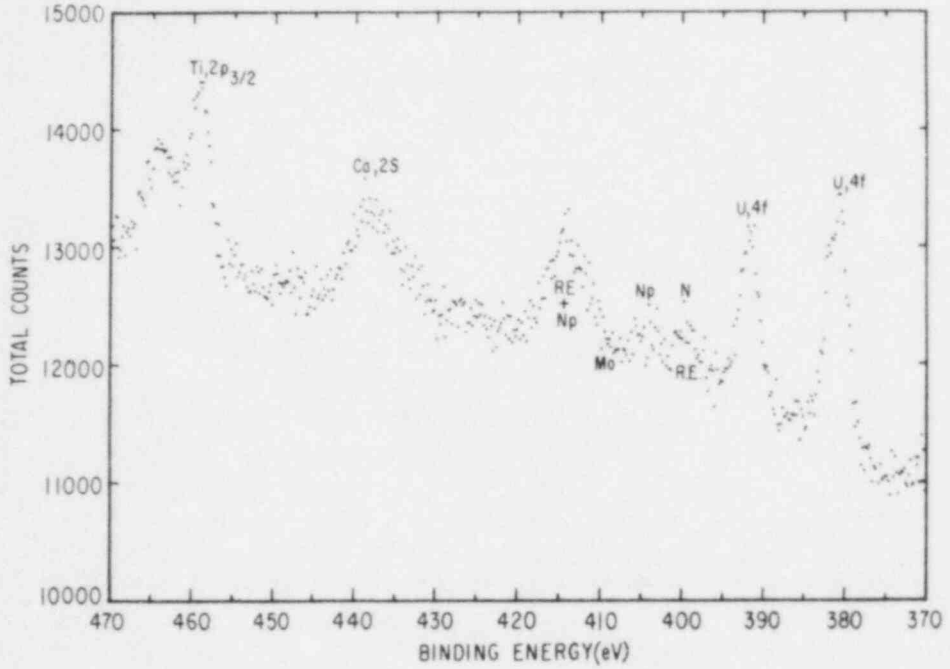

Fig. 2.8. Actinide region of X-ray photoemission spectroscopy spectrum of the radioactive glass before leaching

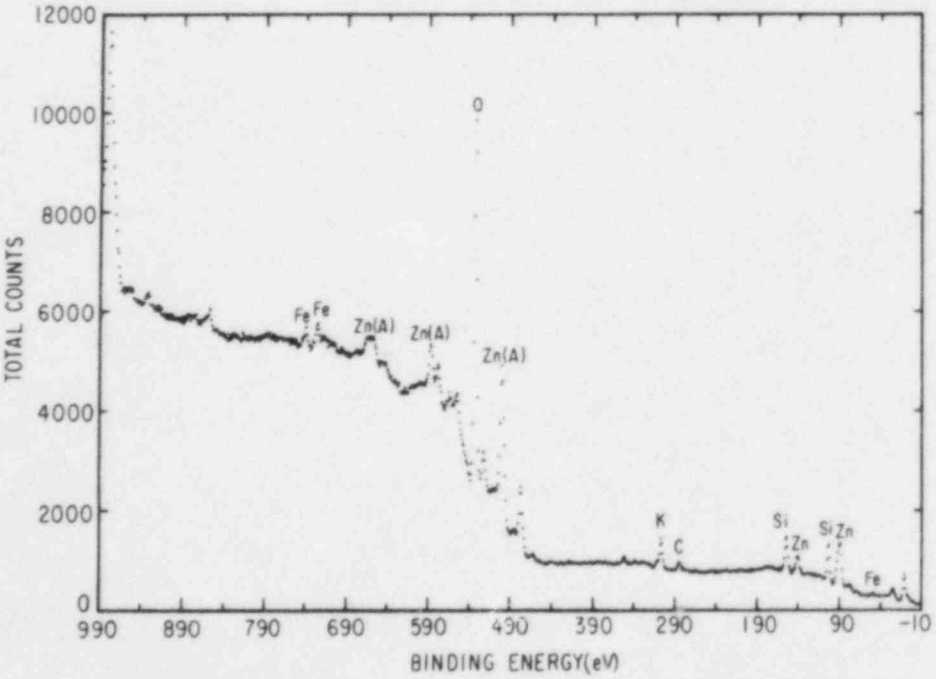

Fig. 2.9. Full X-ray photoemission spectroscopy spectrum of leached radioactive glass

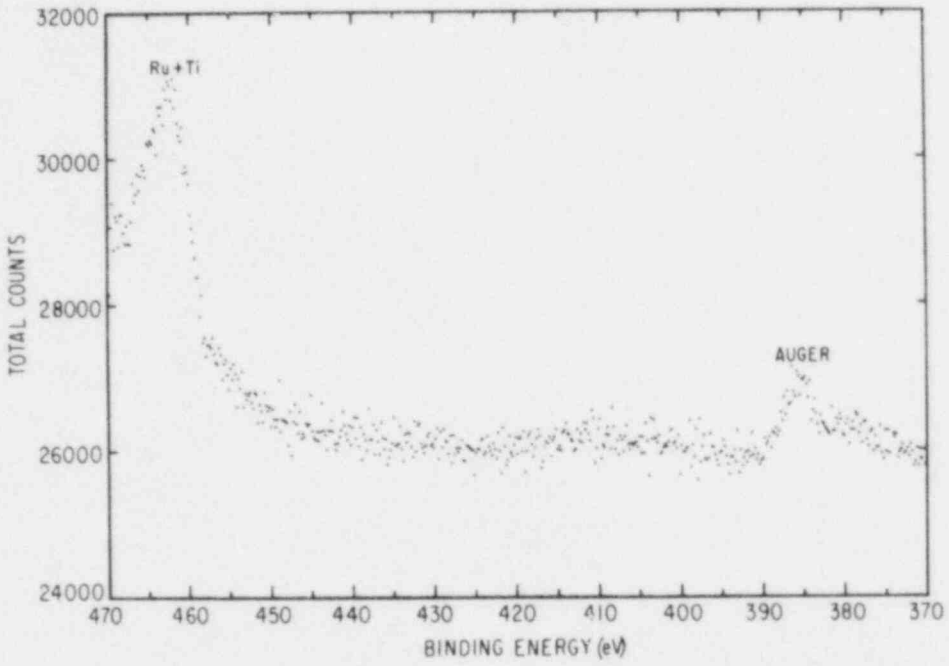

Fig. 2.10. Actinide region of X-ray photoemission spectroscopy spectrum of leached radioactive glass

concentrated HF, HCl, and HNO_3 acids. The solution was diluted with distilled water to a volume of 25 mL. A 20-μL sample of this solution was transferred to a planchet and dried.

The deposit on the planchet was then counted using an alpha-counting chamber. The relative and specific activities of the various isotopes per gram of glass are shown in Table 2.11. As is evident from the table, the measured levels of the three isotopes agree very well with the values expected based on the activity added when preparing the glass.

Table 2.11. Relative and specific activities of neptunium, plutonium, and americium isotopes in the radioactive glass

Isotope	Relative Activity[a] (cps/g)	Relative Activity[a] (μCi/g)	Activity Added in Formulating the Glass (μCi/g)
^{237}Np	1.69×10^4	2.16	2.01
^{239}Pu	2.81×10^5	36.2	35
^{241}Am	8.47×10^4	10.9	12.5

[a] A counting efficiency of 21% was obtained by calibrating with a radioactive standard.

2.3.2 Pomona Basalt

The rock used in this work was taken from the Pomona flow in the vicinity of the Near Surface Test Facility at the Hanford, Washington, site. The Pomona flow is part of the Saddle Mountains basalt formation of the Columbia River Plateau; the Pomona flow consists of high-magnesium (~7.0 wt % MgO) tholeiite (Ames 1980) and occurs at a depth of 250 m at the reference location for the proposed repository (Figure 6-1, Rockwell Hanford Operations 1982).

The Pomona basalt used in these experiments was supplied by personnel of the Basalt Waste Isolation Project. The rock is fine- to medium-grained basalt that is altered and has the average bulk chemical composition shown in Table 2.12. Density of the basalt was determined to be 2.92 g/cm^3 by measuring the weight of a known volume of rock.

Table 2.12. Pomona flow basalt average whole-rock analyses[a]

Oxide	Analysis (wt %)	Population Standard Deviation[b] (wt %)
SiO_2	53.5	2.5
Al_2O_3	13.8	0.3
Na_2O	2.34	0.09
K_2O	0.46	0.16
MgO	7.45	0.19
CaO	9.6	0.5
FeO[c]	11.0	0.2
TiO_2	1.65	0.06
MnO	ND[d]	
P_2O_5	ND	

[a] From Ames (1980).

[b] Standard deviation of 13 analyses.

[c] Fe_2O_3 reported as FeO.

[d] Not determined.

Rock cores were cut from the interior of the basalt, as exhibited in Fig. 2.11, and were ground to size (6.83 cm in diameter by 14.60 cm long, weighing ~1545 g). The unsplit cores could not be permeated by water (a water pressure of 6.9 MPa across the length of the core for one week did not transmit a measurable quantity, 0.1 mL, of water). Therefore, the cores were split, using a blade made of Brown & Sharp gauge stock (tool steel) that had been oil-quenched to about 60 Rockwell hardness and ground.

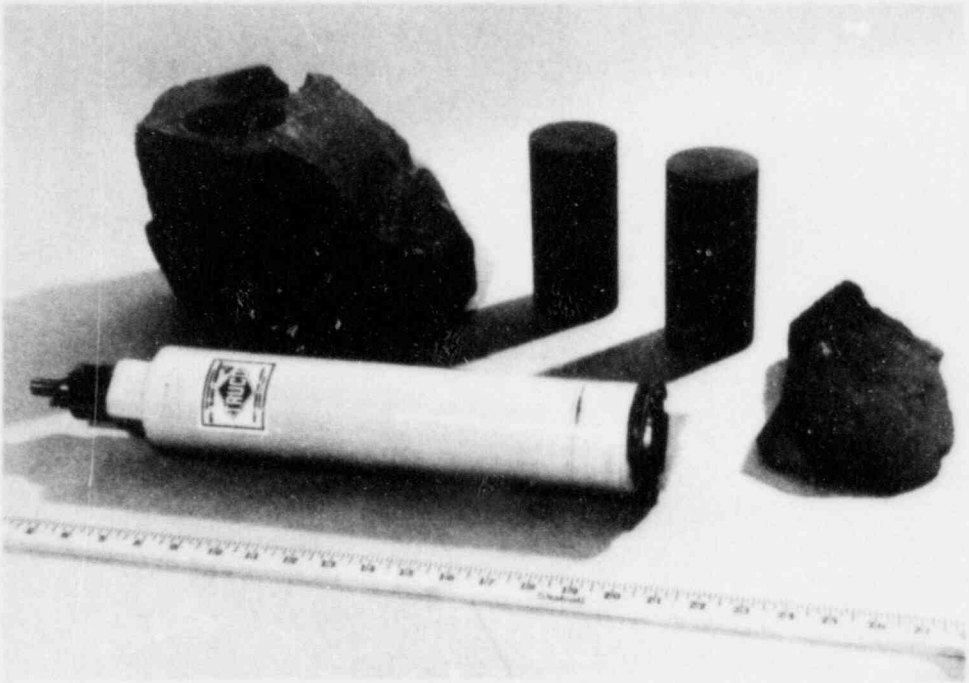

Fig. 2.11. Cores drilled from the interior of a block of basalt for use in the analog experiment

To split a core, the 15-cm-long blade was pressed along the length of the core, using a hydraulic press. When the force exerted on the splitter by the press was increased to about 28×10^3 kg, the core fractured. The newly split core halves were constrained by sandbags to prevent them from falling from the press.

In addition to the cores, chips of the Pomona basalt were used as part of the backfill material in the integrated experiments and as the solid phase in experiments conducted to study the interaction of the basalt with groundwater.

The basalt chips used as a component of the backfill in the analog experiments consisted of pieces 1 to 3 mm in linear dimensions that were hand picked from crushed basalt. The basalt used with bentonite in each holder had a surface area per unit mass of 6 cm^2/g, estimated from measurements of particles in a binocular microscope.

An additional crushed sample was sieved (by being passed through a 10-mesh sieve and retained on an 18-mesh sieve) to form a sample of particle size nominally 1 to 2 mm in diameter. The surface area per unit mass of these chips, as determined by measuring a representative sample of 30 chips and assuming rectangular shapes, was computed to be 230 cm^2/g. This material was used in auxiliary experiments.

2.3.3 Backfill

Backfill that would surround the package of nuclear waste may serve as a primary chemical barrier to radioelement migration. Bentonite mixed with crushed basalt has been proposed as one material to serve this function (Coons 1980; Turcotte 1980), and was used as the backfill in these experiments. Five grams of crushed basalt were used in each holder with Wyoming bentonite. Material called backfill in this project is also often referred to as packing material.

The bentonite is a source clay, SWy-1, of the Clay Mineral Society. It is primarily sodium smectite with albite, quartz, mica, calcite, amorphous silica, aluminum oxide, and iron oxides as minor phases (Van Olphen 1979). The sample is from the Newcastle Formation (Cretaceous), Crook County, State of Wyoming, NE 1/4, SE 1/2, Sec. 18, T 57N, R 65W. Cation exchange capacity was measured to be 76.4 meq/100 g with sodium and, to a small extent, calcium being the exchangeable ions. The bentonite has a surface area measured by nitrogen gas adsorption of 31.8 ± 0.2 m^2/g (Van Olphen 1979). Chemical analyses of the bentonite are given in Table 2.13.

Table 2.13. Chemical analyses of SWy-1 Wyoming bentonite[a]

	Analysis (wt %)	
Constituent	1	2
SiO_2	62.9	62.9
Al_2O_3	19.3	19.6
TiO_2	0.16	0.090
Fe_2O_3	3.85	3.35
FeO	0.12	0.32
MnO	0.01	0.006
MgO	2.80	3.05
CaO	1.80	1.68
Na_2O	1.54	1.53
K_2O	0.56	0.53
Li_2O	ND[b]	ND
P_2O_5	0.06	0.049
S	ND	0.05
F	0.111	ND
Total	99.65	99.22

[a] From Van Olphen (1979).

[b] No data.

2.3.4 Groundwater Solution

Simulated groundwater solutions used in these experiments were prepared to represent the composition of groundwater from well DC-6, Grande Ronde Formation, which was sampled primarily from 200 m below the Umtanum unit on the Hanford, Washington, site (Apps 1979; Gephart 1979). The nominal composition of the simulated groundwater is reported in Table 2.14. While being prepared, the solutions were sparged with nitrogen. After preparation, the basic solutions were stored under nitrogen gas in capped polyethylene bottles to prevent pickup of carbon dioxide. During an experiment, the groundwater was continually sparged with nitrogen gas before entering the apparatus to maintain the dissolved oxygen at a low level and to prevent pickup of carbon dioxide.

Table 2.14. Recipe for simulated groundwater prepared for analog experiments

Compound	Quantity Added to 20 L of water (g)	Concentration (mmol/L)
NaCl	3.51	2.99
Na_2SO_4	3.19	1.12
$Na_2B_4O_7 \cdot 10H_2O$	0.246	0.0331
NaF	1.64	1.95
Na_2CO_3	1.20	0.57
$NaHCO_3$	1.18	0.71
$Na_2SiO_3 \cdot 9H_2O$	11.46	2.01
K_2SO_4	0.085	0.024
$CaSO_4 \cdot 2H_2O$	0.111	0.032
$MgSO_4 \cdot 7H_2O$[a]	0.0036	0.00073
HCl (1M)[b]	61 mL	3.05

[a]Added from a concentrated 1-mL solution.

[b]Added to reduce the pH of the groundwater at 22°C to 9.9.

The chemical composition of each 20-L batch of simulated groundwater was measured before its use by titration, anion chromatography, and inductively coupled plasma emission spectroscopy analyses. The results of these measurements are presented in Section 3.2.1.

2.3.5 Hydrothermal Alteration of Materials

Materials used in some of the analog and auxiliary experiments were altered hydrothermally to produce characteristics similar to those expected of aged materials in the repository. The relationship of hydrothermal alteration to aging is described in Section 4.2.

2.3.5.1 Alteration of Basalt and Bentonite

The bentonite and basalt used in the analog experiments were altered in Hastelloy or stainless steel pressure vessels (autoclaves) under similar conditions of temperature and pressure to produce modifications expected upon aging. Vessel pressure and temperature were monitored and recorded every 15 minutes by computer.

Three fissured basalt cores used in analog experiments 4, 5, and 6 were altered by placing them individually in an autoclave with water and gas at ~320°C for 27 to 60 days. Each of the cores was run with either air or argon, as specified in Table 2.15. The rock cores were found to have reacted with the water and formed secondary minerals (quartz, hematite, anthophyllite, scapolite, sericite, and zeolites) on their surfaces.

Table 2.15. Conditions for alteration of three fissured rock cores[a]

Gas, Quantity	Temperature (°C)	Time at Temperature (d)	Materials for Use in Experiment
Air, 350 mg	320	30	4
Air, 350 mg	320	60	5
Argon, 490 mg	320	27	6

[a]Each run contains a rock core of ~1545 g and 1 L of water solution. The 2-L pressure vessel was made of Type 316 stainless steel.

Basalt rock chips were altered hydrothermally for use in the auxiliary experiments. For this work, a 170-g sample of basalt rock chips was placed in a gold-mesh screen basket suspended in a Hastelloy C-276 pressure vessel that was filled with 1.50 L of groundwater solution and kept at a temperature of 350°C and pressure of 10 kPa for one month. When the altered basalt chips were removed from the autoclave, they were lighter in color than unaltered chips, being covered with a white gray powder. The powder was analyzed by X-ray diffraction and the major crystalline constituent was found to be alpha cristobalite (SiO_2); possible minor constituents found were orthoclase ($KAlSi_3O_8$) and tridymite (SiO_2). We did not analyze the powder for amorphous constituents. The basalt rock cores had shown red coloration from the alteration, indicating that ferrous ion had been oxidized to ferric ion. However, very little red coloration was seen on these altered basalt chips.

The bentonite used in three of the analog experiments was altered hydrothermally by placing 6 g of bentonite, 6 g of groundwater solution, and 3 mg of air in four sealed stainless steel vessels and heating two of them for 30 days and two for 60 days at a temperature of 320°C. The altered bentonite was gray (as opposed to the yellow starting material) and formed

chunks that did not disperse freely in flowing water. Mineralogy of the altered bentonite, revealed by X-ray diffraction, was comparable to that of the original bentonite containing 1M type clay with alpha silica. The 1M type reflection at 12.2 Å had the closest fit to JCPDS 29-1495, $K_{0.7}Al_2(Si,Al)_4O_{10}(OH)_2 \cdot nH_2O$; but after being finely suspended in water the clay exhibited a reflection at 10.7 Å and a fit closest to the illite 1 Md type JCPDS 29-1496, $K_{0.7}Al_2(Si,Al)_4O_{10}(OH)_2$ (JCPDS 1981).

The altered basalt and bentonite were stored at room temperature in humidifed chambers prior to their use in the experiments.

2.3.5.2 Alteration of the Waste Glass

The borosilicate waste glass was hydrothermally altered in saturated steam and air. Two glass wafers (samples 6 and 10, Table 2.5) were suspended in platinum wire loops in a 35.6-mL Hastelloy C-276 autoclave to which was added 10 mL of groundwater solution. The upper portion of the vessel was insulated to prevent condensation on the glass when the pressure vessel was cooled after the alteration process.

The vessel was sealed and then heated to 340°C for 17 days in an oven. At the end of the heating period, the oven was cooled and the vessel opened to recover the glass samples and residual groundwater. No water had escaped from the pressure vessel during heating, as indicated by recovery of 10.0 mL of water from the lower portion of the vessel. The water contained no detectable radioactivity, indicating that liquid water had not contacted the radioactive glass during the aging process.

The two glass samples were removed from the vessel. They were observed to be coated with a yellow-green layer resulting from the reaction of the water vapor with the glass. During gentle handling, the reaction layer on the large surface of glass sample 10 separated from the substrate. Glass sample 6 remained intact. Figure 2.12 is a photograph of the hydrated samples and a sample of fresh glass.

The hydrated glass samples were stored in a humidified jar before being used in analog experiments 4 and 5.

2.4 APPARATUS

The apparatus used in the analog experiments is described generally in Section 2.1. The experiments were done in apparatus, described here more fully, that consisted of three distinct components: a vessel containing backfill (basalt chips and bentonite) and the nuclear waste glass, another vessel similar to the first and containing additional backfill, and a holder with the fissured rock core. The geometry of the first vessel is illustrated in Fig. 2.13. The bentonite was packed in a crimped tube of Hastelloy alloy to allow it to disperse gradually in the flowing stream without clogging the stream. During an experiment, bentonite from the top of the crimped holder continued to fall to the bottom of the vessel where it settled into the basalt chips. The rock core holder with the fissured core of basalt is illustrated in Fig. 2.14.

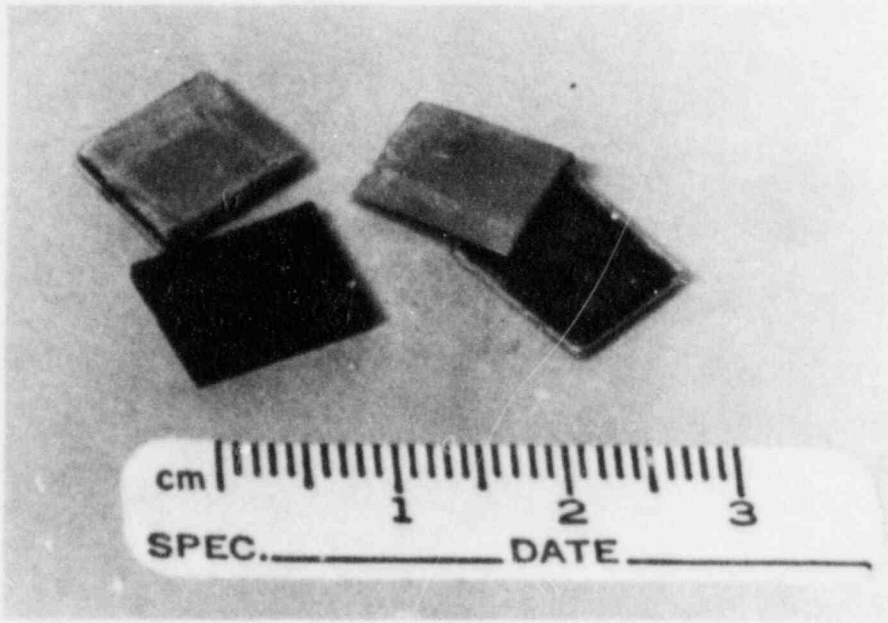

Fig. 2.12. An original (black) glass sample at the lower left, together with two altered samples at the top (the hydration layer of the sample at the upper right has separated from the glass substrate)

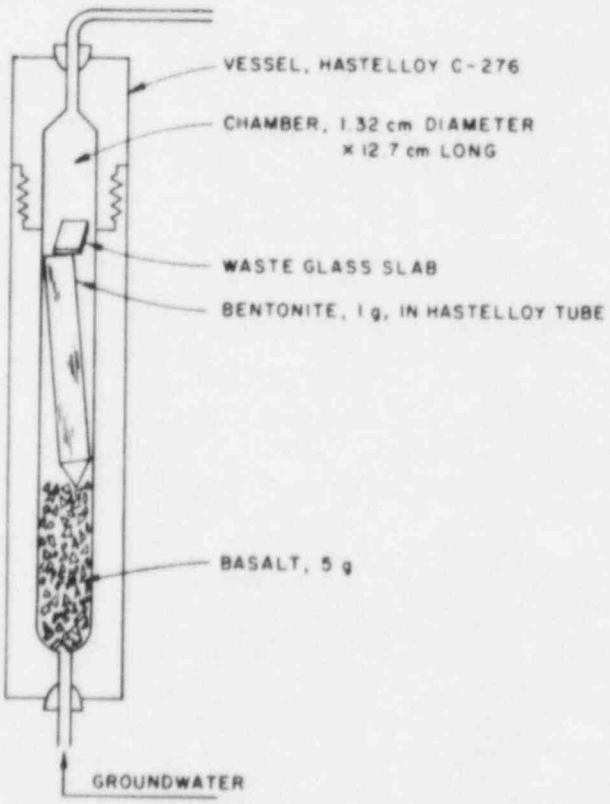

Fig. 2.13.

Schematic of the first vessel in the analog experiments, which held basalt chips, bentonite, and waste glass

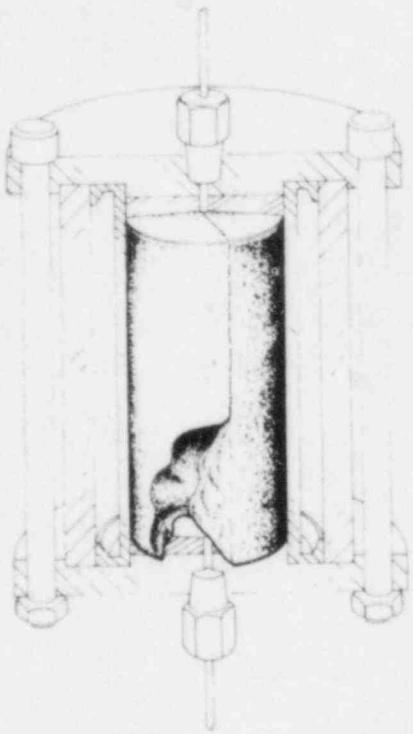

Fig. 2.14.

Cutaway diagram of the rock core holder with fissured basalt

The fissured rock core was enclosed in a Teflon sleeve that was pressurized to seal and prevent water from bypassing the rock core. The Teflon sleeve deformed under pressure to fill the irregularities on the outer surface of the basalt core.

Under ordinary experimental conditions, the Teflon was inert and did not have any measurable chemical influence on the experiments. However, in a radiation field Teflon is known to degrade readily. To avoid this problem, a sleeve of high density polyethylene was substituted for the Teflon sleeve in the one analog experiment that was performed in a radiation field.

The apparatus used in the auxiliary experiments varied in the many experiments that were performed, but generally consisted of one or two components similar to those used in the analog experiments. In the auxiliary experiments with basalt, basalt chips were always substituted in place of the fissured basalt core of the analog experiments.

2.4.1 Materials of Construction

The apparatus used in the experiments consisted of metal components and tubing to hold the experimental materials and to create flow paths for the solution. Alloys of construction of vessels, tubing, and couplings were either Hastelloy C-276* or Monel-400† for the analog experiments and either

*Trademark of the Cabot Corporation. Hastelloy C-276 contains 59% nickel, 17% molybdenum, 15% chromium, and 4% tungsten by weight.

†Trademark of Huntington Alloys. Monel-400 contains 66.5% nickel, 31.5% copper, 1.2% iron, 1.0% manganese, 0.2% carbon, and 0.2% silicon by weight.

Type 316 stainless steel* or glass for the auxiliary experiments. The metals are corrosion-resistant alloys that may be used to make canisters for the waste or, in the case of the stainless steel, to make cans in which the molten glass will be cast.

2.4.2 Dimensions of the Flow System

The volume of the flow system, the volume occupied by materials in the fluid stream, and the rate at which solution is pumped through the system determine the residence time of solution in the apparatus. The volumes of relevance to the analog experiments are shown in Table 2.16. For a flow rate of 0.5 mL/h, the solution in the apparatus will be displaced about every three days.

Table 2.16. Volume of components and materials used in the analog experiments

Component	Volume (mL)		
	Hastelloy Autoclave System[a]	Hastelloy Tubing System	Monel Tubing System
First Vessel	17.8	11.3	16.0
Second Vessel	17.8	11.3	16.0
Solution in Fissure of Basalt	1.45	1.45	1.45
Solution in Connecting Tubing	2.67	2.67	4.57
Solution in Valves and Fittings	0.8	0.8	0.8
Nominal Fluid Volume[b]	29.74	16.74	28.04

[a] The vessels were made by Autoclave Engineers, Erie, PA.

[b] Nominal fluid volume is obtained by adding the volumes of the first vessel, second vessel, solution in the fissure, connecting tubing, and valves and fittings, and subtracting the volumes of basalt (1.71 mL) and bentonite with holders (3.62 mL) for two vessels and the volume of the waste glass (0.12 mL).

The cross sections of the fluid stream and the flow rate of solution determine the fluid velocities at the various locations along the fluid stream. The cross sections at the different locations in the apparatus are shown in Table 2.17. The linear velocities of solution pumped at a rate of 0.5 mL/h are determined from data given in this table to be ~30 m/yr through the first and second vessels and 500 m/yr through the fissured rock.

*Type 316 stainless steel contains 17% chromium, 12% nickel, 2.5% molybdenum, and less than 2% manganese, 1% silicon, and 0.08% carbon by weight. The balance (65-68% by weight) is iron.

Table 2.17. Cross sections of the fluid stream in various components of the analog apparatus

Component	Cross Section (cm^2)		
	Hastelloy-Autoclave System	Hastelloy Tubing System	Monel Tubing System
First Vessel	1.37	0.817	1.00
Second Vessel	1.37	0.817	1.00
Connecting Tubing	0.014	0.014	0.024
Rock Fissure	0.099	0.099	0.099

As described in Section 2.3.2, the basalt cores used in the experiments were 6.83 cm in diameter by 14.60 cm long. They were split along their lengths to form two surfaces each of 99.7 cm^2 surface area. Because water flow could not be maintained through the tightly closed fissure in the basalt in the presence of bentonite, the two halves of the core were held apart in the core holder by two strips of 0.017-cm-thick gold foil, 0.5 cm wide.

2.4.3 Pumps

Solution metering pumps for the analog experiments were used to pump groundwater solution through apparatus at a controlled flow rate. These pumps had internal parts of Hastelloy alloy, stainless steel, Kel-F plastic, or sapphire that were nonreactive with the groundwater solution. The pumps are described in Appendix A.

2.4.4 Atmosphere Control

For the analog experiments, a 2-L quantity of the groundwater solution was placed in an Erlenmeyer flask and sparged throughout the experiment with nitrogen gas to prevent pickup of carbon dioxide and to exclude dissolved oxygen. This reservoir flask and the apparatus to treat the nitrogen gas to establish the low oxygen concentration are shown in Fig. 2.15. In this apparatus, nitrogen gas derived from liquid nitrogen containing about 2 ppm oxygen was humidified and then reacted with ~50 mL of chromous chloride solution, which is highly reactive with gaseous oxygen. After oxygen removal, the gas was washed in water to remove any entrained particulate or liquid. The purified nitrogen was then bubbled through the groundwater solution.

The chromous chloride solution served also as an indicator of the absence of oxygen, because it turns from light blue to dark green upon reaction with oxygen in the atmosphere. It is reasonable to assume that this color change is readily detected when the concentrations of chromous and chromic ions are equal. An aqueous solution at a pH of 10 with equal concentrations of chromous and chromic ions has a calculated oxygen partial pressure of 10^{-76} Pa and an oxidation potential of -0.41 V (calculated using the standard free energies of the chromous and chromic ions as -42.1 and -51.5 kcal respectively, and the disassociation constant of liquid water as 83.1). Inasmuch as

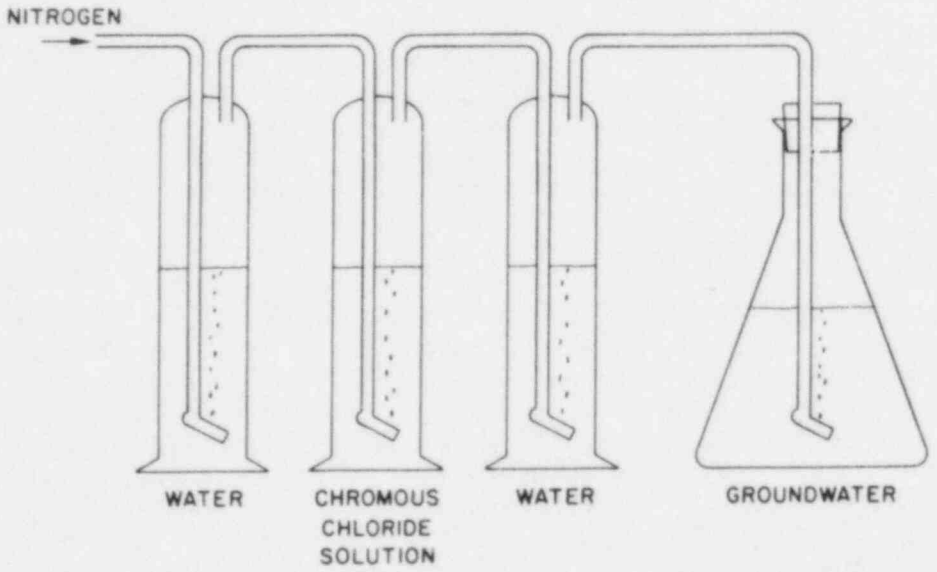

Fig. 2.15. Apparatus to keep oxygen from dissolving in the groundwater solution

the color of the chromous chloride solution did not change (compared with the color of the solution when sealed in a glass jar) while being sparged with nitrogen gas, the oxygen concentration in the nitrogen gas and, thus, in the groundwater solution was considered to have remained low throughout the experiments. The calculated oxygen partial pressure corresponds to an oxygen concentration in solution significantly below the concentrations of radioelements (greater than 1×10^{-15} mol/L) detected in these experiments. Thus, the dissolved oxygen would not be expected to influence the behavior of the radioelements.

Oxygen is removed from solution not to control the oxidation potential of the solution. Rather, the removal of oxygen allows other redox-sensitive elements in the materials and solution, most notably iron, to react and establish redox states that might exist in a deep repository in the absence of oxygen.

2.4.5 Automated Collection of Data

The equipment used for data acquisition in this work consists of a Digital Equipment Corporation (DEC) PDP 11-23 processor with two RL02 discs for storage of digital information. Operator's consoles are a DEC printer (DEC writer) and DEC videoterminal (DEC VT-105). Analog signals were converted to digital signals using Kinetic Systems Crate Controllers (Kinetic Co. Model 3525-A1T, 16-channel controller for T-type thermocouple signals and Kinetic Co. Model 3512, 16-channel controller for 0- to 5-V pressure transducers).

For each analog experiment, two temperatures (ambient and oven) and three pressures (pump, water stream, and core sleeve pressure) were recorded. Pressures and temperatures in pressure vessels that were used to alter materials for the experiments were also recorded using the computer equipment. Temperature and pressure signals were scanned at 10-minute intervals. If a change of 1% or greater occurred in any temperature (compared to the preceding recorded data point), the system recorded the data and the date and time on disc storage and printed the results for operator monitoring.

2.5 RUNNING OF ANALOG EXPERIMENTS

To perform an analog experiment, the apparatus was first assembled without the basalt, bentonite, or waste glass and tested for oven-temperature stability and accuracy of data recorded by the digital equipment. The basalt chips and bentonite were then introduced to the first and second vessels, and the core holder with the fissured basalt was added after a uniform flow of groundwater solution had been established. (The procedure for preparing bentonite for use in the analog experiments is the same as that for the auxiliary experiments and is described in Sec. 3.2.4.1.) The flow was continued for a period of 30 days to allow the solid components of the system to attain chemical compatibility with the groundwater solution, at which time the radioactive waste glass was introduced into the first vessel.

Groundwater solution flowing in the system was collected at the outlet of the rock core and intermittently at the outlets of the first and second vessels. Flow was continued for 90 to 120 days after introducing radioactive glass, before the experiment was terminated.

To terminate an experiment, components were removed in sequence starting at the exit end of the flow stream, with sufficient intervals lapsing between each removal to allow the collection of large (~100-mL) groundwater samples at the outlet. The tubing that connected components was also removed in this process and inspected for accumulation of radioelements using a shielded detector. The rock core and vessels were disassembled at room temperature, and samples of liquids and solids were recovered for detailed analyses. The existence of bentonite downstream from vessels 1 and 2 was generally noted, and the bentonite was sampled at various locations for detailed analyses. The surface of the rock core was inspected for deposits of bentonite and for the existence of features generated during the experiment (mineral growth, changes in coloration, etc.).

All analog experiments except the third one were conducted without gamma radiation. The third analog experiment was installed in the proximity of four rods containing ^{60}Co to create gamma radiation fields of 1.05×10^5 rad/h in the first two vessels and 2.2×10^4 rad/yr in the holder containing the rock core. The radiation fields were measured using cobalt glass dosimeters. The reservoir containing the groundwater solution, the metering pump, and the recording instrumentation were shielded from radiation.

The apparatus, the location of the experimental station, and the experimental record of pressures and temperatures are listed in Table 2.18 for each of the analog experiments.

Table 2.18. Apparatus, experimental station, and data collection files for the six analog experiments

Analog Experiment Number	Apparatus	Experimental Station[a]	Experimental Data Record[b]
1	Hastelloy, Autoclave Vessels	1	Mon587.Dat 2, 3, 4, 5, and 6
2	Monel, Tube Vessels	2	Mon12.Dat 4, 5, 6, 7, 8, 9, and 10
3	Hastelloy, Tube Vessels	3	Strip Chart
4	Hastelloy, Autoclave Vessels	1	Mon78.Dat 1, 2, and 3
5	Hastelloy, Tube Vessels	2	Mon12.Dat 13 and 14
6	Hastelloy, Autoclave Vessels	1	Mon78.Dat 5, 6, and 7

[a]Experimental Stations 1 and 2 are the left and right vacuum frame hoods, respectively, in Room G-133 of Building 205. Experimental Station 3 is the gamma cell of M-Wing, Building 200.

[b]Mon designations are computer files of recorded pressures and temperatures.

2.6 ANALYTICAL METHODS

2.6.1 Bulk Water Analyses

2.6.1.1 Atomic Emission Spectroscopy

Concentrations of 24 metal ions in simulated groundwater solution were measured by E. A. Huff of the Analytical Chemistry Laboratory, Argonne National Laboratory, using inductively coupled plasma/atomic emission spectroscopy. Table 2.19 lists the elements measured and their detection limits.

2.6.1.2 Ion Chromatography

The concentrations of chloride, sulfate, and fluoride ions were measured by F. L. Williams of the Analytical Chemistry Laboratory, using an updated Dionex Corp., System 14, Ion Chromatograph. Detection limits are 50 µg/L for chloride and fluoride ions and 500 µg/L for sulfate, phosphate, and nitrate ions.

2.6.1.3 Fluorimetry

Concentrations of uranium ion were measured by A. M. Essling of the Analytical Chemistry Laboratory using laser fluorescence spectroscopy. The detection limit for measuring uranium in solution is 10 µg/L for 50-µL-sized samples. For large samples (10 mL), the detection limit is below 0.02 µg/L.

Table 2.19. List of elements in simulated groundwater solution measured by atomic emission spectroscopy

Element	Detection Limit (µg/L)
Al	100
B	30
Ba	10
Be	2
Ca	30
Co	20
Cr	10
Cu	5
Fe	10
K	500
Cd	10
Tl	50
Mg	5
Mn	2
Mo	30
Na	100
Ni	10
Pb	100
Si	500
Sn	100
Sr	2
V	10
Zn	5
Zr	10

2.6.1.4 Titrations

Solutions from analog and auxiliary experiments were titrated with a Metrohm Titroprocessor E636 to determine the total alkalinity and the $[CO_3^{2-}]$* and $[HCO_3^-]$ of each sample. The sample size titrated varied from 50 µL to 10 mL and the total burette volumes were either 1 or 5 mL. The titroprocessor is capable of accurately delivering 1/100,000 of the burette volume in a single pulse. Either one or two inflection points were measured for each titration, depending on the initial pH of the solution. The inflection point that was measured for all solutions occurred at a pH of ∿4.6; the other inflection point was at a pH of ∿7.9.

* A chemical species symbol in brackets refers to the concentration of that species.

The equilibria that control the pH of a typical groundwater are

$$H_2O \rightleftharpoons H^+ + OH^- \qquad K_1 = 10^{-14} \tag{2.1}$$

$$HCO_3^- \rightleftharpoons H^+ + CO_3^{2-} \qquad K_2 = 10^{-10.33} \tag{2.2}$$

$$H_2CO_3 \rightleftharpoons H^+ + HCO_3^- \qquad K_3 = 10^{-6.34} \tag{2.3}$$

$$H_4SiO_4 \rightleftharpoons H^+ + H_3SiO_4^- \qquad K_4 = 10^{-9.8} \tag{2.4}$$

$$H_3BO_3 \rightleftharpoons H^+ + H_2BO_3^- \qquad K_5 = 10^{-9.24} \tag{2.5}$$

$$[C]_{Total} = [H_2CO_3] + [HCO_3^-] + [CO_3^{2-}] \tag{2.6}$$

$$[Si]_{Total} = [H_4SiO_4] + [H_3SiO_4^-] \tag{2.7}$$

$$[B]_{Total} = [H_3BO_3] + [H_2BO_3^-] \tag{2.8}$$

where $[C]_{Total}$, $[Si]_{Total}$, and $[B]_{Total}$ are the total concentrations of carbon, silicon, and boron in the groundwater. All equilibrium constants are for 22°C and were obtained from two sources (Phillips 1982; Skoog 1963). The total alkalinity in groundwater in the pH range 4 to 12 is assumed equal to:

$$[HCO_3^-] + 2[CO_3^{2-}] + [H_3SiO_4^-] + [H_2BO_3^-] + [OH^-] \tag{2.9}$$

Table 2.20 shows how the concentrations of these bases vary with pH for the groundwater composition shown in Table 2.14. The concentrations of these species were calculated by standard iterative techniques based on solving the equilibria of Eqs. 2.1 to 2.8. The predicted titration curve for an analog groundwater solution is given in Fig. 2.16.

At a pH value of 10, the pH of simulated groundwater, all the species in Table 2.20 contribute to the basicity of the solution. The carbonate/bicarbonate ratio cannot, therefore, be calculated by the simple relationship that ignores the other bases. A calculated titration curve for groundwater predicts that the first inflection point occurs at a pH of 7.9 and the second at a pH of 4.5. Although the inflection points are nearly the same for the standard CO_3^{2-} - HCO_3^- titration, at the high pH values, this solution is highly buffered by other groundwater ions in solution, e.g., $H_2BO_3^-$ and $H_3SiO_4^-$. Because the first inflection point occurs when essentially all $H_2BO_3^-$, $H_3SiO_4^-$, CO_3^{2-}, and OH^- are neutralized (refer to Table 2.20), the difference in meq/L between this inflection point and the second inflection point is the total carbonate + bicarbonate concentration in mol/L in the groundwater. The $[CO_3^{2-}]/[HCO_3^-]$, $[H_3SiO_4^-]/[H_4SiO_4]$, $[H_2BO_3^-]/[H_3BO_4]$, $[OH^-]/[H_2O]$ ratios at the initial pH of the groundwater solution can be determined using Table 2.20. The total silicon and boron concentrations were measured by spectroscopy using inductively coupled plasma emission and were used to compare the predicted and actual concentration of base in solution.

2.6.1.5 Specific-Ion Electrodes

Three ion selective electrodes were used individually to measure the concentrations of sodium, calcium, and potassium ions in the majority of

Table 2.20. Concentrations of all significant basic species in simulated groundwater as a function of solution pH

	Concentration (meq/L)					
pH	CO_3^{2-}	HCO_3^-	$H_2BO_3^-$	$H_3SiO_4^-$	OH^-	Total Base
Added to Groundwater	-	2.54	0.13	1.82	-	4.49
12	2.48	0.03	0.13	1.81	10	14.45
11.75	2.44	0.05	0.13	1.80	5.62	10.04
11.5	2.38	0.08	0.13	1.78	3.16	7.53
11.25	2.28	0.13	0.13	1.76	1.78	6.08
11.0	2.10	0.22	0.13	1.72	1.00	5.17
10.75	1.84	0.35	0.13	1.64	0.56	4.52
10.5	1.52	0.51	0.12	1.52	0.32	3.99
10.25	1.16	0.69	0.12	1.34	0.18	3.49
10.0	0.80	0.87	0.11	1.12	0.10	3.00
9.75	0.52	1.01	0.10	0.85	0.06	2.58
9.5	0.32	1.11	0.08	0.61	0.03	2.15
9.25	0.20	1.17	0.06	0.39	0.02	1.84
9.0	0.12	1.21	0.05	0.25	0.01	1.64
8.75	0.06	1.24	0.03	0.15	0.01	1.49
8.5	0.04	1.24	0.02	0.09	-	1.39
8.25	0.03	1.24	0.01	0.06	-	1.34
8.0	0.02	1.23	0.01	0.03	-	1.29
7.75	-	1.22	0.01	0.02	-	1.25
7.5	-	1.19	-	0.01	-	1.20
7.25	-	1.13	-	-	-	1.13
7.0	-	1.04	-	-	-	1.04
6.75	-	0.91	-	-	-	0.91
6.5	-	0.72	-	-	-	0.72
6.25	-	0.57	-	-	-	0.57
6.0	-	0.40	-	-	-	0.40
5.75	-	0.26	-	-	-	0.26
5.5	-	0.17	-	-	-	0.17
5.25	-	0.06	-	-	-	0.06
5.0	-	0.02	-	-	-	0.02
4.5	-	0.01	-	-	-	0.01
4.0	-	0.01	-	-	-	0.01
3.5	-	-	-	-	-	0
3.0	-	-	-	-	-	0

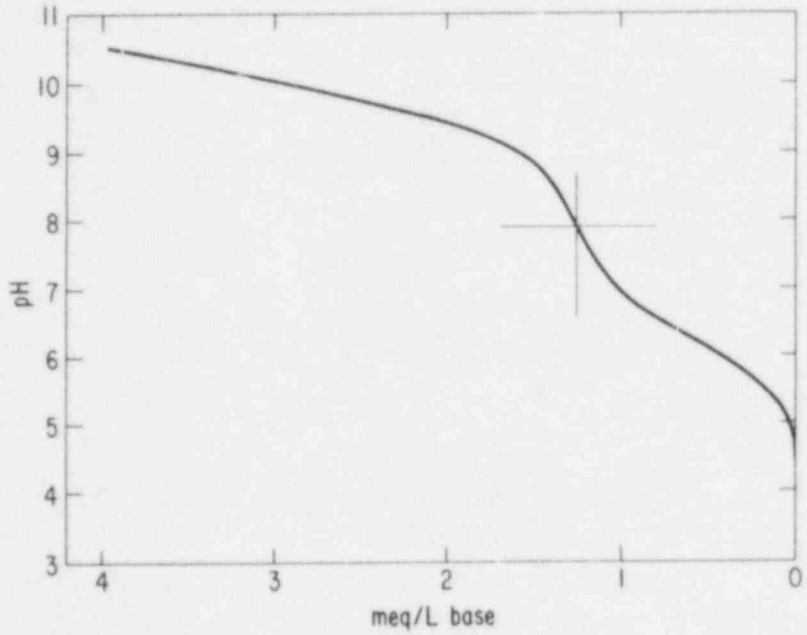

Fig. 2.16. Titration curve of the groundwater solution from pH = 10.5 to pH = 3

auxiliary experiments. These electrodes were calibrated using a series of standard solutions suited for use with the groundwater solutions to be measured.

The sodium selective electrode is an Orion Model 96-11 combination electrode. It was calibrated using a series of solutions produced by (1) preparing simulated groundwater in which most of the sodium salts were substituted by equimolar amounts of potassium salts (Table 2.21), and (2) mixing this low sodium groundwater with normal groundwater in various proportions (Table 2.22). By this technique, a set of standards was prepared with the same ionic strength and a range of $[Na^+]$ from 117 to 326 mg/L.

To measure potassium ion concentrations, an Orion Model 93-19 potassium ion selective electrode was used in conjunction with an Orion Model 90-01 single junction reference electrode. Calibration of these electrodes was performed with the same solutions used to calibrate the sodium ion selective electrode (Table 2.22). The range of $[K^+]$ in the standards varied from 1.9 to 419 mg/L.

An Orion Model 93-20 calcium ion selective electrode, in conjunction with the Orion Model 90-01 single junction reference electrode, was used to measure $[Ca^{2+}]$ in the auxiliary experiments. Standard solutions for this electrode pair were prepared by diluting small volumes of a standard 1.00M $CaCl_2$ solution by 500 mL of analog groundwater. The dilution factors are shown in Table 2.23.

Table 2.21. Recipe for low sodium groundwater

Original Compound	Substituted Compound	Amount Used (g/20 L)
NaCl	KCl	4.481
Na_2SO_4	K_2SO_4	3.641
$Na_2B_4O_7 \cdot 10H_2O$	$K_2B_4O_7 \cdot 8H_2O$	0.1661
NaF	KF	2.2662
Na_2CO_3	K_2CO_3	5.0723
$NaHCO_3$	—	0
$Na_2SiO_3 \cdot 9H_2O$	$Na_2SiO_3 \cdot 9H_2O$	11.46[a]
$CaSO_4 \cdot 2H_2O$	$CaSO_4 \cdot 2H_2O$	0.111[a]
K_2SO_4	K_2SO_4	0.085[a]
$MgSO_4 \cdot 7H_2O$	$MgSO_4 \cdot 7H_2O$	0.0036[a]

[a]This is the same amount of the chemical used to prepare the regular groundwater solution.

Table 2.22. Standard solutions for sodium and potassium ion analyses

Ratio	Amount of Original Groundwater (mL)	Amount of Low Sodium Groundwater (mL)	$[Na^+]$ (ppm)	$[K^+]$ (ppm)
10:0	500	0	326	1.9
9:1	450	50	305	43.6
8:2	400	100	284	85.3
7:3	350	150	263	127
6:4	300	200	242	168
5:5	250	250	222	210
4:6	200	300	201	252
3:7	150	350	180	294
2:8	100	400	159	336
1:9	50	450	138	377
0:10	0	500	117	419

When these electrodes were new, they were very easily calibrated and gave slopes (millivolts of signal per decade of chemical species concentration) very close to theoretical values. When problems such as unresponsiveness or sluggishness began to develop, they were rejuvenated according to the manufacturer's directions. Eventually rejuvenation became ineffective, and they needed to be replaced after about three months of use.

Table 2.23. Standard solutions for calcium ion analysis

Amount of 1M Solution Added to 500 mL of Groundwater (μL)	$[Ca^{2+}]$ (mg/L)
0	1.3
125	2.3
250	3.3
500	5.3
1,125	11.3
2,375	21.3
3,625	31.4
6,125	51.3
12,375	101.3

2.6.2 Radioelement Analyses of Solutions

2.6.2.1 Actinide Analyses

Because measurements showed that the levels of ^{241}Am in all analog solutions were low (<0.02 dpm/mL) and, consequently, of little interest, a procedure was developed for separating and detecting only ^{237}Np and ^{239}Pu by alpha-pulse detection (Bowers 1983).

To determine the concentrations of ^{237}Np and ^{239}Pu in the groundwater, it is necessary to separate these elements from other dissolved solids in solution because, upon evaporation, these solids (~730 mg/L) interfere with determining the alpha disintegration rate using a silicon barrier alpha pulse height detector. The separation procedure is a traditional solvent extraction technique (Burney 1974) using methyl isobutyl ketone (hexone) as the organic solvent. Because, as with many chemical separations, 100% recovery cannot be assumed, it is necessary to spike the solution with a different isotope of the same element to monitor the recovery of the element. The spikes chosen for these analyses were ^{235}Np and ^{236}Pu. The ^{235}Np has a relatively long half-life (396 days) and can be easily detected by its 13.6-keV X-ray. The ^{236}Pu (half-life of 2.8 years) has a high-energy alpha decay of 5.7 MeV, which is easily resolved from the ^{239}Pu (5.1 MeV) and ^{237}Np (4.8 MeV).

The choice of ^{235}Np over the more conventional ^{239}Np as a yield monitor was made because of its availability and relative ease of detection (Ahmad 1983). The ^{239}Np has to be milked from its parent ^{243}Am, and its short half-life (2 days) necessitates quick completion of an entire analysis. (The characteristic gamma-ray decay of the ^{239}Np spike is counted to measure the chemical yield of neptunium.)

Although ^{235}Np spiking eliminates most of the problems associated with ^{239}Np, there is still one precaution that must be addressed in its use. A sufficient amount of the ^{235}Np must be used for good counting statistics and to overshadow the contribution to the ^{235}Np signal by X-rays emitted from the other actinides that may be present; i.e, ^{237}Np with a 13.3-keV X-ray and branching ratio of 59%, ^{236}Pu with a 13.6-keV X-ray and branching ratio of 13%, and ^{234}Pu with a 13.6-keV X-ray and branching ratio of 4.4%. Consequently, care was taken to limit the amount of these interfering isotopes in the analysis. Fortunately, with the high sensitivity and low backgrounds of alpha-pulse counting, it is possible to measure low activities of these isotopes with high precision.

The procedure was as follows: An aliquot (varied from 0.1 to 50 mL, depending on the expected activities of ^{237}Np and ^{239}Pu) was spiked with a known amount of ^{235}Np and ^{236}Pu. Three drops of concentrated HF, three drops of concentrated $HClO_4$, and 2-3 mL of 8M HNO_3 were added. The HF and $HClO_4$ were added to ensure isotopic exchange of the actinides. The sample was evaporated to dryness in a Teflon beaker; after additional 8M HNO_3 redissolved the sample, it was again taken to dryness. The solids were again dissolved in 0.5-0.7 mL of 8M HNO_3 and added to ~6 mL of 2.8M $Al(NO_3)_3$ salting solution containing 0.1 mL of 0.25M $KMnO_4$; the $KMnO_4$ was to ensure that neptunium and plutonium were both in the (VI) oxidation state necessary for extraction. The resultant solution was mixed on a Vortex mixer with 1 mL of hexone for a minimum of three minutes and then centrifuged. The hexone phase was separated from the aqueous phase and a sample was transferred to and dried on a planchet, taking care that none of the aqueous salting solution was on the counting plate. The planchet was then measured for ^{235}Np content (using a high-purity, high-efficiency germanium detector with a beryllium window) and placed on a silicon barrier alpha-pulse detector for determination of ^{237}Np, ^{239}Pu, and ^{236}Pu.

A variation of this procedure was used for some of the samples analyzed in the analog program. In this variation, the sample and spikes were first reduced with HBr, taken to dryness, and oxidized with the $HF-HNO_3-HClO_4$ before extraction with hexone. Also, the extraction step used $NH_4NO_3-KBrO_3$ instead of the $Al(NO_3)_3-KMnO_4$. The data produced from this method were in general agreement with those of the standard method. The range of activities measured varied from background (0.001 dpm/mL) to 90 dpm/mL. The separation yields varied between 20 and 85%, with a mean value of ~50%. There was no identifiable relationship between the percent recovery and the measured activities.

2.6.2.2 Gamma Analyses of Solutions

Because the concentrations of ^{137}Cs, ^{152}Eu, and ^{133}Ba were low in the glass wafers and/or the leach rates of the radionuclide from the glass were low, it was difficult to measure the activity levels of these radionuclides in analog outlet samples. To measure their activities, a large volume (10-34 mL) of an outlet sample was taken to near dryness in a Teflon beaker and the concentrated solution was centered on a stainless steel planchet for subsequent gamma counting on a Ge(Li) detector with a 4000-channel multichannel analyzer. Each sample was counted for $\sim 2.5 \times 10^5$ s.

The samples were placed directly on top of the detector to maximize the counting geometry. The detectors are not calibrated for this condition, so results are not reliable as absolute activity determinations. However, because the second vessel outlet sample and the core outlet sample for each analog experiment were placed on the same detector with nearly the same geometry, the relative activities of each isotope in an experiment are comparable. Also, the ^{237}Np activities for these solutions were previously measured by alpha-counting techniques, which serve as a check of the calibration.

2.6.3 Radionuclide Analysis of Solids

2.6.3.1 Gamma Counting of Tube Rinses and Bentonite Samples

Gamma count data have been acquired from several bentonite samples and various rinse solutions collected during the dismantling of the analog experiments. Bentonite samples from eight locations along the liquid flow path were analyzed for ^{241}Am, ^{237}Np, ^{152}Eu, ^{137}Cs, and ^{133}Ba using the same instrumentation and technique described in the gamma characterization of the waste glass (Sec. 2.3.1.3). Counting time for each sample was about one day. The sample activities were calibrated with a standard source. These analyses were intended to provide a measure of radioactive isotope transport through the system and to provide data on the total quantities of radionuclides present in the system at the completion of an experiment.

Figure 2.17 is a schematic of the analog experimental apparatus, showing the locations where samples were obtained for subsequent gamma analyses. Samples 1 and 4 are bentonite from the metal holders. Samples 2 and 5 are bentonite that overflowed the holders and settled to the bottom of the vessels. Samples 3 and 6 are solids rinsed from the connecting tubing, and samples 7 and 8 are bentonite samples from the inlet and outlet to the core.

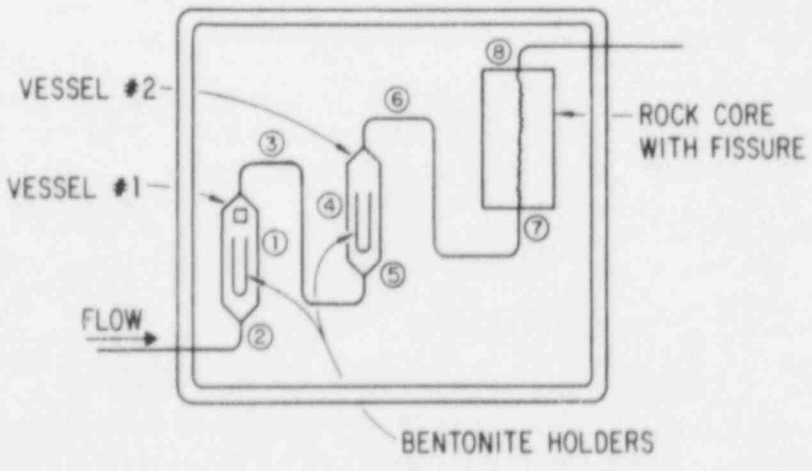

Fig. 2.17. Schematic of experimental apparatus (numbers correspond to the sampling locations described in the text)

2.6.3.2 Basalt Core Profile of ^{237}Np

The final component in the analog flow system is a basalt rock core that had been split axially to provide a fissure through which fluid flows. The simulated groundwater flowing into the rock core contained low concentrations of radioactive materials leached from the glass waste form; most of this activity was deposited on the rock surface. The distribution of radioactive materials retained on the rock surface was measured by counting the gamma activity through an opening of 8 by 58 mm in a 4-mm-thick lead plate using a Ge(Li) detector. The lead plate shielded the detector from low-energy radiation originating from other than the exposed part of the rock's surface. The 86.5-keV gamma ray of ^{237}Np and the 662-keV gamma ray of ^{137}Cs were the only signals detectable from the rock surface; ^{152}Eu, ^{133}Ba, and ^{241}Am were looked for, but their activities were below detectability. The highly irregular surface geometry of the rock faces precludes quantitative data being obtained by this method.

2.6.3.3 Extracting Radioelements from the Core

Although gamma counting of the rock core surface can give a relative profile of ^{237}Np activity, it cannot be used as a quantitative measurement. To quantitate the amount of neptunium and plutonium sorbed on the rock core, it was necessary to extract these elements chemically from the core. The chemical solution that was used was one developed for removing plutonium from sediments--sodium citrate/sodium dithionate solution (Edgington 1976) followed by extraction with a strong acid solution. The results of this analysis were coupled with results of ^{237}Np groundwater analyses to check the mass balance of the first analog experiment.

A solution consisting of 0.3M sodium citrate-0.1M sodium dithionate was used to extract radioelements from the face of one of the half cores. The split core was placed fissured face down in a trough-like Pyrex vessel; the chemical solution was added to ~0.5 cm above the face, and heated at ~70°C for two hours. The solution with extracted radioelements was transferred to a 200-mL volumetric flask, and an aliquot was analyzed for ^{237}Np and ^{239}Pu using the same procedure as described in Section 2.6.2.1.

To determine the extent that these isotopes were extracted, a portion of the core was counted on a Ge(Li) detector for the characteristic 86.5-keV gamma decay of ^{237}Np and compared with the activity level of the other half core. A second extraction was performed using 1M HCl-0.5M HNO_3 under the same conditions as the first extraction. The core was recounted on the Ge(Li) detector to indicate the amount of ^{237}Np removed from the core by each extraction.

2.6.3.4 Conversion Units for Radioelement Concentrations

Amounts of radioactive isotopes were measured in units of disintegrations per minute (dpm) by relating count rates measured on gamma- or alpha-particle detectors to count rates obtained from known standards. The amounts of radioactive isotopes were converted in some instances to concentrations in units of dpm/mL by dividing the amounts of radioactive isotopes by the volume of the solutions from which they were derived.

Concentrations of the elements neptunium, plutonium, and americium in units of dpm/mL can be converted to units of mol/L using the radiodecay half-lives given in Table 2.3 (Sec. 2.3.1.2) and Avagadro's number, 6.022×10^{23} atoms per mole. The conversion factors from units of dpm/L to units of mol/L for ^{237}Np, ^{239}Pu, and ^{241}Am are 2.69×10^{-9}, 3.04×10^{-11}, and 5.44×10^{-13}, respectively. Units of mol/L can be converted to units of mg/L using the atomic weight of the isotope.

For the radioelements cesium, strontium, barium, cerium, and europium, the conversion from units of radioactive decay to units of element concentration requires consideration of the stable isotopes of these elements. These elements originate, primarily, from the radioactive waste glass, so the concentrations of the stable elements in glass given in Table 2.2 of Section 2.3.1.2 can be used together with the radioactive decay half-life of cesium given in Table 2.3 to obtain the conversion factor from dpm/mL to mol/L. For cesium, the conversion factor is 2.28×10^{-9}. These conversion factors are used specifically in this report.

3. EXPERIMENTAL RESULTS

3.1 EXPERIMENTAL CONDITIONS OF THE ANALOG EXPERIMENTS

Pressures and temperatures monitored during the analog experiments with pressure transducers and thermocouples were recorded in computer memory or on strip charts to provide a continuous record of the conditions experienced. Groundwater flow rates were adjusted by setting the metering pumps and were measured by weighing the amount of solution exiting the system during a known period of time.

The pressure used to seal the Teflon sleeve around the rock core remained relatively constant during experiments, being initially 12.4 MPa (1800 psi) and decreasing slowly to 11.0 MPa (~1600 psi) over the four- to five-month duration of the experiments. Ambient air temperature during the experiments varied from 19.3 to 23.3°C (as recorded in computer memory) in work stations 1 and 2. The ambient air temperature in the gamma cell was 25°C rising to ~30°C after the gamma source had been exposed for 10 or more hours. The ranges and average values of flow rate, metering-pump pressure, and oven temperature are given in Table 3.1. The solution flow was maintained in the first two experiments but was erratic due to the increasing restriction to flow, which caused the pump pressure to rise. Plots of flow rate and pressure vs. time for the first experiment are given in previous reports (Steindler 1982e, 1984b). The increase in pressure with time in the experiment was due to bentonite clogging the fissure in the rock core. An analysis of the hydraulic aspects of the clogging and the description of a model that accurately describes the pressure buildup with time is reported elsewhere (Steindler 1984c).

Table 3.1. Experimental conditions recorded for the six analog experiments

Analog Experiment Number	Flow Rate (mL/h)		Range[a] of Metering-Pump Pressure (MPa)	Oven Temperature (°C)	
	Average	Range		Average	Range
1	0.58	0.20 to 0.92	0.04 to 1.06	88.9	88.5 to 89.3
2	0.86	0.72 to 1.20	0.00 to 0.43	90.2	84.6 to 90.6
3	0.60	0.0 to 1.0	0.0 to 0.5	90.0	89 to 120
4	0.47	0.45 to 0.49	0.00 to 0.02	90.1	89.3 to 90.8
5	0.48	0.46 to 0.50	0.00 to 0.02	90.1	89.3 to 90.8
6	0.48	0.46 to 0.50	0.00 to 0.03	89.9	89.3 to 90.3

[a]The lowest pressures existed at the start of the experiments, the highest pressures at the end of the experiments. The entire pressure drop occurred across the rock core holder as evidenced by the pressure dropping to zero when removing each rock core holder from the system.

For a given flow setting of the pump, the flow rates decreased with increasing pump pressure; so, the pump flow setting had to occasionally be adjusted upward as the back pressure increased. In experiment 3, failure of the pump seals, then of the pump motor, produced the large range of flow rates reported for this experiment. When the third experiment was nearly completed, the insulation in the oven failed in the radiation field, which caused the oven temperature to rise, requiring the experiment to be halted for repair of the oven. These variations are reflected in the data of Table 3.1.

Experiments 4, 5, and 6 used metering pumps that were accurately controlled near the desired ∿0.5-mL/h rate. Furthermore, the pressure required to pump the solution did not increase substantially, and no additional adjustments of flow were required.

3.2 COMPOSITIONAL CHANGES IN SOLUTION

As groundwater solution passed through the analog experiments, changes in its composition occurred. These changes were much more substantial in experiments that used unaltered repository components than in those that used hydrothermally altered materials. Furthermore, interactions with unaltered basalt during an experiment had a much more profound effect on solution composition than did those with bentonite or the waste form. Groundwater composition data from the analog experiments are given in this section along with results of auxiliary experiments that were run to elucidate them.

3.2.1 Effluents of Analog Experiments 1, 2, and 3, Unaltered Repository Components

The data in Fig. 3.1 for the first three analog experiments (which used unaltered waste form, bentonite, and basalt cores) show that the groundwater exiting the basalt fissure reaches a steady-state composition for $[Na^+]$ and $[Ca^{2+}]$ soon after the start of the experiment. (The term "cold" in the figure legend refers to the conditioning period of the experiments, before the waste form was put into the first vessel. The term "hot" refers to the part of the experiment where the waste form was in place.) The steady-state $[Na^+]$ in the groundwater eluant at the core's exit is ∿2/3 of its original groundwater concentration. The $[Ca^{2+}]$ is higher by almost an order of magnitude at the steady-state condition reached inside the core than at its original concentration.

An auxiliary experiment, performed at 90°C with groundwater and a column of crushed basalt chips and with a ratio of basalt surface area to groundwater volume equivalent to that of the analog basalt fissure (2×10^2 cm^{-1}), has elucidated this phenomenon. Data from this experiment, which are presented in Fig. 3.2, show that the $[Na^+]$ of the groundwater does not decrease gradually from its initial value of 13.7 meq/L to its steady-state value of 13.0 meq/L; rather, it initially falls to a much lower concentration, ∿2 meq/L. Gradually, over an "equilibration" period, the $[Na^+]$ rises to its steady-state value. The analog experimental data, Fig. 3.1, show a steady-state $[Na^+]$ of only 9.6 meq/L. This difference may be a function of slightly different ratios of surface area to groundwater volume for the two experiments. The $[Ca^{2+}]$ shows an opposite, yet similar, behavior. The initial $[Ca^{2+}]$ in the groundwater of 0.08 meq/L increases dramatically to 15 meq/L before gradually dropping to a steady-state value of 0.4 meq/L.

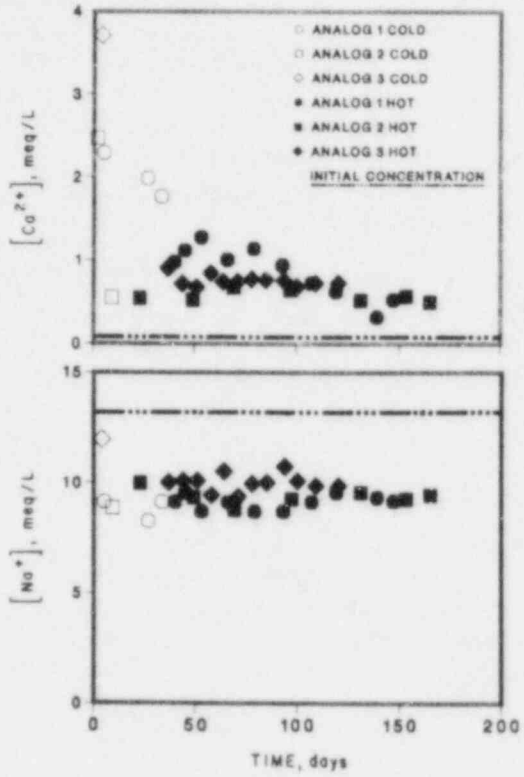

Fig. 3.1.

Concentrations of sodium and calcium ions in the first three analog experiments

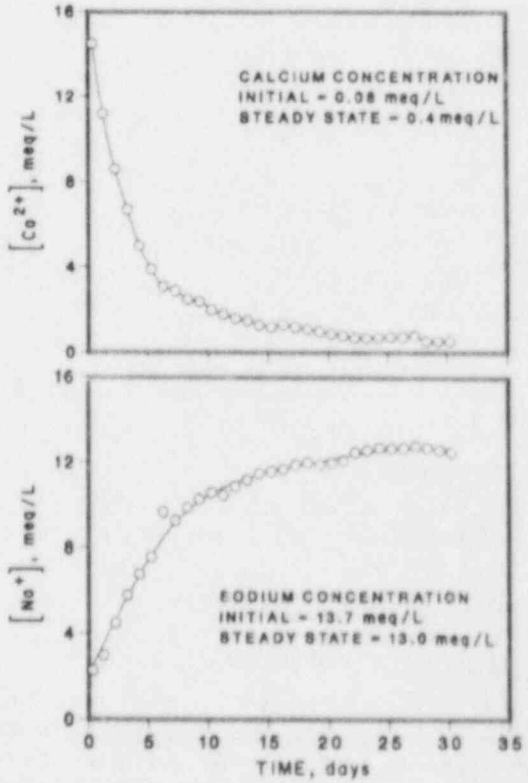

Fig. 3.2.

Concentrations of sodium and calcium ions in an auxiliary experiment showing, in detail, the approach to steady state at the start of the experiment

Tables 3.2, 3.3, and 3.4 show inductively coupled plasma emission, ion chromatography, and uranium concentration data for outlet groundwaters from the first three analog experiments. The data for all three analog experiments show the same trends. In general, alkaline-earth elements show the same behavior as does calcium; an initial very high concentration gradually falls to a steady-state concentration much higher than that of the initial groundwater. Results of auxiliary experiments, discussed in Section 3.2.3, show that the potassium ion also follows the trend of the calcium ion. The variation in anion concentrations is small in comparison to that of cationic species.

Table 3.5 shows the major cationic and anionic constituents in the first analog experiment groundwater in (1) its initial condition, (2) its condition at steady-state on exiting the second vessel, and (3) its condition at steady-state on exiting the unaltered basalt fissure. Quite apparent from these data is the small change in groundwater composition caused by interaction of the groundwater with the bentonite and waste form* compared to that caused by interaction with unaltered basalt. The major changes in the groundwater after it passed through the two bentonite-containing vessels were slightly lower pH and $[Na^+]$. (Lower $[H_3SiO_4^-]$, $[H_2BO_3^-]$, and $[CO_3^{2-}]$ are all attributable to the lower pH value.) Passage of the groundwater through the basalt fissure greatly modified its cationic content and its pH. Again, there was no perceptible change in the total $[SO_4^{2-}]$, $[F^-]$, $[Cl^-]$, [Si], or [B]. The charge balance is accomplished by the decrease in pH (10 to 8) that occurs in the rock fissure. This decrease in pH decreased the negative ions in solution by neutralizing much of the $H_3SiO_4^-$, $H_2BO_3^-$, and CO_3^{2-} in the groundwater. The total $[HCO_3^-]$ plus $[CO_3^{2-}]$ also decreased by ~40% by passage through the rock core.

3.2.2 Effluents of Analog Experiments 4, 5, and 6, Hydrothermally Altered Repository Components

Analog experiments 4, 5, and 6 were all run using hydrothermally altered basalt core and bentonite. There were, however, differences in the laboratory alteration procedures for each of these experiments (Sec. 2.3.5.1). Briefly, the bentonite and rock cores for analog experiments 4 and 5 were treated with simulated groundwater at 320°C for 30 and 60 days, respectively; no provisions were made for eliminating air from the reactor before it was sealed and heated. The bentonite and rock core used in experiment 6 were hydrothermally altered for 27 days, as were the others, but argon was used in this case to purge the vessel for two days before startup. The glass waste forms in experiments 4 and 5 were treated by water vapor at 340°C for 14 days to simulate aging in a repository by steam. The glass waste form in experiment 6 was altered only by leaching. (It was the same wafer that was used in analog experiment 1.)

*The effects on groundwater compositional changes due to leaching of the waste form are discussed in Section 3.4, in which the radioelement migration in analog experiments is described.

Table 3.2. Major constituent concentrations of groundwater samples that exited analog experiment 1

Sampling Period	Collection Time (days)	Chemical Constituent[a] (mg/L)									
		B	Ca	Mg	Na	Si	Sr[b]	F^-	Cl^-	SO_4^{2-}	U[b]
Original Groundwater:		1.30	1.5	<0.02	316	53.0	<2	35	165	110	0.04
Conditioning	-38 - -28	1.37	45.9	14.4	210	63.5	220	15	175	140	0.16
Conditioning	-14 - -7	1.43	39.9	12.3	190	51.2	170	20	165	125	0.12
Conditioning	-7 - 0	1.42	35.6	7.2	210	49.3	130	25	165	125	0.13
Radioactive	1 - 3	1.50	19.7	5.0	210	47.4	110	ND[c]	ND	ND	ND
Radioactive	6 - 9	1.58	22.4	3.1	220	51.7	100	ND	ND	ND	ND
Radioactive	13 - 17	1.53	25.7	6.5	200	55.7	120	20	165	115	2.7
Radioactive	27 - 29	1.46	20.3	2.8	210	47.8	90	ND	ND	ND	ND
Radioactive	37 - 45	1.51	22.8	5.6	200	51.2	110	ND	ND	ND	ND
Radioactive	52 - 59	1.46	18.8	5.4	200	54.8	100	25	165	110	6.1
Radioactive	66 - 73	1.46	14.7	4.7	210	49.2	80	ND	ND	ND	ND
Radioactive	78 - 85	1.38	12.7	2.4	220	49.6	60	30	160	105	6.7
Radioactive	98 - 105	1.38	6.4	0.5	215	50.9	44	30	160	115	ND
Radioactive	105 - 114	1.38	10.6	0.7	211	54.0	48	ND	ND	ND	ND
Radioactive	114 - 120	ND	ND	ND	ND	ND	ND	30	165	115	ND

[a] Total $[CO_3^{2-} + HCO_3^-]$ was 1.54 mmol/L in the original groundwater and was a nearly constant 1.15 ± 0.05 mmol/L for outlet samples taken during the experiment.

[b] Reported in µg/L.

[c] No data collected.

Table 3.3. Major constituent concentrations of groundwater samples that exited analog experiment 2

Sampling Period	Sampling Location	Collection Time (days)	Chemical Constituent (mg/L)										
			B	Ca	K	Mg	Na	Si	Sr[a]	F^-	Cl^-	SO_4^{2-}	U[a]
Original Groundwater:			1.31	1.0	ND[b]	<0.1	307	48	<5	40	200	125	ND
Conditioning	Outlet	-21 - -17	1.31	11.2	ND	2.62	204	51	78	21	170	128	0.05
Radioactive	Outlet	0 - 5	1.49	11.0	ND	2.42	230	63	45	ND	ND	ND	2.25
Radioactive	Outlet	28 - 34	1.33	10.6	ND	0.47	215	47	43	31	170	118	8.7
Radioactive	Outlet	49 - 54	1.35	13.9	ND	1.60	202	45	55	ND	ND	ND	10.9
Radioactive	Outlet	77 - 82	1.37	13.1	ND	1.49	213	46	53	30	190	118	8.76
Radioactive	Outlet	109 - 114	1.34	10.4	ND	0.44	220	47	41	ND	ND	ND	14.1
Radioactive	Outlet	132 - 138	1.33	11.5	ND	1.17	213	46	48	33	172	118	12.5
Radioactive	Outlet	144 - 150	1.33	10.0	ND	0.73	217	46	40	33	168	117	11.1
Radioactive	2nd Vessel	150 - 160	1.37	0.9	2.7	<10	282	58	19	35	164	106	27.3
Radioactive	1st Vessel	160 - 170	1.37	0.9	2.5	<10	281	58	18	34	154	106	26.9

[a]Reported in µg/L.

[b]No data collected.

Table 3.4. Major constituent concentrations of groundwater samples that exited analog experiment 3

Sampling Period	Sampling Location	Collection Time (days)	Chemical Constituent (mg/L)										
			B	Ca	K	Mg	Na	Si	Sr[a]	F^-	Cl^-	SO_4^{2-}	U[a]
Original Groundwater:			1.31	1.05	ND[b]	<0.1	307	48	<5	40	200	125	ND
Conditioning	2nd Vessel[c]	-33 - -32	2.03	4.6	ND	0.3	291	38	59	50	275	185	ND
Conditioning	2nd Vessel	-32 - -31	2.15	3.7	ND	0.7	275	44	64	105	205	130	ND
Conditioning	Outlet	-25 - -19	1.55	74.2	ND	24.2	156	56	240	20	210	160	ND
Conditioning	Outlet	-19 - -12	1.68	50.8	ND	15.9	191	55	180	35	225	150	ND
Radioactive	Outlet	0 - 8	1.61	18.3	ND	3.50	230	51	66	35	199	123	8.0
Radioactive	Outlet	8 - 14	1.57	14.4	ND	2.33	232	52	56	34	197	122	8.6
Radioactive	Outlet	14 - 22	1.54	13.6	ND	2.66	232	53	54	34	196	123	6.5
Radioactive	Outlet	22 - 28	1.53	17.1	ND	3.75	217	51	66	30	192	122	3.3
Radioactive	Outlet	28 - 35	1.63	15.1	ND	2.89	242	54	60	35	206	125	3.5
Radioactive	Outlet	35 - 42	1.55	15.0	ND	2.99	216	51	61	33	194	122	2.2
Radioactive	Outlet	42 - 49	1.51	15.7	ND	2.69	229	52	65	33	197	123	1.9
Radioactive	Outlet	49 - 56	1.66	15.5	ND	2.58	230	51	64	34	198	123	1.5
Radioactive	Outlet	56 - 64	1.77	15.2	ND	2.40	247	54	63	35	206	130	1.6
Radioactive	Outlet	64 - 71	1.53	13.8	ND	2.19	232	51	57	35	195	122	1.6
Radioactive	Outlet	71 - 81	1.57	14.7	ND	2.62	227	53	60	34	197	124	0.84
Radioactive	Outlet	81 - 93	1.63	14.7	ND	2.72	227	54	60	31	196	123	0.70
Radioactive	2nd Vessel	93 - 103	2.11	0.99	2.9	0.85	323	54	28	ND	ND	ND	7.5

[a] Reported in µg/L.

[b] No data collected.

[c] Gamma field not yet on.

Table 3.5. Major constituent concentrations of analog experiment 1 groundwater solution, unaltered basalt[a] (meq/L)

Solution	pH	Na^+	Ca^{2+}	Mg^{2+}	Sum of Cations
Initial Groundwater	9.9	13.7	0.075	nil	13.8
2nd Vessel Outlet (~90 days)	9.6	12.3	0.018	nil	12.3
Core Outlet (~100 days)	7.8	9.6	0.63	0.20	10.4

Cl^-	F^-	SO_4^{2-}	OH^-	$H_3SiO_4^-$	$H_2BO_3^-$	CO_3^{2-}	HCO_3^-	Sum of Anions
4.65	1.84	2.29	0.08	1.10	0.10	0.96	1.33	12.4
4.84	1.82	2.43	0.04	0.67	0.08	0.82	1.05	11.8
4.51	1.58	2.19	nil	0.02	0.01	nil	1.33	9.6

[a]Concentrations of OH^-, $H_3SiO_4^-$, $H_2BO_3^-$, CO_3^{2-}, and HCO_3^- and pH are listed for solutions at 25°C. These concentrations would, of course, change dramatically at 90°C, where $H_2SiO_4^{2-}$ is also an important anionic species.

The data in Tables 3.6 and 3.7, for analog experiments 4 and 5, respectively, imply that much of the material on the surfaces of the altered bentonite and altered basalt is readily soluble in the groundwater and probably precipitated from the solution inside the reactor as it cooled from 320°C to room temperature over several days. This is indicated, for example, by the high [Ca] and $[SO_4^{2-}]$ in the groundwater effluents when the flowing groundwater first contacted both the bentonite (outlet of the second vessel) and the rock core fissure. The initially high [Si] must also be attributed to this surface-dusting phenomenon, and is consistent with the precipitate at the bottom of the pressure vessel being found to be primarily SiO_2.

In a short period of time (~14 days) for both experiments, a steady-state condition was established in which there was little perceptible alteration in the groundwater composition as it passed through the experimental apparatus; only [K] continued to be higher in the effluent of the basalt core than in the original groundwater. This is a far different behavior than was noted previously for the analog experiments that used fresh basalt and bentonite (Sec. 3.2.1).

The same trends noted above for analog experiments 4 and 5 are seen in the limited data from analog experiment 6, Table 3.8.

Table 3.9 shows the charge balance relationships for three solutions of analog experiment 4 that can be used as a comparison to the charge balance of the three solutions of Table 3.5 (analog experiment 1).

Table 3.6. Major constituent concentrations of groundwater samples that exited analog experiment 4

Sampling Period	Sampling Location	Collection Time (days)	Chemical Constituent[a] (mg/L)									
			B	Ca	K	Na	Si	Sr[b]	F^-	Cl^-	SO_4^{2-}	U[b]
Original Groundwater:			1.38	1.0	2	320	72	<5	35	214	115	0.041
Conditioning	2nd Vessel	-25 - -22	1.15	3.7	11	218	47	48	26	146	89	ND[c]
Conditioning	2nd Vessel	-22 - -14	1.62	2.7	9	318	68	27	35	236	122	ND
Conditioning	Outlet	-15 - -7	1.52	6.1	146	387	82	24	36	298	290	ND
Conditioning	Outlet	-7 - -5	1.37	2.2	77	329	79	5	ND	ND	ND	ND
Conditioning	Outlet	-5 - 0	1.38	2.0	74	319	79	<5	ND	ND	ND	ND
Radioactive	Outlet	0 - 9	14.2	2.2	89	354	104	6	38	228	168	<10
Radioactive	Outlet	14 - 19	4.05	1.9	84	328	97	<5	ND	ND	ND	<10
Radioactive	Outlet	40 - 47	2.19	1.6	79	317	86	<5	36	218	144	398
Radioactive	1st Vessel	70 - 71	ND	ND	ND	ND	ND	ND	ND	ND	ND	556
Radioactive	Outlet	78 - 88	1.73	1.2	66	307	79	<5	ND	ND	ND	387
Radioactive	Outlet	88 - 98	1.60	1.2	55	314	70	<5	35	205	131	ND
Radioactive	Outlet	98 - 106	1.66	1.1	63	302	78	<5	ND	ND	ND	323
Radioactive	2nd Vessel	113 - 123	1.72	0.9	8	339	88	15	39	190	77	358
Radioactive	1st Vessel	123 - 133	1.74	0.6	4	326	85	8	ND	ND	ND	319

[a] Magnesium concentrations were below the detectability limit for the entire series of samples.

[b] Reported in µg/L.

[c] No data collected.

Table 3.7. Major constituent concentrations of groundwater samples that exited analog experiment 5

Sampling Period	Sampling Location	Collection Time (days)	Chemical Constituent[a] (mg/L)									
			B	Ca	K	Na	Si	Sr[b]	F^-	Cl^-	SO_4^{2-}	U[b]
Original Groundwater:			1.38	1.0	2	320	72	<5	35	214	115	0.041
Conditioning	2nd Vessel	-36 - -35	1.58	8.35	9.5	295	50	84	32	208	131	ND[c]
Conditioning	2nd Vessel	-35 - -23	1.36	3.30	10.1	301	66	16	34	208	109	ND
Conditioning	2nd Vessel	-23 - -15	1.37	1.76	6.7	321	66	7	33	206	107	ND
Conditioning	2nd Vessel	-15 - -12	1.37	1.49	5.6	331	65	6	33	209	107	ND
Conditioning	Outlet	-12 - -5	1.51	8.48	185	331	60	32	33	272	322	ND
Conditioning	Outlet	-5 - 0	1.40	1.74	123	260	59	3	35	219	173	ND
Radioactive	Outlet	0 - 6	16.8	1.91	127	323	90	4	34	216	157	<10
Radioactive	1st Vessel	6 - 7	ND	ND	ND	ND	ND	ND	ND	ND	ND	<10
Radioactive	Outlet	7 - 16	8.00	1.57	113	306	88	2	33	214	147	<10
Radioactive	Outlet	16 - 26	ND	ND	ND	ND	ND	ND	ND	ND	ND	700
Radioactive	Outlet	26 - 36	ND	ND	ND	ND	ND	ND	ND	ND	ND	825
Radioactive	Outlet	36 - 44	ND	ND	ND	ND	ND	ND	ND	ND	ND	880
Radioactive	Outlet	44 - 47	ND	ND	ND	ND	ND	ND	ND	ND	ND	760
Radioactive	1st Vessel	47 - 49	ND	ND	ND	ND	ND	ND	ND	ND	ND	710
Radioactive	Outlet	49 - 58	1.87	1.25	87	298	65	<2	39	215	140	650
Radioactive	Outlet	58 - 68	ND	ND	ND	ND	ND	ND	ND	ND	ND	600
Radioactive	Outlet	68 - 77	ND	ND	ND	ND	ND	ND	ND	ND	ND	475
Radioactive	Outlet	77 - 87	ND	ND	ND	ND	ND	ND	ND	ND	ND	460
Radioactive	Outlet	87 - 98	ND	ND	ND	ND	ND	ND	ND	ND	ND	420
Radioactive	Outlet	98 - 108	1.62	1.13	76	302	64	<2	48	215	131	320
Radioactive	2nd Vessel	108 - 118	1.56	1.20	5.0	350	67	9	50	214	108	310
Radioactive	1st Vessel	118 - 126	ND	ND	ND	ND	ND	ND	ND	ND	ND	310

[a] Magnesium concentrations were below the detectability limit for the entire series of samples.

[b] Reported in µg/L.

[c] No data collected.

Table 3.8. Major constituent concentrations of groundwater samples that exited analog experiment 6

Sampling Period	Sampling Location	Collection Time (days)	Chemical Constituent[a] (mg/L)									
			B	Ca	K	Na	Si	Sr[b]	F^-	Cl^-	SO_4^{2-}	U[b]
Original Groundwater:			1.95	2.09	2.6	360	83	<5	38	218	109	ND[c]
Radioactive	Outlet	80 - 86	1.90	0.89	64	330	96	<5	28	175	103	5.2
Radioactive	2nd Vessel	86 - 92	1.92	1.27	3.8	356	99	14	39	218	109	11

[a] Magnesium concentrations were below the detectability limit for the entire series of samples.

[b] Reported in µg/L.

[c] No data collected.

Table 3.9. Major constituent concentrations of analog experiment 4 groundwater solution, altered basalt[a] (meq/L)

Solution	pH	Na^+	Ca^{2+}	K^+	Sum of Cations[b]
Initial Groundwater	9.9	13.7	0.060	0.05	13.8
2nd Vessel Outlet (∿10 days)	9.8	14.7	0.045	0.2	14.9
Core Outlet (∿90 days)	9.5	13.6	0.061	1.4	15.0

Cl^-	F^-	SO_4^{2-}	OH^-	$H_3SiO_4^-$	$H_2BO_3^-$	CO_3^{2-}	HCO_3^-	Sum of Anions
6.0	1.9	2.4	0.10	1.56	0.11	0.86	0.82	13.8
5.4	2.1	1.6	0.07	2.6	0.13	1.36	1.57	14.6
5.8	1.9	2.7	0.04	0.80	0.08	0.52	2.00	13.9[c]

[a] Concentrations of OH^-, $H_3SiO_4^-$, $H_2BO_3^-$, CO_3^{2-}, and HCO_3^- and pH are listed for solutions at 25°C. These concentrations would, of course, change dramatically at 90°C, where $H_2SiO_4^{2-}$ is also an important anionic species.

[b] Concentration of Mg^{2+} is nil in these solutions.

[c] This low value could be increased significantly by a small increase in pH.

A comparison of the first and third data rows of Table 3.9 (concentrations in original groundwater solution vs. those in solution exiting the rock core after 90 days) shows only limited compositional changes in the two solutions. The steady-state compositions of major groundwater constituents in the exiting groundwater are much closer to those of the original groundwater than are those noted in the fresh-basalt experiments. The major differences that did occur in analog experiment 4 were substantial increases in [K] and the total of $[HCO_3^-]$ plus $[CO_3^{2-}]$. The decreases of $[H_3SiO_4^-]$ and $[H_2BO_3^-]$ are due to partial neutralization at the lower pH of the exiting groundwater.

The differences in the sums of the anionic and the cationic charges in the data presented in Tables 3.5 and 3.9 are within the experimental error of the analytical methods (inductively coupled plasma emission, ion chromatography, and acid/base titration and pH measurement) used to measure the concentrations of these species. The measurement of the initial solution pH is especially critical to $[H_3SiO_4^-]$ and the relative values of $[CO_3^{2-}]$ and $[HCO_3^-]$. The differences in sums of the anionic and the cationic charges are small enough in all analyses to allow modeling of the water with the WATEQ2 model of the solute speciation and solubilization program (Truesdell 1973).

3.2.3 Auxiliary Experiments with Bentonite and Basalt

A series of auxiliary experiments was performed to learn more about the compositional changes that the groundwater underwent as it passed through the analog experimental apparatus. As discussed in previous sections, these changes were much more dramatic for contact with unaltered basalt. Whether altered or unaltered, bentonite had little effect on groundwater composition. Likewise, hydrothermally altered basalt had only a marginal effect on the groundwater.

3.2.3.1 Auxiliary Basalt Experiments

The auxiliary experiments described here were run using a much simpler apparatus than that for analog experiments. These were still flow experiments, but only a single vessel was involved. No waste form or bentonite was placed in the system, only basalt. Instead of a fissured rock core, ground and sized basalt chips were placed in a vessel to approximate the ratio of rock surface area to groundwater volume inside the fissure. Parameters examined by these experiments were ion exchange capacity, rock surface area, initial groundwater composition, and flow rate.

Ion Exchange Capacity of Basalt

Calcium and potassium ions on the rock surface were readily replaced by Na^+ from the groundwater. Early in the experiments, the equivalents of Na^+ lost from solution were exactly made up for by those of Ca^{2+} and K^+ dissolved into solution. As fresh groundwater continued to pass through the basalt-chip column, the loss of Na^+ from the exiting solution continued, but at incrementally lesser amounts. For example, in one experiment with an entering $[Na^+]$ of 315 mg/L, the first sample of exiting solution contained 53 mg/L of Na^+; the fourth sample's $[Na^+]$ was 134 mg/L; the sixteenth sample's $[Na^+]$ was 265 mg/L. The values of $[Ca^{2+}]$ and $[K^+]$ showed the same effect but in the opposite direction. For example, the values of $[Ca^{2+}]$ in those same three samples were 290, 135, and 25 mg/L; the initial groundwater had a $[Ca^{2+}]$ of 1.3 mg/L.

As the uptake of Na^+ by the basalt chips continued, the contribution to the groundwater was no longer made up by dissolution of Ca^{2+} and K^+ from the basalt chips. Instead, the loss of cationic content of the groundwater was balanced by neutralization of anionic bases in the groundwater. As the pH of the groundwater that passed over the previously unaltered basalt chips dropped from 10 to 8, the anionic species in solution (CO_3^{2-}, HCO_3^-, $H_3SiO_4^-$, and $H_2BO_3^-$) picked up hydrogen ion from the rock surfaces.

Typically, after 60 mL of groundwater passed by 64 g (22-cm^2 surface area) of crushed basalt, about 0.9 meq/100 g basalt of Na^+ from solution was replaced by Ca^{2+} and K^+ from the basalt. After 400 mL of groundwater had passed, a total of 2.4 meq/100 g basalt was replaced by 1.4 meq/100 g basalt of Ca^{2+}, 0.2 meq/100 g basalt of K^+, and the remainder by hydrogen ion. After 2000 mL, ~4.5 meq/100 g basalt was replaced by 1.7 meq/100 g basalt of Ca^{2+} and 0.3 meq/100 g basalt of K^+; the remaining 2.5 meq/100 g basalt was replaced by hydrogen ion.

Rock Surface Area

Most of the auxiliary experiments were performed with a 20-cm-long, 1-cm-I.D. column containing <65 g of +18-10 mesh size (i.e., 0.98- to 1.91-mm) basalt chips. The average dimension of these basalt chips was measured under a microscope to be 0.93 mm on a side. Two experiments were performed under different conditions of surface area to test the proportionality of physical (i.e., optically measured) surface area to ionic exchange capacity of the basalt.

In the first experiment, the standard column was packed with finer mesh size basalt chips. These chips passed through a 0.85-mm screen and were stopped by a 0.5-mm screen, and were measured microscopically to have an average dimension of 0.67 mm on a side. The increased surface area of <30% caused an average increase in the ion exchange capacity of the basalt, in terms of meq/100 g basalt, of 50%. Because of the crudeness of the optical surface area determinations, these results agree well with a one-to-one correlation of ion exchange capacity and basalt surface area.

In the second experiment, the column length was reduced by half, thus reducing the surface area of the basalt rock (and its mass) by 50%. The average loss of ion exchange capacity for the shorter column was 50% of that in the first experiment.

Groundwater Composition

Although there was a large change in composition of the groundwater when fresh basalt was used in an analog experiment, there was little to no change in groundwater composition as it passed through a hydrothermally altered basalt core. Basalt chips were altered in the same manner as were these basalt cores, and the passivity of the hydrothermally altered surfaces was studied as a function of groundwater composition.

The effect of altered basalt on the groundwater was confirmed to be minimal in these auxiliary experiments; but, when the composition of the groundwater entering the apparatus was modified considerably, the altered basalt would begin to react. For example, although the pH of both eluants was 9.8, the analog groundwater contained 320 mg/L Na^+, 2 mg/L K^+, and 1 mg/L Ca^{2+} and the modified groundwater contained 680 mg/L Na^+, 8 mg/L K^+, and 4 mg/L Ca^{2+}. After 100 mL of this new, high sodium solution entered the basalt column, the eluate pH dropped to 7.8 and its [Na^+], [K^+], and [Ca^{2+}] were 380, 24, and 2 mg/L, respectively. As more fluid passed through the apparatus, the composition of the eluate trended toward that of the eluant.

The conclusion from this experiment is that basalt surfaces are not activated or passivated by groundwater; rather, they reach a steady-state condition with the groundwater in contact with them. The reaction surface formed by contact with a groundwater is not so much a protective coating as it is an equilibrium region. If that groundwater is modified (say by creating new surfaces and new water channels by building a repository), there will be basalt/groundwater reequilibration, which can affect both rock sorption properties and species concentrations in the groundwater.

Flow Rate

Experiments were run at two well-controlled flow rates, 2.5 and 0.5 mL/h, the volumetric flow rates of the analog experiments. Figure 3.3 presents $[Ca^{2+}]$ in the exiting stream vs. volume of effluent, and shows that the effect of flow rate was minimal for Ca^{2+} ion exchange. However, as shown by Fig. 3.4, Na^{+} behavior is a bit more complex. At low throughput volumes, where ion exchange has been shown to be the major contributor of Na^{+} loss from solution, the two sets of flow rate data look very similar. As the supply of K^{+} and Ca^{2+} from the basalt surface available to exchange for Na^{+} from solution decreases and hydrolysis of surface species leading to exchange of hydrogen ion for Na^{+} becomes the dominant reaction, there appears to be a divergence of the two curves. The apparent longer time to reach steady state for the higher flow rate experiment leads to the conclusion that, although ion exchange, as expected, is a comparably fast reaction, surface hydrolysis is not instantaneous and limits the reaction at the flow rate of 2.5 mL/h.

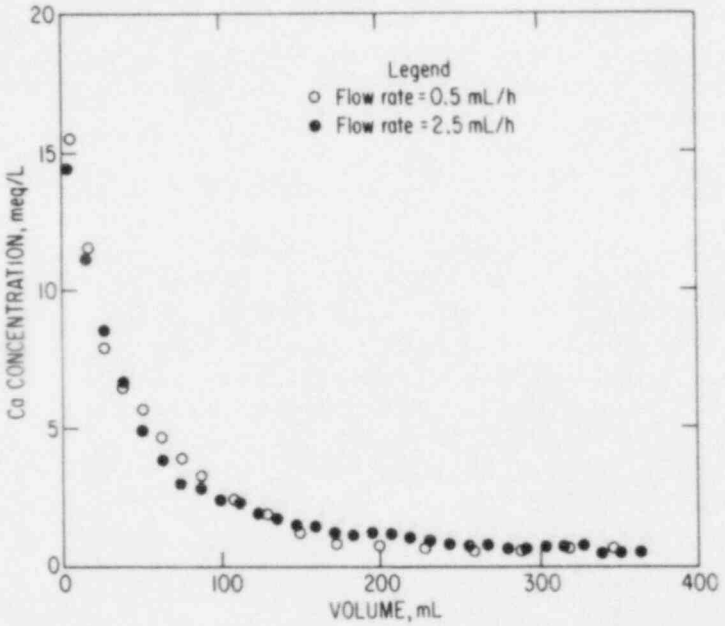

Fig. 3.3. Calcium concentrations in exiting groundwater vs. volume of groundwater for auxiliary experiments 2 and 4

A series of batch extractions were performed to test this hypothesis. In the first two series of experiments, 30 minutes equilibration of fresh basalt chips and groundwater lead to an equilibrium constant of 5×10^{-3}. This dimensionless equilibrium constant is based on treating the system as an ion exchange equilibrium:

$$Na^{+}_{aq} + M\ Rock_{s} \overset{Keq}{\rightleftharpoons} M^{+}_{aq} + Na\ Rock_{s} \qquad (3.1)$$

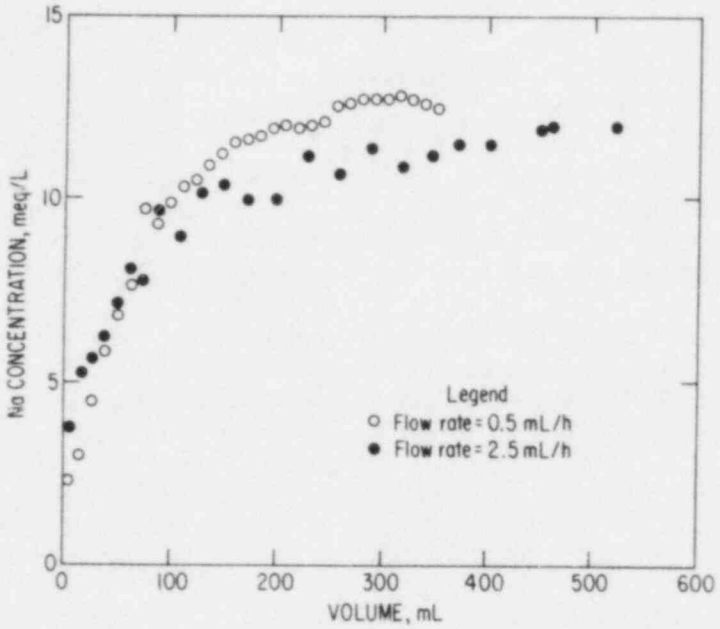

Fig. 3.4. Sodium concentrations in exiting groundwater vs. volume of groundwater for auxiliary experiments 2 and 4

where M $Rock_S$ and Na $Rock_S$ are two species on the rock surface with the same anionic component. The species M^+ in this experiment would be the sum of Ca^{2+}, K^+, and H^+. Mass balance equations for the system are

$$[M^+]_{eq} = [M^+]_o + [Na^+]_o - [Na^+]_{eq} \tag{3.2}$$

$$[\text{Na Rock}] = [\text{Na Rock}]_o + (\text{Groundwater Volume/Surface Area})([Na^+]_o - [Na^+]_{eq})$$

$$[\text{Na Rock}] + [\text{M Rock}] = [\text{Sat}] \tag{3.3}$$

where the o subscript refers to initial concentrations and the eq subscript to concentrations at equilibrium. The [Sat] value was determined by the total exchange of Na^+ in the flow auxiliary experiments. The equilibrium constant for these series of experiments was an average of 23 experiments that were run at two ratios of groundwater volume to basalt surface area. The two sets of data each showed a large degree of variation but, when each set was averaged out, the precision was surprisingly high, 5.8×10^{-3} and 4.5×10^{-3}.

In contrast to these 30-minute contacts, one solution was allowed to equilibrate for 5 days. The equilibrium constant measured in this experiment was almost an order of magnitude higher, 3.2×10^{-2}.

3.2.3.2 Auxiliary Bentonite Experiments

Flow Experiments with Bentonite in One Vessel

The objective of four auxiliary experiments described here was to identify behavior of the bentonite and groundwater exhibited during the analog experiments. Results of these experiments include swelling rates of the backfill, permeability of the vessel to flow, and changes in composition including pH of groundwater after passing through the vessel.

Bentonite was packed in 5.1-cm-long pieces of Hastelloy tubing that were crimped on one end (the same as used in the analog experiments, see Fig. 2.13, Sec. 2.4). The Hastelloy tubes containing bentonite were each placed on a bed of basalt (5 g) in a glass flow test tube. The setup for these four experiments is comparable to the pump and first vessel of the apparatus shown in Fig. 2.1, Section 2.1. The inner dimensions of the glass flow test tube were 19 cm long by 1.5 cm diameter, and it held about 22 mL of liquid.

After it filled the glass flow tube, the groundwater solution was pumped through the apparatus at a rate of 0.1 mL/min for the duration of each experiment.

The amount of bentonite packed into each tube and the temperature for each experiment are shown in Table 3.10. The results showed that as groundwater was pumped through the vessel, the bentonite would swell. Once it reached the height of about 2 cm in the time indicated in the table, pieces of bentonite would fall to the bottom of the glass flow tube and be assimilated into the basalt chip layer.

Table 3.10. Amount of bentonite and the temperature used in each of four auxiliary bentonite flow experiments

Experiment	Bentonite Packed in 5.1-cm Column (g)	Temperature (°C)	Time Required For the Bentonite to Expand 2 to 3 cm Above the Tube (h)
1	<4	22	72
2	2.22	22	120
3	1.00	90	24
4	1.00	90	24

Based on these results, the procedure used to introduce bentonite into an analog experiment was to pack one gram of bentonite into a crimped Hastelloy tube and submerge the tube in groundwater solution for 24 hours. The bentonite that expanded above the top of the tube was removed and the tube inserted in the flow stream above the basalt chips. In this fashion the tube provided a slow but continuous supply of bentonite to the solution

stream and basalt chips. The amount of bentonite that expanded above the tubes in 24 hours and was removed prior to insertion into the analog experiments was 0.1 g per tube.

Bentonite exhibited very good swelling potential in all the auxiliary experiments conducted. In sufficient quantity, it took up all available space in the glass flow tube as well as space in the basalt chips. A good aspect with regard to conducting these flow experiments was that bentonite did not inhibit the flow of groundwater in the system when used in the moderate amounts introduced from the metal tubes. Based on these results, the Hastelloy-tube method of introducing bentonite to the flow stream was adopted for use in the analog experiments.

Analyses of Water from Flow Experiments with Bentonite

The groundwater effluents from the one vessel containing bentonite were analyzed without prior filtering to examine the effects of suspended bentonite particles on solution analyses. Unfiltered (and visibly cloudy) samples of water that were passed through the auxiliary experiments were analyzed by emission spectroscopy using inductively coupled plasma emission techniques. The samples analyzed were collected at different time intervals during the course of each experiment.

The results of compositional changes in the groundwater after contacting bentonite are shown in Table 3.11. The elements Ag, Ba, Be, Co, Cr, Ru, Nd, Ce, Mn, Mo, W, Pb, Sn, V, Zr, Cd, and Te were not detected in any of the samples. Detection limits are given in Table 2.19, Section 2.6.1.1. Graphs were plotted from the analytical results on key cation constituents. In the

Table 3.11. Analysis of unfiltered groundwater solution after flowing through auxiliary bentonite apparatus[a]

Elapsed Time at Collection (h)	pH	Chemical Constituent (µg/L)								
		Al	B	Ca	Fe	Mg	Si[b]	Sr	Ti	Zn
Original Groundwater:	11.0	490	1510	2020	<20	120	44.6	5	26	—
24	10.3	4100	3470	2470	1000	680	64.2	18	39	10
48	10.2	3150	3290	2260	670	590	61.4	18	34	21
224	10.7	4450	4190	1350	1030	750	71.4	24	40	15
624	10.3	4350	6120	1090	930	630	88.4	20	42	<10
648	10.6	1700	3780	1120	190	130	70.7	17	28	—

[a]Estimated accuracy is 10%. The major cation, Na, was not determined in these analyses.

[b]Reported in µg/mL.

cases examined, the graphs showed linear relationships when two elements were observed simultaneously. The data in Table 3.12 indicate that relative rates of change of element ratios in solution equal the ratios of these elements in the bentonite itself.

Table 3.12. Element ratios in bentonite and in material detected in groundwater solutions

Elements	Ratio	
	Unfiltered Groundwater	Bentonite
Aluminum/Iron	4	4.0
Aluminum/Magnesium	5	3.5
Silicon/Aluminum	7	2.8

The particulates in the groundwater resulted in poorly reproducible data, so that analyses of these groundwaters were not determined accurately. Even with this uncertainty, it appears from a comparison of the analyses of groundwaters and bentonite that the major chemical changes exhibited in unfiltered samples were due to bentonite suspended in solution.

The data in Table 3.12 suggest that silica from the bentonite, possibly as amorphous silica or as quartz, may have been suspended in groundwater preferentially to suspension of the bulk of the bentonite. The analyses of aluminum and iron can be used to estimate the amounts of bentonite suspended in the groundwater samples. These amounts were 10 to 40 mg/L in the unfiltered samples.

Filtering Experiments

To determine the degree of filtration necessary to remove bentonite particulate from the collected effluents, bentonite was mixed with three different solutions; groundwater, distilled water, and a NH_4Cl solution. Portions of these solutions were filtered through 1.2-, 0.8-, 0.4-, and 0.2-μm pore size filters, and 20-μL samples of each filtered and unfiltered solution were placed onto optical microscope slides and scanning electron microscope mounts for observation.

Observations by optical microscopy on the residue from the distilled water solution and NH_4Cl solution are presented here. Also, observations by scanning electron microscopy of residues from the groundwater solutions are given.

Optical Microscope Observations. Glass slides containing evaporate of 20 μL of the solutions were viewed in transmitted light at magnifications from 100 to 600X. Polarized light with a crossed analyzer was used to detect crystallinity within the observed particles. The conclusion made from these observations using optical microscopy alone is that the 0.8-μm pore size filter is adequate to remove the bentonite particles from solution.

Scanning Electron Microscope Analysis. The sample of unfiltered bentonite solution left a fairly common uniform texture with grains averaging ~5 μm. The bentonite particles were found to be high in Fe, Ca, and K, with smaller amounts of Mg. Due to the fact that the groundwater is relatively low in these elements, their presence can be attributed to their presence in the bentonite.

The sample filtered through a 1.2-μm sieve showed no obvious traces of bentonite. The particles observed were (1) small 8-μm particles high in S, presumably as SO_4, and (2) larger 25-μm particles cubic in form and high in Na and Cl. These particles were the residues caused by evaporation of the sample.

The sample filtered through a 0.8-μm sieve also showed no detectable sign of bentonite. No samples that passed through smaller pore size filters were examined.

Auxiliary Experiment with Bentonite in Two Vessels

This experiment was run to examine the effects of filtering of solutions on analyzed groundwater composition.

Analysis of Filtered Samples. The effluent collected between day 7 and day 10 of the experiment was filtered through 1.2-, 0.8-, 0.45-, 0.2-, and 0.1-μm pore size filters; 15-mL samples of solution were filtered through each of the 0.8-, 0.2-, and 0.1-μm filters and 30-mL samples were filtered through each of the 1.2- and 0.45-μm filters. Of the latter samples, 15 mL of each were treated with 150 μL 8M HNO_3 to dissolve any particulate in solution. The remaining 15 mL of each were left untreated for comparison with the acidified samples.

Table 3.13 presents the inductively coupled plasma emission analysis of these filtered samples. Decreases in the concentration of Al, Ca, Fe, Mg, Si, and Ti upon initial filtration indicate that most of the bentonite particles were eliminated by the 1.2-μm pore size filter. The concentrations of Fe and Mg dropped below the detectable level using 0.45-μm pore size filters, suggesting that this filter adequately eliminated any measurable amounts of the bentonite. There appeared to be no noticeable change in composition between the acidified and unacidified samples; therefore, the procedure was adopted that solutions to be analyzed in this program were filtered through 0.45-μm pore size filters but were not acidified.

Inductively Coupled Plasma Emission Results. The effluent from the experiment was collected in 11 samples, over 17 days, in 1- to 3-day periods. All the samples were filtered through a 0.45-μm sieve for analysis. Table 3.14 reports the results of these analyses along with an analysis of the original groundwater. It appears that interaction with bentonite alone has a negligible effect on the groundwater composition. The only noticeable change is an increase in Al concentration, probably due to Al from the bentonite remaining with the solution.

Table 3.13. Analysis of filtered groundwater samples collected from day 7 to day 10 of an auxiliary experiment with bentonite in two vessels

Filter Pore Size (μm)	Chemical Constituents (μg/L)									
	Al	B[a]	C[a]	Fe	Mg	Mn	Na[a]	Si[a]	Sr	Zn
Unfiltered	18,200	4.89	2.36	5,500	3,400	17	304	127	64	30
1.2 (acidified)	490	4.98	1.31	40	12	<5	333	79	35	19
1.2 (unacidified)	530	4.99	1.25	35	13	<5	352	81	32	16
0.8	530	4.88	1.32	39	17	<5	318	80	34	12
0.45 (acidified)	400	4.72	1.37	<20	<10	<5	312	76	36	<10
0.45 (unacidified)	460	4.85	1.27	<20	<10	<5	313	81	34	<10
0.2	430	4.98	1.32	<20	<10	<5	306	82	35	<10
0.1	480	4.86	1.38	35	<10	<5	307	82	37	<10

[a]Reported in mg/L.

Table 3.14. Analysis of groundwater samples filtered through a 0.45-μm sieve

Elapsed Time at Collection (h)	pH	Chemical Constituent (μg/L)							
		Al	B	Ca	Fe	Mg	Na[a]	Si[a]	Sr
Original Groundwater:	10.00	<30	1330	1020	<20	<10	300	41	<5
72	9.49	100	5280	1210	27	<10	331	62	45
96	9.20	300	6940	1530	34	<10	322	74	52
120	9.29	130	8380	1480	38	<10	320	76	48
144	9.38	270	7180	1400	40	<10	322	75	42
168	9.57	380	4920	1270	40	<10	306	66	42
240	9.55	460	4850	1270	<20	<10	313	81	34
264	9.60	440	4860	1220	<20	<10	303	66	35
288	9.59	460	4910	1220	<20	<10	319	65	35
312	9.61	700	4600	1200	71	<10	299	61	32
336	9.64	690	4900	1490	27	<10	286	67	37
408	9.60	700	5010	1510	25	<10	303	69	36

[a]Reported in mg/L.

Bentonite Interaction with Groundwater

A 10-g sample of bentonite was reacted in distilled water at 90°C for 17 hours to see if it was a source of anions. The filtrate obtained from the test was found to have the anion constituents shown in Table 3.15. The bentonite did not add fluoride or chloride to the water in sufficient quantities to modify the composition of the groundwater used in the analog experiments. (Water from the Grande Ronde structure, which is proposed for the waste repository, contains 37 mg/L fluoride and 148 mg/L chloride.)

Table 3.15. Analyses of anions in solution after extraction from bentonite[a] (mg/L)

Fluoride	Chloride	NO_3^-	SO_4^{2-}	PO_4^{3-}
0.95	3.39	6.35	149.9	1.00

[a]Analyzed by F. Williams, Analytical Chemistry Laboratory, Argonne National Laboratory. Analysis No. 80-0556-01, 11 Sep 81, of sample Bent-F.

The quantity of sulfate extracted from the bentonite also is not significant, as exemplified by the following comparison. From 10 g of bentonite, 3.0 mg of sulfate was extracted. In an experiment typically using 2 g of bentonite, only 0.6 mg sulfate would be available from the bentonite. With a flow of 0.5 mL/h in the experiments, this amount of sulfate, released in 90 days, would raise the sulfate level of the water by 0.3 mg/L, which is not significant in comparison to the 114 mg/L of sulfate already in solution.

Summary of Results from Auxiliary Bentonite Experiments

The auxiliary experiments revealed that the use of Hastelloy tubes is an effective means of introducing bentonite to a groundwater flow stream without obstructing the flow path. Concentrations of 10 to 40 mg/L bentonite in solution are readily visible, are apparent in chemical analyses showing elevated levels of aluminum and iron, and can readily be removed by filtering with 0.45-μm pore size filters. Using filters with smaller pores did not produce any additional effects observable in the chemical analyses. Therefore, the use of the 0.45-μm pore size filter was sufficient to remove particulate from groundwater solutions for analyses in this program.

3.3 MINERALOGICAL CHANGES IN BASALT

Knowledge of the mineralogical changes on the basalt surfaces that occurred during alteration or during experimentation can contribute to the prediction of the geochemical behavior of this rock. Therefore, a detailed study of basalt surfaces that have been used in the analog experiments has been made. Because of the fragility and small size (~1 μm) of these

secondary phases, this analysis was carried out by using a scanning electron microscope. As a check on whether the experimentally produced minerals reflect authigenic minerals in a natural environment, several studies of naturally altered basalts also were reviewed.

3.3.1 Conditions

Chips of basalt (and vesicle material) from the analog experiments and from auxiliary experiments associated with the analog program were placed on aluminum mounts and carbon coated. The chips were then scanned for crystal phases that originated at the smooth primary fracture surface. Eight mounts were examined, each representing different experimental conditions and each mount holding from one to five chips.

During preliminary scanning, X-ray spectral data were obtained so that compositional as well as crystal habit information could be combined for mineral identification. After preliminary viewing, the dominant secondary phases were reexamined using mineral standards to increase stoichiometric precision, especially for those minerals that did not show a well-defined single-crystal habit.

The experimental conditions to which the basalt was subjected are summarized in Table 3.16.

3.3.2 Observations

The largest, most euhedral crystals were located on the mounts of basalt that were exposed to groundwater at 90°C (mounts 242-02 and 242-05). Spectral analysis indicates a Ca:S mole ratio present in this material of 1:1. Coupling this with habit indicates that this is probably gypsum, $CaSO_4 \cdot 2H_2O$, or a semihydrated gypsum (see Fig. 3.5). In addition to these large euhedral crystals (0.13-0.06 mm), smaller twinned subhedral grains (5 μm) were noted. However, these grains were too small for reliable X-ray analysis, but they have been identified as gypsum by habit and association.

Of the five chips on mount 242-02, one showed an extremely irregularly cracked surface. Within those cracks, trigonal needlepoint crystals were noted. The spectrum associated with these 3- to 23-μm sized crystals was almost entirely calcium, indicating that calcite ($CaCO_3$) crystals had formed in the cracks.

Only two other phases on the nonartificially aged surface were notable. One phase was a sparsely present open net mineral that formed a thin fibrous weave over local sections of two of the chips' surfaces. While not stoichiometrically exact, these compositions are closest to the zeolite erionite, $Ca_{4.5}Al_9Si_{27}O_{72} \cdot 27H_2O$. The other phase was a thin, almost fibrous phase identified as fibrous epidote and was extremely sparse. Sulfur in the composition probably replaced (OH) groups. The spectral analyses of these chips are summarized in Table 3.17.

Platelets of SiO_2 were found to be the dominant surface phase on the basalt hydrothermally altered at 340°C (mounts 242-03, -04, -06, -07, and -08). This phase was not identified on the specimens that were not

Table 3.16. Description of eight basalt samples examined for mineralogical changes

Basalt Sample	Ref. No.	Hydrothermally Altered[a] (days)	Time Exposed to Groundwater[b] (days)	Flow Rate (mL/h)
Fresh	242-01	0	0	—
Auxiliary 2	242-02	0	44	—
Analog 1	242-05	0	120	0.56
Hydrothermally Altered	242-03	30	0	—
Auxiliary 3	242-04	30	39	—
Analog 4	242-06	30	128	0.50
Analog 4	242-08 (Vesicle filling)	30	128	0.50
Analog 5	242-07	60	123	0.50

[a]The basalt was maintained in stock groundwater at a pressure of 102 atm at 350°C for the times specified.

[b]The rock samples were exposed to groundwater solution at 90°C and ∿1 atm fluid pressure for the times specified.

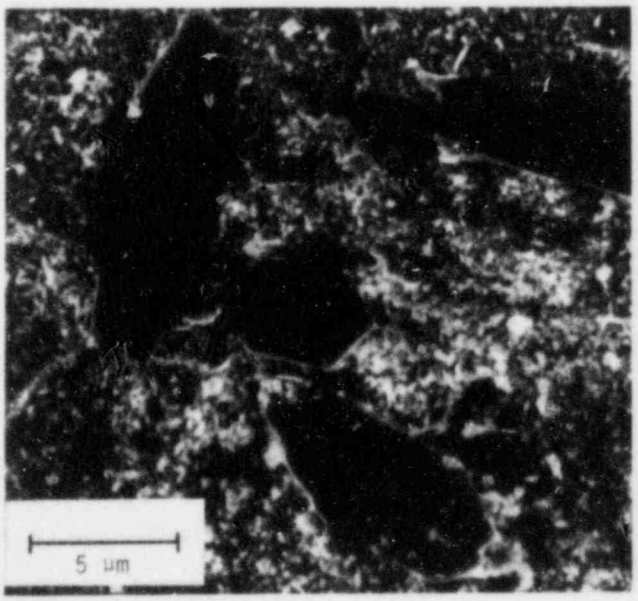

Fig. 3.5. Euhedral gypsum crystals

Table 3.17. Summary of surface mineralogical analyses of basalt hydrothermally altered at 320°C

Mount Designation	Measured Cation Proportions	Identified Mineral Formula	Mineral
424-02	$Ca_{1.03}S_{1.00}$	$CaSO_4 \cdot (2H_2O)$	Gypsum
424-02	$Ca_{1.00}S_{1.12}$	$CaSO_4 \cdot (2H_2O)$	Gypsum
424-02	$Ca_{1.00}$	$CaCO_3$	Calcite
424-02	$Ca_{4.5}Al_{13.5}Si_{22.5}$	$Ca_{4.5}Al_9Si_{27}O_{72} \cdot 27H_2O$	Erionite
424-02	$Ca_{4.5}Fe_{2.25}Al_{11.25}Si_{22.5}$	$Ca_{4.5}Al_9Si_{27}O_{72} \cdot 27H_2O$	Erionite
424-05	$Ca_{0.86}Si_{0.06}Al_{0.06}$	$CaCO_3$	Calcite
424-05	$Ca_{2.8}Mg_{1.0}Al_{2.0}Si_{3.5}S_{4.5}$	$Ca_2(Al,Fe)_3Si_3O_{12}(OH)$	Epidote

hydrothermally altered and, hence, indicates a major mineralogic difference between the two experimental approaches. These SiO_2 platelets averaged about 4 μm in diameter and were generally flattened. Usually the plates formed an even coating (that is, one or two plates thick) on the grain's surface, rarely producing protruding aggregates. The X-ray spectra acquired from these plates identified 96% of the cation to be silicon, with the remainder chiefly aluminum (2.4%). Minor amounts of K, Ca, and Fe were detected (<0.6%). Besides the aluminum, which may actually have been within the mineral structure, the impurities were probably either adsorbed on the plate's surface or were small inclusions within the poorly crystallized mass. The SiO_2 mineral usually shows an anhedral form, occasionally evidencing hexagonal symmetry. Therefore, we may conclude that this SiO_2 phase is at least in part cryptocrystalline quartz, and we shall refer to this mineral, for convenience, as quartz.

A zeolite-type solid solution tektosilicate called scapolite and two true zeolites, mordenite and phillipsite, have compositions corresponding to other surface phases analyzed. Again, these were minor, each probably covering less than 0.5% of the rock surface, but showing some tendency to clump and grow to larger volumes. Notable about these minerals are their high alkali contents and known ability to readily adsorb ions. These may be the sodium sink responsible for sodium loss from groundwater in the analog experiments. Crystals of these phases generally are no larger than 16 μm along the longest dimension.

Probably the most interesting and, other than quartz, ubiquitous phase located on the altered samples was an open net mineral occurring as protruding infundibuliform aggregates and as a matrix beneath and between the quartz plates (see Fig. 3.6). The elemental proportions most closely resembled an amphibole, ideally magnesium-rich anthophyllite.* Unlike the other minerals identified in this examination, the amphibole family is not predicted by recent works (Deutsch 1982; Wollenberg 1984) to occur under our experimental conditions. However, this mineral occurred on all altered specimens in fairly regular elemental proportions and with a consistent habit. This phase may

*This mineral is now identified as stevensite.

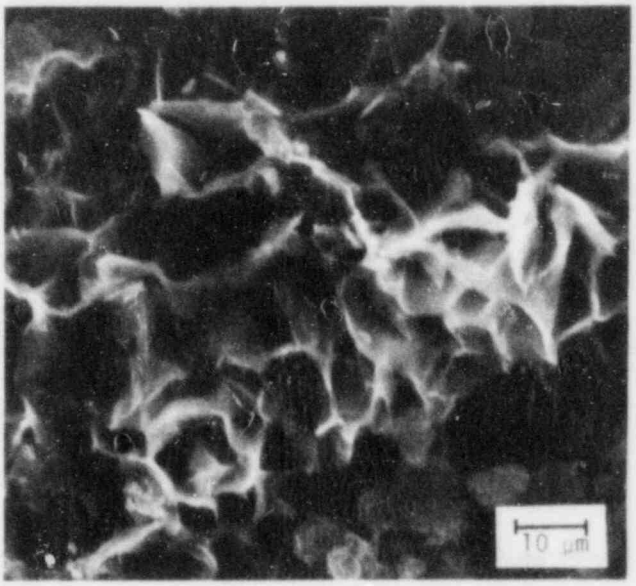

Fig. 3.6.

Aggregate of infundibuliform anthophyllite

represent as much as 30 to 40% of the alteration products forming on a chip's surface.

On mounts 242-03 and 242-04, a quartz platelet and amphibole net blanketed large areas of the basalt. The quartz showed the same relatively anhedral shape with a size range of about 3 to 5 µm. The 39-day exposure to groundwater at 90°C affected the quartz with more of the platelets showing the rudiments of hexagonal symmetry.

The sodium bearing zeolite, chabazite, was identified spectrally on sample mount 242-04. Again, this phase is extremely sparse, but its ion exchange capacity may make it noteworthy. In Table 3.18, the surface minerals of the chips on mounts 242-03 and 242-04 are summarized.

The specimens on mounts 242-06 and 242-07 both had the same mineral assemblage; quartz, amphibole, and sericite (Table 3.19). Occurrences of both quartz and anthophyllite were similar to those on the other hydrothermally altered samples, with an even intergrowth of the two minerals spread thinly over more of the chip's surface. Quartz crystals maintained a fairly constant 3-µm size. The sericite presence was evident on both crystals through X-ray analysis as well as by noting crystal shape (Sudo 1981).

Vug filling from the basalt core surface on mount 242-08 had some areas monochromatic in iron that were assumed to be hematite rich, which accounted for the reddish color of the sample. Similar vug-filling material that was aged naturally was subjected to examination by X-ray diffraction and showed calcite with montmorillonite clay.

3.3.3 Summary of Minerals Produced by Alteration of Basalt

Several mineral trends are evident from this investigation:

(1) Calcite and gypsum are the initial secondary phases precipitated onto basalt when exposed to groundwater at 90°C.

Table 3.18. Surface minerals of chips on mounts 242-03 and 242-04

Sample Designation	Cation Proportions	Mineral Formula	Mineral Name
Mount 242-03			
A-1	$Si_{1.6}Al_{0.04}K_{0.01}Ca_{0.01}Fe_{0.01}$	SiO_2	Quartz
A-2	$Na_{1.0}Mg_{5.0}Al_{1.02}Si_{7.6}Fe_{1.01}$	$Na_2(Mg,Fe,Al)_5Si_8O_{22}(OH)_2$	(Alkali) Amphibole
A-3	$Mg_{4.25}Fe_{1.8}Al_{1.0}Si_{7.8}$	$(Mg,Fe)_7Si_8O_{22}(OH)_2$	Anthophyllite
A-4	$Mg_{5.0}Fe_{3.0}Al_{1.0}Si_{10.5}$	$(Mg,Fe)_7Si_8O_{22}(OH)_2$	Anthophyllite
A-5	$K_{1.0}Al_{1.6}Si_{8.9}$	$K_2Al_2Si_{10}O_{24}\cdot 7H_2O$	Mordenite
B-1	$Mg_{5.3}Fe_{1.8}Al_{1.0}Si_{8.5}$	$(Mg,Fe)_7Si_8O_{22}(OH)_2$	Anthophyllite
B-2	$Mg_{5.3}Fe_{1.8}Al_{1.0}Si_{8.4}$	$(Mg,Fe)_7Si_8O_{22}(OH)_2$	Anthophyllite
B-3	$Mg_{2.7}Al_{1.0}Si_{9.7}$	$(Mg,Fe)_7Si_8O_{22}(OH)_2$	Anthophyllite
B-4	$Mg_{3.3}Fe_{1.2}Al_{1.0}Si_{7.1}$	$(Mg,Fe)_7Si_8O_{22}(OH)_2$	Anthophyllite
B-51	$Na_{5.8}K_{1.0}Al_{1.4}Si_{10.9}$	$(Na,K)_4[Al_3Si_9O_{24}](OH)$	Scapolite
B-52	$Na_{5.8}K_{1.0}Al_{1.4}Si_{10.8}Cl_{1.2}$	$(Na,K)_4[Al_3Si_9O_{24}](Cl)$	Scapolite
C-1	$Na_{3.2}K_{1.0}Al_{1.3}Si_{11.2}S_{1.1}Cl_{1.2}$	$(Na,K)_4[Al_3Si_9O_{24}](Cl,SO_4)$	Scapolite
C-2	$Na_{1.0}K_{1.0}Al_{2.3}Si_{5.8}$	$(Na,K)_3[Al_3Si_5O_{16}]\cdot 6H_2O$	Phillipsite
C-3	$Mg_{4.9}Fe_{1.4}Al_{1.0}Si_{8.3}$	$(Mg,Fe)_7Si_8O_{22}(OH)_2$	Anthophyllite
C-4	$Mg_{3.7}Fe_{1.3}Al_{1.0}Si_{8.4}$	$(Mg,Fe)_7Si_8O_{22}(OH)_2$	Anthophyllite
C-5	$Mg_{4.7}Fe_{1.3}Al_{1.0}Si_{7.3}$	$(Mg,Fe)_7Si_8O_{22}(OH)_2$	Anthophyllite
Mount 242-04			
A-2	$Mg_{1.7}Fe_{1.0}AlSi_{7.1}$	$(Mg,Fe)_7Si_8O_{22}(OH)_2$	Anthophyllite
A-3	$Na_{1.0}Ca_{1.7}Al_{4.6}Si_{9.9}$	$(Ca,Na_2)[Al_2Si_4O_{12}]\cdot 6H_2O$	Chabazite

Table 3.19. Surface minerals of chips on mounts 242-06 and 242-07

Mount Designation	Ion Proportions	Mineral Formula	Mineral Name
242-06	$Mg_{3.8}Fe_{1.0}Al_{1.0}Si_{7.9}$	$(Mg,Fe)_7Si_8O_{22}(OH)_2$	Anthophyllite
242-06	$Si_{1.6}Al_{0.03}$	SiO_2	Quartz
242-06	$K_{1.2}Al_{1.0}Si_{3.8}$	$KAl_2(AlSi_3O_{10})(OH)_2$	Sericite
242-07	$Mg_{7.8}Al_{1.0}Si_{10}$	$(Mg,Fe)_7Si_8O_{22}(OH)_2$	Anthophyllite
242-07	$K_{1.0}Al_{1.5}Si_{5.1}$	$KAl_2(AlSi_3O_{10})(OH)_2$	Sericite
242-07	$Mg_{3.7}Fe_{1.4}Al_{1.0}Si_{7.2}$	$(Mg,Fe)_7Si_8O_{22}(OH)_2$	Anthophyllite

(2) Quartz will not readily form upon exposure of the basalt to groundwater at a temperature of 90°C, but does so rapidly at the elevated pressure and temperature imposed during hydrothermal alteration.

(3) A magnesium-iron alumino silicate, here identified as the amphibole anthophyllite, in conjunction with quartz forms rapidly during alteration at elevated temperatures and pressures and is fairly stable upon contact with groundwater at 90°C. These two minerals dominate basalt alteration under the given experimental conditions.

(4) Several similar zeolites and scapolite are formed and stabilized during both alteration at elevated temperature and reaction with groundwater at 90°C during the experiments.

(5) Sericite is formed in minor amounts during alteration at elevated pressure and temperature.

(6) The zeolites and clay may be the major mineral sinks for sodium, potassium, and most of the calcium during both hydrothermal alteration and upon contact with groundwater at 90°C.

3.4 RADIOELEMENT DISTRIBUTION IN ANALOG EXPERIMENTS

3.4.1 Solutions

The primary objective of the laboratory analog program was to study the migration of radioelements through a laboratory-simulated repository breach situation, with special emphasis on actinide migration. To meet this end for each experiment, a great number of data were collected for solution concentrations of uranium, neptunium, and plutonium. Data were also collected on migration of fission products (Cs, Ba, and Eu). In this section we describe the data collected for all six analog experiments. Presentation of these results is divided into four topics: (1) predicted levels of elements leached into the moving groundwater, (2) general solution behavior of actinides, (3) specific actinide behavior for different analog conditions, and (4) fission product behavior.

3.4.1.1 Predicted Concentrations of Elements in Analog Experiment Eluate Due to Leaching of the Waste Form

Results of continuous flow leaching experiments performed at Lawrence Livermore National Laboratory (LLNL) (Coles 1982) and Pacific Northwest Laboratory (PNL) (Strachen 1982) were used to predict the concentrations of waste form constituents that would leach from the radioactive glass into the groundwater eluate during analog experiments. The LLNL data used in this analysis were measured in continuous-flow experiments run at 25°C and 75°C with a bicarbonate leach solution at a linear flow velocity (22 m/yr) comparable to that seen by the waste form in analog experiments (38 m/yr). The PNL data were also collected in a continuous-flow system, but distilled water was the leachant; these experiments were run at 90°C with a linear flow velocity equal to that of the analog experiments (38 m/yr). Table 3.20 lists these data and shows each step of the calculations used to convert leach rate data in terms of $g/(cm^2 \cdot day)$ into analog leachate steady-state concentrations.

Table 3.20. Calculation steps leading to metal ion concentrations in analog experiment eluant from leaching of waste form

Element	Leach Rate [g/(cm^2·day)] Reference Bicarbonate at 25°C	Reference Bicarbonate at 75°C	Predicted at 90°C	Predicted Rate for Wafer of 2.63 cm^2 and 0.4 g (parts/h)	Amount of the Element in Glass Wafer	Predicted Loss Rate (h^{-1})	Predicted Concentration in Leachate at a Flow Rate of 0.6 mL/h (mL^{-1})
Pu	5×10^{-7}	9×10^{-8}	1×10^{-7}	7×10^{-9}	14 µCi	0.1 pCi	0.4 dpm
Np	2×10^{-6}	9×10^{-5}	2×10^{-4}	1×10^{-5}	0.8 µCi	8 pCi	30 dpm
B	4×10^{-6}	9×10^{-5}	2×10^{-4}	1×10^{-5}	11.3 mg	1×10^{2} ng	2×10^{2} ng
Si	2×10^{-7}	7×10^{-5}	3×10^{-4}	2×10^{-5}	76.9 mg	1.5×10^{3} ng	2.6×10^{3} ng
Cd	4×10^{-5}	4×10^{-5}	4×10^{-5}	3×10^{-6}	0.2 mg	0.6 ng	1 ng
Fe	3×10^{-6}	-	3×10^{-6}	2×10^{-7}	27.2 mg	5 ng	1 ng
Mo	9×10^{-5}	1×10^{-5}	6×10^{-6}	4×10^{-7}	5.4 mg	2 ng	0.3 ng
Ni	3×10^{-5}	3×10^{-5}	3×10^{-5}	2×10^{-6}	0.7 mg	1.4 ng	2 ng
Sr	1×10^{-5}	1×10^{-4}	6×10^{-5}	4×10^{-6}	1.4 mg	6 ng	1×10^{1} ng
U	6×10^{-5}	8×10^{-5}	9×10^{-5}	6×10^{-6}	12.4 mg	7×10^{1} ng	1×10^{1} ng
Ce	no data	no data	no data	($<5 \times 10^{-8}$)[a]	16.4 µCi[b]	8×10^{-1} pCi	<3 dpm[b]
Ca	6×10^{-5}	1×10^{-4}	1×10^{-4}	7×10^{-6}	6.2 mg	4×10^{1} ng	7×10^{1} ng
Eu	no data	no data	no data	($<5 \times 10^{-8}$)[a]	20 µCi	<1 pCi	<4 dpm
Na	3×10^{-3}	8×10^{-4}	3×10^{-4}	2×10^{-5}	33.5 mg	7×10^{2} ng	1×10^{3} ng
Ba	no data	1×10^{-5}	8×10^{-5}[c]	5×10^{-6}	0.45 µCi	2 pCi	(2×10^{1} ng) 7 dpm
Cs	no data	1×10^{-4}	3×10^{-4}[d]	2×10^{-5}	0.0065 µCi	0.1 pCi	(1.4×10^{3} ng) 0.4 dpm (4×10^{1} ng)[e] 0.1 dpm[e]
Am	no data	no data	no data	($<5 \times 10^{-8}$)[a]	5 µCi	<0.2 pCi	<1 dpm

[a] Estimated from Cs and Nd data from Strachen (1982); less than 5 ppm Eu and less than 5 ppm Ce (the detectability limit) was in the leachate solution.

[b] No correction for ^{141}Ce half-life (32.5 days).

[c] Predicted from Ca^{2+} and Sr^{2+} behavior.

[d] Predicted from Na^{+} behavior.

[e] From Strachen (1982).

The Arrhenius equation was used to predict the leach rate at 90°C from the data produced by Coles (1982) at 25 and 75°C:

$$\ln\left(k_1/k_2\right) = -\frac{E^*}{R}\left(\frac{1}{T_1} - \frac{1}{T_2}\right) \tag{3.4}$$

where k_1 and k_2 are leach rates, E^* is an effective activation energy (in units of cal/mol), R is the universal gas constant [1.987 cal/(deg·mol)], and T_1 and T_2 are temperatures in kelvin. A value of $-E^*/R$ was calculated from the data at these two temperatures, and this value and the leach rate at 75°C were used to calculate the leach rate at 90°C. The use of this relationship for a complex phenomenon such as leaching is not always valid. For example, in situations such as plutonium leaching, when the rate of leaching decreases with increasing temperature, the equation is clearly not applicable. Nevertheless, because the extrapolation is small (75-90°C), this procedure was followed, in the absence of sufficient data to devise a more rigorous method.

To relate the normalized leach rates to the analog system, the leach rates must be multiplied by the surface area of the glass wafer used in these experiments (2.63 cm^2) and divided by its mass (0.40 g), then multiplied by the amount of material in that wafer (in milligrams or microcuries). These operations are shown in Table 3.20. To convert the leach rate in terms of ng/h or dpm/h to concentrations (ng/mL or dpm/mL) in the leachate, they must be divided by the volumetric flow rate of the eluant in these experiments (0.6 mL/h). The rightmost column in the table lists the predicted concentrations of waste glass constituents in the analog eluate due to their being leached from the waste form. In Table 3.21, in comparison, are the concentrations of these constituents in the initial groundwater and in several sampled analog experiment fluids.

A comparison of (1) the concentrations of waste form constituents added to the groundwater eluant by leaching of the waste form to (2) their concentrations in the initial groundwater shows that, for the major and minor constituents of groundwater, the effect of waste form leaching is either insignificant or imperceptible. The notable cases of substantial changes in composition are uranium and the radioelements that are not present in the starting solution. Allowing for the significant uncertainties in the predicted leach rates (e.g., a factor of four in different leach data for cesium), the leach data in flowing systems are comparable to those observed in the analog experiments (first vessel). This is true explicitly for U, Pu, Np, and Cs, where concentrations were sufficiently high in both leach tests and analog experiments to be measured. This suggests that no new phenomena are encountered in the more complex analog experiments than occurred in flowing leach tests that would need to be considered for a realistic estimate of leach behavior. It indicates, for example, that the leached concentrations of U, Pu, Np, and Cs are not affected by the proximity of the backfill in the analog experiments.

The leach data are also consistent with the analog results for other elements that were below detectability in leach tests (e.g., Am) or where incremental increases from leaching are masked by large changes in the initial analog groundwaters (e.g., B, Si, Na, etc.).

Table 3.21. Predicted and measured concentrations of constituents due to leaching from the waste form in groundwater of analog experiment 1

Element	Concentration (mg/L except as noted)					
	In Original Groundwater[a]	Predicted to be Added to Groundwater from Leaching of Glass Wafer[b]	Measured in First Vessel	Measured in Second Vessel	Rock Core Outlet (78-85 days after waste form was added)	Rock Core Outlet 24-31 Days After Flow Started (7 days before waste form was added)
Pu	0.00	(0.4 dpm/mL)	(1.1 dpm/mL)[c]	(0.4 dpm/mL)[c]	(<0.01 dpm/mL)[c]	0.00
Np	0.00	(30 dpm/mL)	(5.2 dpm/mL)[c]	(3.1 dpm/mL)[c]	(0.03 dpm/mL)[c]	0.00
B	1,340	200	1,340	1,260	1,380	1,430
Si	53,000	2,600	49,000	48,000	49,600	51,200
Cd	<10	1	<10	<10	<10	<10
Fe	<20	1	<20	<20	<20	<20
Mo	<100	0.3	<30	<30	<100	270
Ni	<20	2	<20	<20	<20	22
Sr	<2	10	21	35	60	170
U	0.04	10	35.6	35.0	6.72	0.16
Ce	-	(<3 dpm/mL)[d,e,f]	(-)[f]	(-)[f]	(-)[f]	(0.0)[f]
Ca	1,500	70	720	670	12,700	39,900
Eu	-	(<4 dpm/mL)[g]	(0.24 dpm/mL)[h]	no data	(0.02 dpm/mL)[h]	(0.0)
Na	316,000	1,000	281,000	243,000	220,000	190,000
Ba	<10	20[i] (7 dpm/mL)[i]	<10 (0.66 dpm/mL)[h]	<10 no data	<10 (<0.01 dpm/mL)[h,j]	18
Cs	-	140[k] 40[d] (0.4 dpm/mL)[k] (0.1 dpm/mL)[d]	0.04[h]	no data	(<0.02 dpm/mL)[h,j]	-
Am	-	(<1 dpm/mL)[h]	(<0.03 dpm/mL)[h]	no data	(<0.02 dpm/mL)[h,j]	(0.0)

[a]Measured by inductively coupled plasma emission; < symbol implies detection limit of the method.

[b]Derived from Coles (1982) from flow leach rate data on PNL 76-68 glass at 25 and 75°C at a comparable flow rate, except where noted otherwise.

[c]By alpha counting.

[d]Derived from Strachen (1982) from flow leach rate data on PNL 76-68 glass under comparable temperature and flow rate conditions.

[e]The < symbol means that Strachen (1982) was unable to detect these elements above his concentration detectability limits; this activity level corresponds to his detectability limit for analog glass samples.

[f]Not corrected for the half-life (32.5 days) of ^{141}Ce. This amount of activity would have diminished by one to two orders of magnitude before being counted in the eluate.

[g]Estimated from Nd data from Strachen (1982).

[h]By gamma counting.

[i]Coles (1982) reported only 75°C leach rate, estimated from Ca^{2+} and Sr^{2+} temperature effects.

[j]Detectability limit--defined as the background count.

[k]Coles (1982) reported only 75°C leach rate, estimated from Na^{+} temperature effect.

3.4.1.2 General Solution Behavior of Actinides

In general, the bulk of the retention of actinides in the analog experiments was observed to be in the basalt core fissure. Significant interaction was noted between fresh basalt and plutonium in analog experiment 1, as evidenced by the retention of plutonium on the rock core. Before the effect of the rock core is discussed, however, the effect of bentonite in analog experiment 1 (unaltered bentonite) and in analog experiment 6 (hydrothermally altered bentonite) must be described. Table 3.22 shows the concentrations of plutonium, neptunium, and uranium as the groundwater exited each of the two vessels and the rock core in analog experiment 1. The fact that concentrations of both neptunium and uranium were constant in the outlets of both bentonite-containing vessels, whereas plutonium concentration decreased, implied that plutonium had at least to some degree associated with the bentonite. (The samples leaving both the first and second vessels appeared cloudy; the basalt core outlet samples appeared clear.) To test this hypothesis, samples from the two bentonite-containing vessels were passed through a 0.1-μm pore size filter. Although there was no loss of uranium or neptunium, the concentration of plutonium was reduced by 60% in the sample from the first vessel and to below detectability in the sample from the second vessel. To reiterate, the results of these studies imply that, with the waste form leaching and groundwater composition of the analog experiments, unaltered bentonite sorbs plutonium from solution, but has no tendency to sorb either the uranium or neptunium chemical species.

Table 3.22. Actinide concentrations in unfiltered outlet samples of analog experiment 1

Outlet Sample Location	Pu[a] (dpm/mL)	Np[a] (dpm/mL)	U (ng/mL)
1st Vessel	1.1 ± 0.1	5.3[b]	35.0
2nd Vessel	0.4 ± 0.1	5.1[b]	35.6
Rock Core	<0.005	0.02	9.6

[a]Units of dpm/mL can be converted to units of mg/L using the conversion factors given in Section 2.6.3.4.

[b]Initial determinations of these values were 3.2 and 3.1 dpm/mL, respectively. The numbers in the table result from an iterative analysis with closer balance between solution activity and yield monitor activity.

The results of analog experiment 6 imply quite a different set of circumstances for hydrothermally altered bentonite (Table 3.23). These data show that both the uranium and neptunium species drop in concentration between the first and second outlets. So, uranium and neptunium, in contrast to plutonium, appear to interact with altered bentonite, but not with the fresh bentonite.

Table 3.23. Actinide concentrations in outlet samples of analog experiment 6[a]

Vessel Outlet	Sampling Period (days)	^{237}Np,[b] (dpm/mL)	^{239}Pu,[b] (dpm/mL)	U (µg/L)
1st	1-2[c]	7.0	1.1	40
Core	3-12[c]	0.16	0.45	2.2
Core	33-42	0.30	0.47	5.2
1st	43-44	2.4	1.1	25
2nd	50-51	1.0	1.0	15
Core	61-70	0.31	0.54	-
1st	71-72	2.3	1.6	25
Core	73-77	-	-	5.2
2nd	78-83	0.9	0.9	11
1st	84-109	1.7	1.5	-

[a]The errors in these numbers are about 10%, based on counting statistics for ^{237}Np and ^{239}Pu and on calibration error for U analyses.

[b]Units of dpm/mL can be converted to units of mg/L using the conversion factors given in Section 2.6.3.4.

[c]Taken very early in the experiment.

Table 3.24 was compiled to show (1) the important part that fresh basalt fissures might have in retarding actinide migration away from a breached waste canister and (2) the far smaller effectiveness of hydrothermally altered basalt surfaces to do the same. The data, which are presented elsewhere in this report in units of dpm/mL, are presented here in terms of mol/L to give the reader a feeling for the concentration of these species present in the analog experiments. Data extracted from this table are presented in the Executive Summary of this report. These data are discussed in more detail in Section 3.4.1.3.

3.4.1.3 Specifics of Actinide Migration

Unaltered Repository Components--Analog Experiments 1 and 2

Both these experiments were run with [illegible] ratory alteration of the waste form, the bentonite, or the freshly fissured basalt. The experiments differed only in the materials of construction of the apparatus (Hastelloy for analog experiment 1 and Monel-400 for analog experiment 2) and in flow rate (0.58 mL/h for experiment 1 and 0.86 mL/h for experiment 2). Neither of the variables was observed to have a measurable effect on the distances the actinide elements migrated. The results reported in Table 3.25 for experiment 1 and Table 3.26 for experiment 2 indicate that all (~98% or

Table 3.24. Actinide concentrations at the inlet and outlet of the fissured basalt core

Experiment		Plutonium (10^{-11} mol/L)	Neptunium (10^{-9} mol/L)	Uranium (10^{-9} mol/L)
1	Inlet	1.2	15	149
	Outlet	≤0.02	0.08	40
2	Inlet	0.3	14	114
	Outlet	≤0.02	0.2	47
3	Inlet	16	2.2	31
	Outlet	0.003	≤0.003	2.5
4[a]	Inlet[b]	89	109	2560
	Outlet	41	67	1660
5[a]	Inlet[b]	128	120	3000
	Outlet	105	120	2730
6	Inlet[b]	3.0	2.4	50
	Outlet	0.5	0.8	22

[a]Plutonium, neptunium, and uranium concentrations decreased significantly with time throughout the course of experiments 4 and 5. These values are near the maximum values.

[b]This sample was from the outlet of vessel 1, but is expected to be similar to a sample collected at the inlet to the core.

more) the neptunium and plutonium leached from the waste and observed in solution from the first vessel was removed by the time the solution had passed through the rock core.

The Effect of Gamma Radiation--Analog Experiment 3

The concentrations of the actinide elements, uranium, neptunium, and plutonium, leached into the groundwater were quite different for this experiment than in the other experiments using unaltered waste glass (experiments 1, 2, and 6). The solution from the second vessel outlet taken at the end of this experiment contained a much higher concentration of plutonium (by a factor between 5 and 50) and greatly reduced concentration of neptunium (by a factor of 7) than for other experiments. The uranium concentration in the second vessel outlet was lower by about a factor of 5 compared with results from the first two experiments.

A complication in the data from analog experiment 3 was the declining uranium concentration with time in samples from the outlet of the core. Either the amount of uranium leaching from the waste form decreased with time or the basalt core became a better sink for uranium as the experiment

Table 3.25. Analyses of actinides in effluent solutions from analog experiment 1 (Hastelloy apparatus)

Sample Location	Collection Time (days)	Concentration[a] (dpm/mL)	
		^{237}Np[b]	^{239}Pu[c]
Rock Core	17-26	≤0.005	≤0.006
Rock Core	45-53	0.014	≤0.009
Rock Core	45-53	0.018	≤0.003
Rock Core	66-72	0.008	≤0.006
Rock Core	78-86	0.03	0.04
Rock Core	92-99	0.034	≤0.004
1st Vessel	130-140	5.3	1.1
2nd Vessel	120-130	5.1	0.4

[a] A 50-mL aliquot of each solution was used for the analyses.

[b] Errors, estimated on the basis of counting statistics only, are about 20%. The analyses for ^{237}Np in units of dpm/mL may be multiplied by 2.69×10^{-9} to convert to units of mg/L.

[c] The symbol ≤ is used to designate an activity not discernible from background. The analyses for ^{239}Pu in units of dpm/mL may be multiplied by 3.04×10^{-11} to convert to units of mg/L.

Table 3.26. Analyses of actinides in effluent solutions from analog experiment 2 (Monel apparatus)

Sample Location	Collection Time (days)	Concentration[a] (dpm/mL)	
		^{237}Np	^{239}Pu
Rock Core	14-18	0.122	0.030
Rock Core	22-28	0.181	0.015
		0.095	≤0.003
Rock Core	63-68	0.083	0.074
		0.097	≤0.008
Rock Core	72-77	0.074	≤0.007
Rock Core	114-125	0.076	0.050
1st Vessel	160-170	5.2	1.0
2nd Vessel	150-160	4.5	0.1
Groundwater Blank		0.008	0.036

[a] Errors, estimated on the basis of counting statistics only, are about 5% for ^{237}Np and 25% for ^{239}Pu.

progressed. Table 3.27 shows that both plutonium and neptunium were effectively retarded by the fresh basalt fissure in the presence of the gamma field. In this regard, the results of experiment 3, performed in a radiation field, are identical to those of experiments 1 and 2.

Table 3.27. Analyses of actinides in effluent solutions from analog experiment 3 (gamma environment)

Sample Location	Collection Time (days)	Concentration[a] (dpm/mL)	
		^{237}Np	^{239}Pu
Rock Core	38-35	0.0090	0.0060
Rock Core	35-42	0.0070	0.0044
Rock Core	42-49	0.0044	0.0053
Rock Core	49-56	0.0056	0.0038
Rock Core	56-64	0.0114	0.0078
Rock Core	71-81	0.0066	0.0060
Rock Core	81-93	0.0070	0.0040
1st Vessel	103-113	0.67	11.6
2nd Vessel	93-103	0.75	5.3

[a]Errors, estimated on the basis of counting statistics only, are about 20%. Units of dpm/mL can be converted to units of mg/L using the conversion factors given in Section 2.6.3.4.

Hydrothermally Altered Waste Form, Bentonite, and Basalt--Analog Experiments 4 and 5

These experiments were designed to test the importance of the hydrothermal history of the repository components. Experiment 4 was run with bentonite and basalt that had been hydrothermally altered by groundwater at elevated temperature for about a month; for experiment 5, the materials had been treated for two months. The waste forms for these experiments were hydrated in water vapor at 340°C for 17 days (Sec. 2.3.5.2).

Tables 3.28 and 3.29 present the outlet ^{239}Pu and ^{237}Np data for analog experiments 4 and 5, respectively. These data and the data for uranium given in Tables 3.6 and 3.7 (Sec. 3.2.2) indicate increasing groundwater concentrations of these actinide elements for the first 40 days, followed by continuously dropping concentrations with time. The amount of activity that exited the system during the experiments was substantial; in the ~130 days of running each experiment, 6% of the uranium, 3% of the neptunium, and 0.1% of the plutonium contained in the waste forms exited the apparatus. In addition, substantial amounts of activity were found on the walls of vessels and tubing and on bentonite dispersed throughout the system. Table 3.30 shows the extent of the activity in the system.

Table 3.28. Analyses of actinides in effluent solutions from analog experiment 4

Sample Location	Collection Time (days)	Concentration[a] (dpm/mL)	
		^{237}Np	^{239}Pu
Rock Core	14-19	23.9	14.0
1st Vessel	19-21	75.7	32.7
Rock Core	21-28	24.5	14.5
Rock Core	28-40	30.9	25.8
Rock Core	47-56	42.7	16.3
Rock Core	56-65	38.4	13.7
Rock Core	65-70	NA	NA
1st Vessel	70-71	40.2	29.3
Rock Core	71-78	24.7	13.5
Rock Core	88-98	30.1	13.7
Rock Core	106-113	17.6	7.6
2nd Vessel	113-123	22.6	8.6
1st Vessel	123-133	29.8	7.4

[a]Units of dpm/mL can be converted to units of mg/L using the conversion factors given in Section 2.6.3.4.

Table 3.29. Analyses of actinides in effluent solutions from analog experiment 5

Sample Location	Collection Time (days)	Concentration[a] (dpm/mL)	
		^{237}Np	^{239}Pu
1st Vessel	6-7	40.8	42.2
Rock Core	7-16	37.3	34.4
Rock Core	16-26	55.3	54.8
Rock Core	26-36	76.6	51.7
Rock Core	36-44	49.4	60.3
Rock Core	44-47	68.5	50.3
1st Vessel	47-49	67.8	62.8
Rock Core	49-58	43.5	40.7
Rock Core	58-68	38.3	31.0
Rock Core	77-87	59.8	15.6
Rock Core	98-108	22.9	11.0
2nd Vessel	108-118	21.7	10.8
1st Vessel	118-126	20.5	8.0

[a]Units of dpm/mL can be converted to units of mg/L using the conversion factors given in Section 2.6.3.4.

Table 3.30. Alpha analyses of rinses of equipment used in analog experiments 4 and 5 after completion of the experiments

Rinse Location	Rinse Volume (mL)	Concentration (dpm) ^{237}Np	Concentration (dpm) ^{239}Pu
Analog Experiment 4			
Core to Outlet	7.05	225	70
2nd Vessel to Core	4.90	1070	825
2nd Vessel to 1st Vessel	12.41	300	1300
1st Vessel	21.27	1260	9900
Analog Experiment 5			
Core to Outlet	3.81	165	960
2nd Vessel to Core	3.09	60	1530
2nd Vessel to 1st Vessel	6.30	380	1630
1st Vessel[a]	ND	ND	ND

[a]There are no data for the first vessel of analog experiment 5 because the vessel contained an abundance of bentonite-basalt chips that precluded obtaining a homogeneous sample.

Even with the close interaction of actinide elements and bentonite, it is interesting that the plutonium and neptunium that passed through the rock core were not removed by filtering the solution. These data are presented in Table 3.31. This finding is contrary to that found in analog experiments with unaltered materials.

Table 3.31. Effects of filtering on the concentration of ^{237}Np and ^{239}Pu in an eluate sample from analog experiment 5

Sample	Concentration[a] (dpm/mL) ^{237}Np	Concentration[a] (dpm/mL) ^{239}Pu
Previously Analyzed (unfiltered)	76.6	62.7
Unfiltered Replicate	89.8	64.2
Filtered	81.3	64.3

[a]Units of dpm/mL can be converted to units of mg/L using the conversion factors given in Section 2.6.3.4.

Hydrothermally Altered Bentonite and Basalt, Unaltered Waste Form--Analog Experiment 6

The conditions of analog experiment 6 were much like those of experiment 4 but for one important difference, an unaltered waste form was used (except that it had been used previously in analog experiment 1).

This experiment reveals that, with lesser amounts of radioactivity, altered basalt continues to be incapable of retarding neptunium, uranium, and plutonium, as does the unaltered basalt. Several first vessel, second vessel, and outlet samples obtained throughout the duration of the experiment have been analyzed for U, ^{239}Pu, and ^{237}Np. The results of these analyses, presented in Table 3.23, show that steady-state behavior developed quickly in the system. Activity levels of the actinides in the three vessels appear to be independent of time.

An interesting result of this study, not noted with the much higher activity levels in analog experiments 4 and 5, is that the altered basalt core and altered bentonite appear to have some ability to retard radionuclide migration. The decrease in [^{237}Np] and [U] between the first and second vessels may be explained by their sorption on bentonite, an effect not seen in unaltered bentonite experiments.

3.4.1.4 Fission Product Behavior--Activities of ^{125}Eu, ^{133}Ba, and ^{137}Cs in Outlet Samples of Analog Experiments 1 and 4

Results of this study are presented in Tables 3.32 and 3.33. The most interesting result is the comparision of cesium sorption by the altered rock core (experiment 4) and the unaltered core (experiment 1). The laboratory-altered basalt appears to be a much better retarder of cesium than fresh basalt; yet, it does not retard any of the other isotopes as well as the unaltered rock. Europium, a good stand-in for americium, appears to pass through the altered fissure with no retardation; barium shows some measurable degree of retardation, and neptunium only a limited amount. (Neptunium results are in good agreement with those measured by alpha analyses, where the neptunium activities measured in the second vessel and rock core outlets of analog experiment 4 were 23 and 24 dpm/mL, respectively.) The unaltered core, although it did not appear to effectively retard cesium ions, stopped most, if not all, the other isotopes represented in Table 3.33.

3.4.2 Radioactivity Relative to Mineralogical Changes on Rocks

An association of alpha-emitting radionuclides with secondary mineral phases on the fissured rock surfaces was looked for by exposing the fissured surfaces to cellulose nitrate plastic for periods of weeks to months, then etching the plastic to reveal the tracks of the alpha particles (Gerding 1979). The alpha tracks were uniformly distributed on a local scale (~5-mm scale). Therefore, no single mineralogical phases of the rock or its alteration products could be associated with the sorption of alpha-emitting radionuclides. The track technique can resolve point sources of ~0.002-dpm activity that are separated by ~10 μm. The results suggest that the alpha radionuclides are not associated with a single phase of the basalt. Because the secondary products are generally small (<10 μm), with some products uniformly coating

Table 3.32. Activities of ^{137}Cs, ^{152}Eu, ^{133}Ba, and ^{237}Np measured in second vessel and core outlet samples of analog experiment 4

Radioisotope	Activity[a] (dpm/g)	
	Second Vessel Outlet	Rock Core Outlet
^{137}Cs	1.9 ± 0.1	-0.2 ± 0.1[b]
^{152}Eu	2.3 ± 0.1	2.0 ± 0.1
^{133}Ba		
(80 keV)	0.42 ± 0.09	0.2 ± 0.1
(356 keV)	0.47 ± 0.07	0.05 ± 0.06
Average	0.45 ± 0.05	0.1 ± 0.1
^{237}Np		
(86 keV)	18.2 ± 0.1	13.5 ± 0.2
(312 keV, ^{233}Pa daughter)	20.1 ± 0.2	14.0 ± 0.2
Average	19.1 ± 0.2	13.8 ± 0.2
Sample Size	10 g	10 g

[a]The errors shown are based on the counting statistics for each measurement.

[b]That is, ^{137}Cs radiation level was less than background count, possibly due to sorption by the sample.

Table 3.33. Activities of ^{137}Cs, ^{152}Eu, ^{133}Ba, and ^{237}Np measured in second vessel and core outlet samples of analog experiment 1

Radioisotope	Activity[a] (dpm/g)	
	First Vessel Outlet[b]	Rock Core Outlet
^{137}Cs	0.04 ± 0.01	0.02 ± 0.01
^{152}Eu	0.24 ± 0.03	0.02 ± 0.02
^{133}Ba		
(80 keV)	0.69 ± 0.03	0 ± 0.02
(356 keV)	0.63 ± 0.02	0.01 ± 0.01
Average	0.66 ± 0.02	0.01 ± 0.01
^{237}Np		
(86 keV)	2.01 ± 0.05	0 ± 0.03
(312 keV, ^{233}Pa daughter)	2.04 ± 0.03	0.06 ± 0.02
Average	2.03 ± 0.03	0.06 ± 0.02
Sample Size	26.9 g	33.7 g

[a]The errors shown are based on the counting statistics for each measurement.

[b]Samples from the first and second vessel outlets are comparable in activity.

the surface of the basalt, the alpha-emitting radionuclides could be associated with a single alteration phase that would be undetectable by the alpha radiographs.

3.4.3 Radioelement Activity of the Rock Core Fissure Surfaces

After each analog experiment, the rock core fissure was counted for gamma-emitting radionuclides in 18 thin bands along the groundwater flow path. Although five radioisotopes were looked for, only neptunium, and in some cases cesium and europium, radioisotopes were located.

3.4.3.1 Neptunium Profiles

Figure 3.7 shows the spatial profiles of ^{237}Np activity on the rock core faces from the first three analog experiments. The profiles are remarkably similar and show that the sorption of neptunium had occurred in the first third of the unaltered rock cores. Furthermore, sorption is not noticeably affected by gamma radiation, as indicated by the similarity of the results from experiment 3 with those of experiments 1 and 2. The smaller area under the peak for analog experiments corresponds to the smaller quantity of neptunium that entered the core.

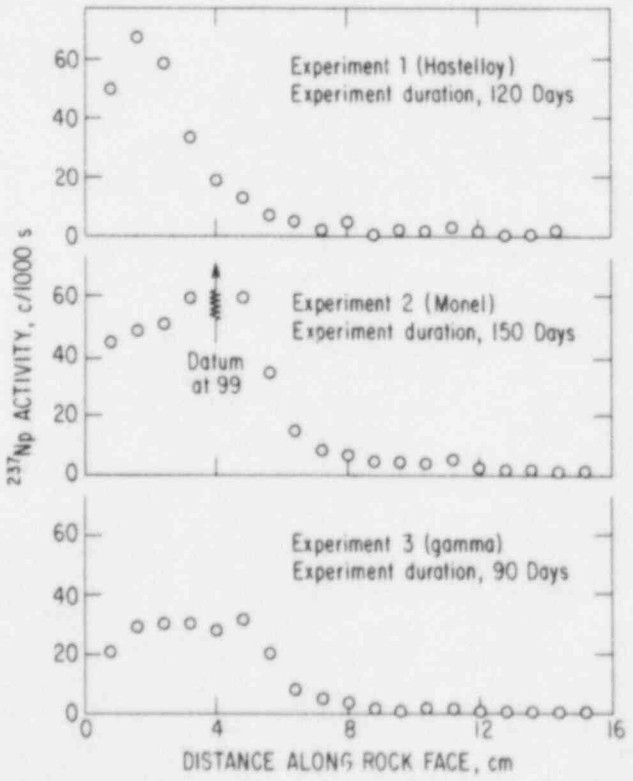

Fig. 3.7.

Spatial profiles of neptunium activity in analog experiments using unaltered basalt cores

To check for mass balance in the rock core vessel and to quantitate the neptunium activity profiles of Fig. 3.7, one face of the rock core fissure from analog experiment 1 was chemically treated to remove the neptunium and plutonium that had sorbed on it. The results of the extractions (described in Sec. 2.6.3.3) are shown in Table 3.34. The measured content of ^{239}Pu of the second extraction was at background levels, which implies that all the plutonium on the rock core was removed in the first extraction. The calculated amounts of the ^{237}Np on the rock core, determined independently for each of two extraction steps, compared well with each other. The calculations were made by comparing the amount of ^{237}Np in the respective extracted solutions to the fractional loss of ^{237}Np activity measured on the rock core face (Bowers 1983).

Table 3.34. Extraction data for ^{237}Np and ^{239}Pu from a basalt core used in an analog experiment

Extraction Number	Volume of Leachate (mL)	Actinide Extracted in Solution (dpm/mL)		Activity of ^{237}Np Remaining on Core After Extraction (%)	Total Actinide Deposited on Core (dpm)	
		^{237}Np	^{239}Pu		^{237}Np	^{239}Pu
1	200	7.16	0.70	57.1	6670	680
2	100	13.34	$\leq$0.007[a]	17.8	6730	

[a]No ^{239}Pu activity was detectable above background levels.

The concentration of ^{237}Np entering the rock core was ~5.7 dpm/mL and was ~0.03 dpm/mL at the rock core's exit. The total volume of groundwater passing through the rock core was 1675 mL. These data would predict 9500 dpm of ^{237}Np was retained in the core vessel (on either the rock surface or on the bentonite at the face of the core inlet). Previous results of gamma spectroscopic analyses of bentonite samples in the experiment showed there was ~1600 dpm ^{237}Np in bentonite deposited at the core inlet. When this amount is subtracted from the total ^{237}Np activity that entered the core holder, the predicted ^{237}Np activity on the rock fissure is 7900 dpm. This compares well to the measured value of 6700 dpm.

No mass balance of ^{239}Pu was attempted. Since bentonite with associated ^{239}Pu was found at the inlet to the core, a relevant mass balance for ^{239}Pu would entail the destructive analysis of all bentonite samples to measure their alpha activity.

3.4.3.2 Cesium Behavior

Figures 3.8 through 3.10 show the spatial profiles of ^{137}Cs along the rock core face of analog experiments 1, 2, and 3, respectively. The error bars represent the statistical error in counting and do not show other errors such as those generated by counting geometry and surface roughness. The background count rate (~17 c/1000 s) has not been subtracted from the total net count rate. The gamma counting data from experiment 6 (presented in Fig. 3.11),

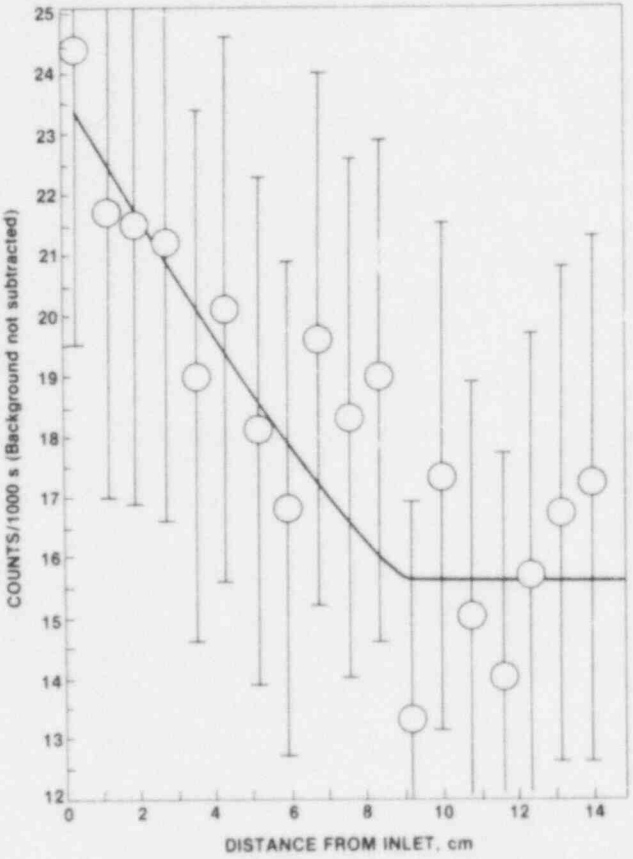

Fig. 3.8.

Gamma signal from ^{137}Cs vs. distance along the axis of the rock core from analog experiment 1. The inlet of the rock core is at the left of the figure.

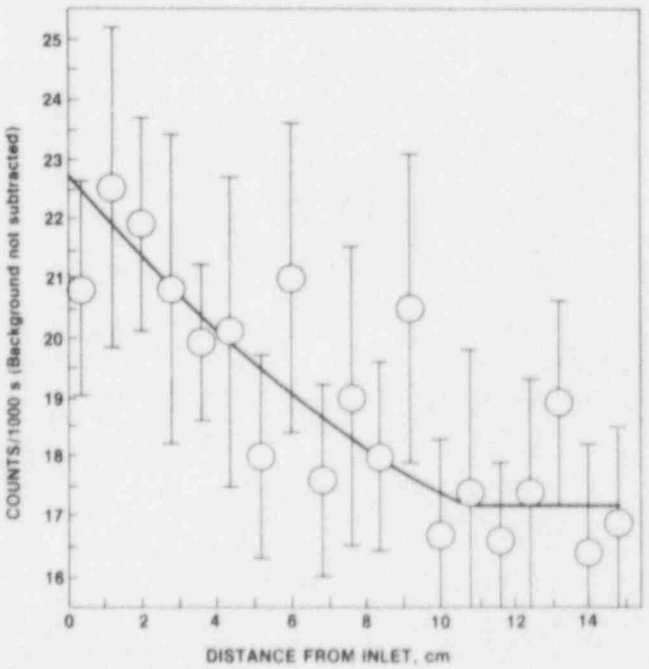

Fig. 3.9.

Gamma signal from ^{137}Cs vs. distance along the axis of the rock core from analog experiment 2. The inlet of the rock core is at the left of the figure.

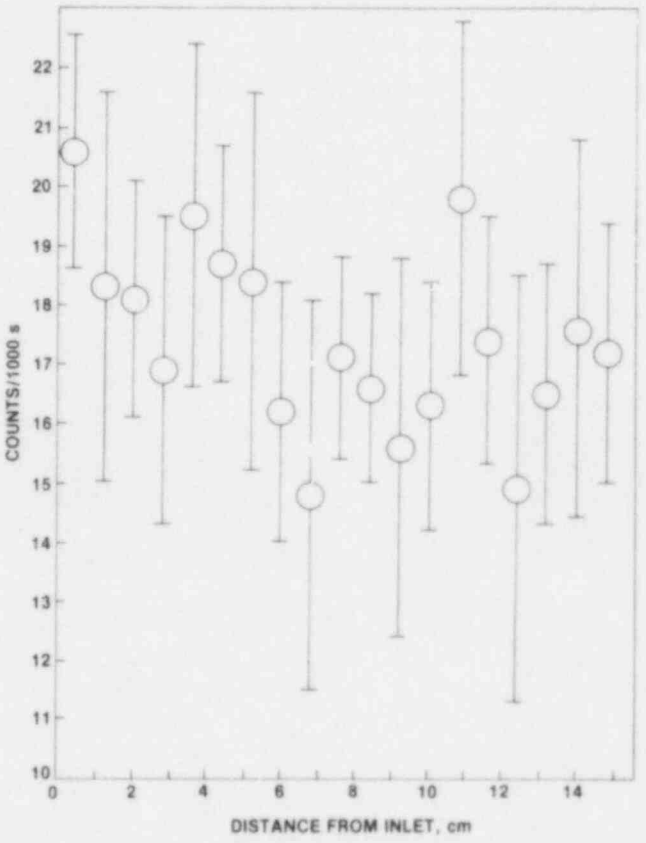

Fig. 3.10.

Gamma signal from ^{137}Cs vs. distance along the axis of the rock core from analog experiment 3. The inlet of the rock core is at the left of the figure.

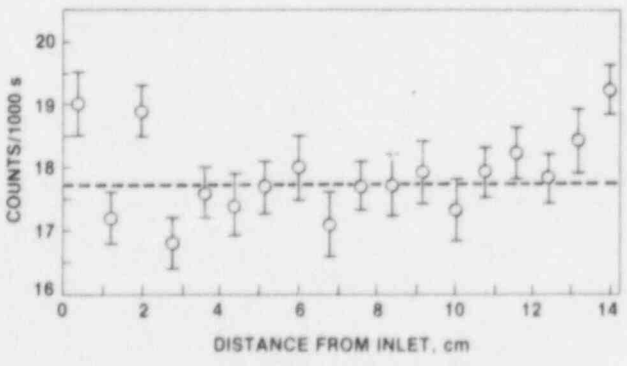

Fig. 3.11.

Gamma signal from ^{137}Cs vs. distance along the axis of the rock core from analog experiment 6. The inlet of the rock core is at the left of the figure.

where the experimental duration and the activity levels on the rock core were lower than in experiments 1, 2, and 3, showed no measurable ^{137}Cs profile. These data for experiment 6 establish the fact that, except for perhaps the first and last positions, the measured gamma signals (due to background in the laboratory) do not depend on the position of the rock core over the detector.

These gamma-scanning experiments of the rock were performed primarily to measure activity levels of ^{237}Np and ^{241}Am, which emit gamma rays of 86.5 and 59.5 keV, respectively. A shield made of 4-mm-thick lead was used so that the signal measured from one 0.8-cm section of the rock core did not include counts from another section. Because ^{137}Cs emits an energetic gamma ray (662 keV), this thickness of lead was inadequate for totally isolating the shielded portions of the rock core. Based on the geometry of the detector and the rock core and on the attenuation of the gamma signal through the lead shield, the signal from one 0.8-cm section would contribute 14% of its signal to its neighboring sections and 3% to the signal recorded two sections away from it. This effect makes the signal of ^{137}Cs appear broader than it actually is, but does not invalidate the conclusions stated below.

The dearth of cesium on the fresh rock cores is consistent with analyses showing little loss of cesium from solutions (Sec. 3.4.1.4). Unaltered basalt surfaces have some ability to retain cesium, but little cesium occurs on unaltered cores compared to the greater amounts on altered cores (analog experiments 4 and 5, Figs. 3.12 and 3.13). This is consistent with sorption data that show greater retention of cesium (higher distribution coefficients) on hydrothermally altered basalt than on fresh basalt (Guzowski 1983).

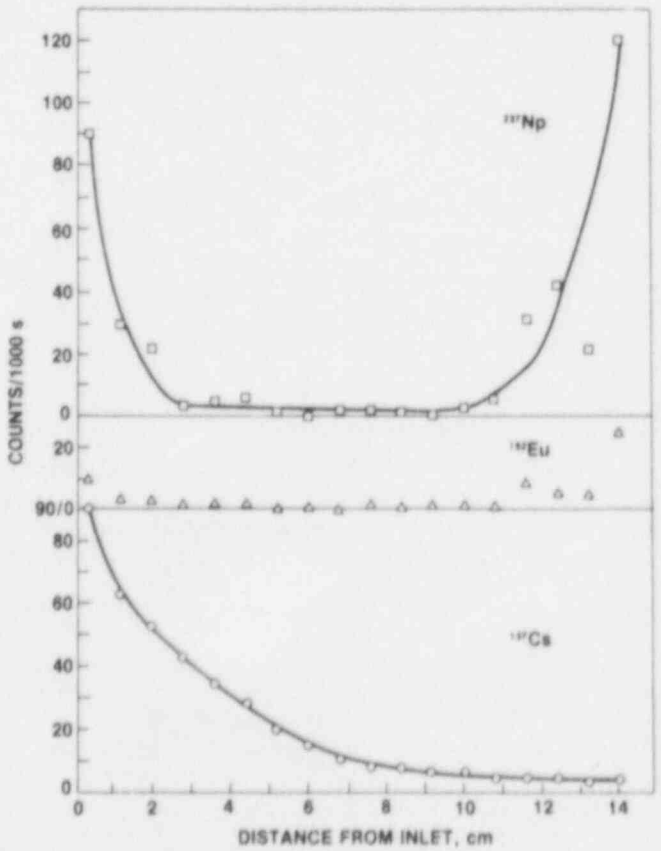

Fig. 3.12.

Gamma signals from ^{137}Cs, ^{152}Eu, and ^{237}Np vs. distance along the axis of the rock core from analog experiment 4. The inlet of the rock core is at the left of the figure.

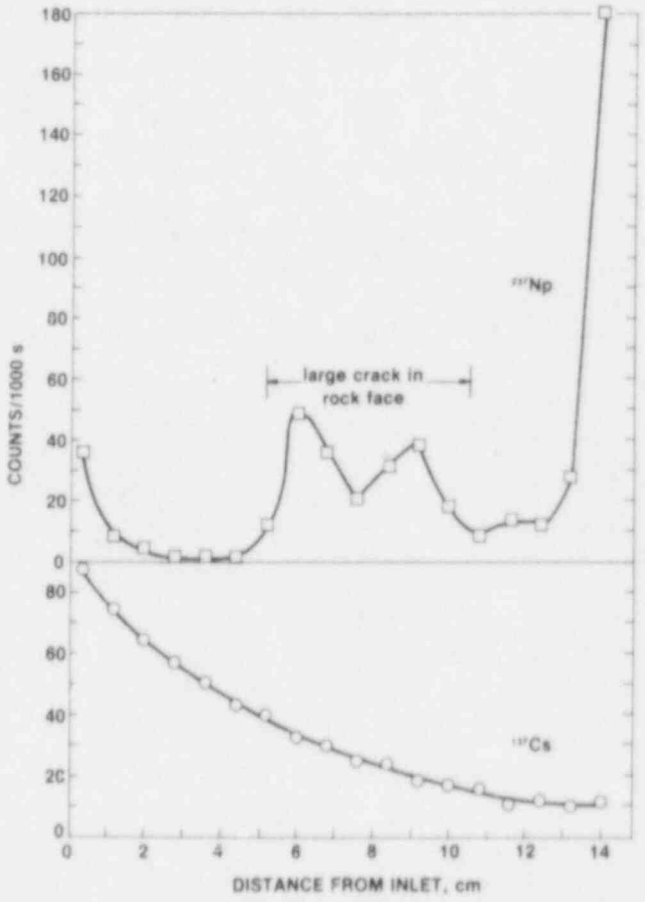

Fig. 3.13.

Gamma signals from ^{137}Cs and ^{237}Np vs. distance along the axis of the rock core from analog experiment 5. The inlet of the rock core is at the left of the figure.

Looking more closely at the profiles of ^{137}Cs on the altered rock cores of experiments 4 and 5, one should note that the maximum signals recorded at the inlets of both rock cores are experimentally equivalent; furthermore, they are about 14 times higher than what appears to be a saturation value for the unaltered cores.* Also noteworthy is that experiment 5, which contained the altered waste glass wafer with the separated surface layer and consequently had higher concentrations of glass leach products (as evidenced by high Pu, Np, and U outlet sample concentrations), showed higher saturation of the surface by cesium.†

---

*The saturation surface concentrations of cesium in the unaltered rock cores (Figs. 3.8-3.10) are inferred by comparing the activity levels at the inlet (~22 c/1000 s) and at the outlet (~17 c/1000 s), thus estimating the background level to be 17 c/1000 s and the saturation level to be 5 c/1000 s.

†It should be noted that ^{137}Cs was not the only isotope of cesium in the waste glass. The radioactive glass contained 1.14% Cs_2O and 0.65 μCi/40 g of ^{137}Cs; for every atom of ^{137}Cs in the glass, there are 6×10^7 atoms of stable cesium.

The ^{237}Np data for experiments 4 and 5 (Figs. 3.12 and 3.13) corroborate the results of the outlet-sample analyses. Almost all the neptunium that entered these cores passed through them. The only locations where signals were recorded were at the entrance and exit in both experiments and in the vicinity of a large fracture on the core face in experiment 5. The fracture is perpendicular to the major fracture in the rock and did not conduct water.

There was a small signal due to ^{152}Eu measured on the core of analog experiment 4 (Fig. 3.12) that appears to follow the behavior of neptunium. There was no measurable ^{152}Eu signal for the core of experiment 5. No gamma signals were found for the core of analog experiment 6.

3.4.3.3 Possible Mechanism for the Differing Profiles of Neptunium and Cesium on Basalt Cores for Analog Experiments 1, 2, and 3

The following three observations can explain the spatial profiles of neptunium and cesium and the differences between them: (1) neptunium was retained by fresh basalt fissures and not at all by laboratory-altered basalt fissures (Sec. 3.4.1.2); (2) cesium was retained far less effectively by fresh basalt fissures than by laboratory-altered basalt fissures (Sec. 3.4.1.4); and (3) basalt possesses a finite capacity to modify groundwater--as a basalt surface is continually contacted with fresh groundwater, the surface eventually modifies to become passive to that groundwater (Sec. 3.2.3.1).

At the beginning of analog experiments 1, 2, and 3, which used unaltered repository components (see Table 2.1 in Sec. 2.1), all the basalt fissures were unaltered and, therefore, had a high ability and/or capacity to sorb neptunium ions and a fair ability and/or capacity to sorb cesium ions from the groundwater. As neptunium ions entered the fissure they would react with the rock and be removed from solution. Based on the expected low distribution ratio of cesium, some of the cesium ions would be sorbed, some would pass farther down the fissure to be eventually sorbed, and some would pass completely through the fissure.

As fresh groundwater continued to enter the core fissure, it modified the rock with which it first came in contact, and it was likewise altered by that surface to be a solution more compatible with unaltered basalt surfaces. Therefore, the basalt surfaces at the inlet of the core would be more greatly altered by the groundwater than would subsequently contacted surfaces. This process would continue until all the basalt fissure was modified and, therefore, compatible with the groundwater entering it. Because the exiting groundwater of analog experiments 1, 2, and 3 had a steady-state composition far different than its entering composition (Sec. 3.2.1), the time required to completely modify the basalt fissure is greater than the four- to five-month duration of these experiments.

But, as this alteration process proceeded in an experiment, cesium and neptunium species responded differently. Because cesium is sorbed more strongly by altered basalt than by unaltered basalt, cesium ions would remain in solution initially, and would begin to be adsorbed later at the entrance of the fissure as it became altered by the passing groundwater. As time progressed, the cesium profile on the initially unaltered rock surface would look more and more like that on an altered rock core.

Because neptunium sorption behavior is different than that of cesium, its spatial profile on the rock would also be different. As neptunium ions entered the fissure, they were sorbed by the rock surface (as would be characterized by a high distribution ratio). Most ions were sorbed immediately; some moved downstream as dictated by the magnitude of the neptunium interaction with basalt. As the entering groundwater began to alter the rock surface near the inlet, the distribution ratio dropped dramatically for that region. Neptunium that was sorbed in that region went back into solution to be resorbed on the unaltered surfaces downstream. As this process continued, the profile seen in Fig. 3.7 developed. These profiles suggest, by the positions of the maxima, that in the time span of these analog experiments less than one-fourth of the basalt fissure was altered to be compatible with the incoming groundwater.

4. DISCUSSION

4.1 RELEVANCE OF EXPERIMENTAL RESULTS TO REPOSITORY PERFORMANCE

Basalt from the Pomona flow of the Pasco Basin was used in this study. The Pomona flow is part of the Saddle Mountains basalt, which is in the Columbia River Basalt Group. The Columbia River basalts have limited ranges of chemical, mineralogical, and physical characteristics. However, the basalts can be distinguished chemically. For example, in terms of magnesium content, high magnesium basalts such as the Pomona contain ∿7 wt % MgO, and low magnesium basalts contain ∿3.6 wt % MgO with a range of 3.3 to 4.4 wt % experienced in individual flows such as the Umtanum. On a chemical and mineralogical basis, the Pomona flow is typical of the high magnesium basalts, which need to be understood in terms of radioelement migration for evaluations of repository performance.

The characteristics of radioelement transport in the Pomona basalt itself are of direct relevance to performance because the basalt is at a depth of 250 m at a proposed repository location (Rockwell Hanford Operations 1982) and, therefore, would lie between the proposed repository and the surface. This is true of the Pomona flow if either the Umtanum or the Middle Sentinel Bluffs is selected for the repository. The Pomona will be part of a geologic barrier isolating the waste from the biosphere. The Pomona flow is the flow in which the Near-Surface Test Facility of the Basalt Waste Isolation Project is constructed.

The groundwater solution used in this work was prepared to represent the composition of groundwater from Well DC-6, Grande Ronde Formation, with the water primarily from 200 m below the Umtanum unit. The composition was reported by Gephart (1979).

For an understanding of issues relating to the performance of a proposed repository, element behavior in solutions having a variety of compositions will have to be known. These composition are not <u>just</u> those sampled from the site, but as we have seen, reactions with fresh rock surfaces can produce compositions that do not now exist at the site. Based on the results of the work presented here, water having lower sodium levels and higher calcium and magnesium levels than currently existing groundwaters would be expected to form in the repository due to the fresh basalt surfaces that are produced by mining basalt and crushing basalt for backfill.

The basalt used in this work initially had fresh surfaces produced by mechanically splitting the rock. Similarly, in the repository, new rock fissures will be introduced by the mining operation and by backfilling with crushed basalt. Therefore, the work with fresh surfaces reported here is of immediate relevance to repository performance. Also, the results with fresh surfaces are most likely to be comparable to results of the myriad of simpler tests of leaching, sorption, and solubilization that have been run using rock with fresh surfaces. Most of the data that exist from these tests are for crushed rock.

The understanding of radioelement behavior on old rock surfaces is also of fundamental importance to repository performance. One way of studying this, demonstrated in this program, is to alter the material in the laboratory to represent expected conditions caused by aging.

Another approach that has been demonstrated (Seitz 1981a) is to core old fissures from rock in the field, take the cores back to the laboratory, and study migration in the fissures of these old cores. By relating the results from this type of study to results from fissures altered in the laboratory, we can understand more fully how natural aging will affect element migration.

Sampling of natural fissures exhibits the complication that the evolution of the fissure surfaces is generally poorly known. Groundwater composition, groundwater flow, and temperature (all as a function of time) together with the age of the fissure should be known if we are to be able to generalize the results of migration in natural fissures to migration in fissures created or disturbed by repository siting.

The nominal water flow rate used in the analog experiments reported here was ~0.5 mL/h. This flow rate produced a flow through the bentonite- and glass-containing vessels of 31 m/yr (0.36 cm/h) and through the rock fissure of 252 m/yr (2.88 cm/h). The Darcy velocity for the rock core is ~1 m/yr (0.014 cm/h). [The Darcy velocity is the specific discharge (discharge per unit area). The specific discharge is easily measured and may be cited as the groundwater flow rate, but it must be clearly differentiated from the microscopic velocities associated with the actual paths of water as it winds its way through the rock.]

The ambient temperature of the Umtanum flow, which is a flow proposed for the repository, is 58°C (Rockwell Hanford Operations 1982). Thus, the temperature of 90°C used experimentally represents a temperature slightly above ambient that may exist, for example, after a time when the rock has cooled from a higher temperature achieved due to heat from radioactive decay.

The groundwater solution used in the analog program was purged with nitrogen to remove dissolved oxygen, which would be a dominant oxidant in the water, having a dissolved concentration of ~8 mL/L when equilibrated with air. By removing the oxygen, the redox potential of the constituents of the groundwater can be governed by the reaction of redox-sensitive species in solution, such as neptunium, with backfill, basalt, etc. Therefore, the experimental results would be most representative of the redox state that would occur in a repository with essentially all air excluded.

The situation in which oxygen is introduced to the groundwater solution is also of interest because the repository will initially contain large quantities of air. This issue was not addressed in the limited number of experiments that were done in this program.

The use of artificially introduced reductants such as hydrazine to the groundwater solution was excluded in this work because the chemicals would override the very attractive possibility for these experiments that the repository constituents be allowed to influence the redox states of the solute ions.

The oxidation states of the actinide elements, plutonium, neptunium, and uranium, are initially those in the simulated waste glass. The oxidation states can change upon reaction with the ferrous-ferric redox couple in the water and the ferrous ion on the rock surfaces (Jacobs 1981; Meyer 1984). At the pH range of 8 to 10, the ferrous ion would reduce higher oxidation states to Np(IV), Pu(IV) and U(IV) (Apted 1982; Duffy 1982; Moody 1982; Rydberg 1981). This is most likely still true with the complexants, e.g., the CO_3^{2-} and F^-, that are present in the groundwater.

The radiochemical species in solution can be estimated from published thermodynamic data knowing the composition of the groundwater. For example, in groundwater having concentrations of 1.26×10^{-3} M total carbonate and 1.36×10^{-2} M Na^+, and a pH of 10 (such as the solution used in this work), the major neptunium species are the oxo-cation of Np(V), NpO_2^+, and its complexes NpO_2OH, NpO_2HCO_3, $NpO_2CO_3^-$, and $NpO_2(CO_3)_3^{5-}$, the last being the dominant species (Carnahan 1984). We can expect that the oxidized neptunium constituting these species is reduced upon contact with basalt (Meyer 1984).

The approach represented in the work reported here is one of only a few approaches that combine repository components and is the only approach in which groundwater is moved across the components. Flowing groundwater is the most credible dispersant that could upset the isolation of nuclear waste in a repository. From this approach, one can examine whether the results of systems experiments are understood in terms of simpler experiments (batch adsorption experiments, solubility limits, etc.). If the results are understood, then there is confidence that the important phenomena have been identified in the cases that are studied. If the results are not understood, then the important fact can be sought that has been left out of the analyses.

Results from these specific analog experiments can be generalized by comparing the results to predictions of models of element migration. The analog experiments are very simple compared to a repository because flow paths, flow rates, temperature, solution composition along the flow path, etc., are known with great accuracy. Models of element migration should be able to predict such experimental results quite accurately. Then the models, confirmed for a few key cases studied experimentally, can be used to generalize to other cases.

The comparison of laboratory results with model predictions has begun (Carnahan 1984; Steindler 1984b) and could be accelerated by identifying other models that include descriptions of rock alteration, distinctions between fresh and altered rock, and other phenomena identified in these experiments to be important to descriptions of repository performance.

4.2 LABORATORY ALTERATION RELATIVE TO EXPECTED AGING

4.2.1 Alteration of Repository Materials

One objective of the laboratory analog program was to assess changes in radioelement migration that would be expected as a result of the aging of nuclear waste, clay backfill, and rock. This was done by observing migration in materials that had been altered to reflect aging in a waste repository.

Aging of the radioactive waste glass, the engineered barrier, and the host rock will occur after emplacement of waste in a nuclear waste repository. The aging will involved many processes, such as devitrification, hydration, dissolution, radionuclide transmutation, radiolysis, radiation damage, and chemical reaction.

The aging depends on the compositions of the materials (waste loading, chemical additives, etc.) and is influenced by open-system variables (groundwater flow, groundwater composition, etc.) that may be influenced by the rock (e.g., the composition of groundwater will change upon contact with fresh rock surfaces). The aged states of repository materials also depend on the size and geometry of breaches of the waste package.

Responding to so many variables, a material may acquire any one of many possible outcomes (aged conditions) depending on the exact conditions experienced. Indeed, many different aged conditions of one material (for example, the nuclear waste glass) may exist in a single repository. In fact, several different aged conditions of a waste glass could plausibly be expected in a single canister. The generation of three different aged conditions simultaneously on one waste solid is illustrated in Fig. 4.1.

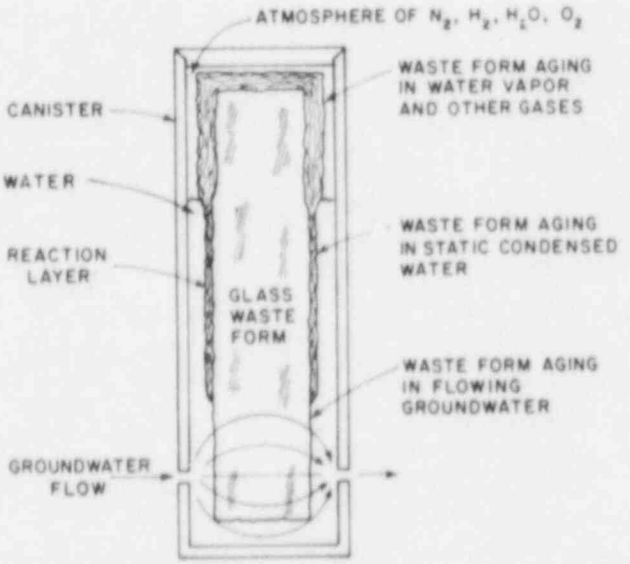

Fig. 4.1.

Waste solid undergoing a variety of aging processes

To illustrate the possible results of aging, we use the model of a breached canister shown in Fig. 4.2, in which a small hole in the canister would allow hydration but no loss of leached constituents from the canister. Cesium is considered here to represent the leached constituents. Two holes in the canister would allow both hydration and the loss of cesium by flowing water. The final condition of the waste would depend on the times of formation of the holes and the sizes of the holes. A hypothetical plot of the possible results described by the hydration and mass-loss parameters is illustrated in Fig. 4.3 for the three periods, 500, 1000, and 2000 yr. Another breach model would give different results.

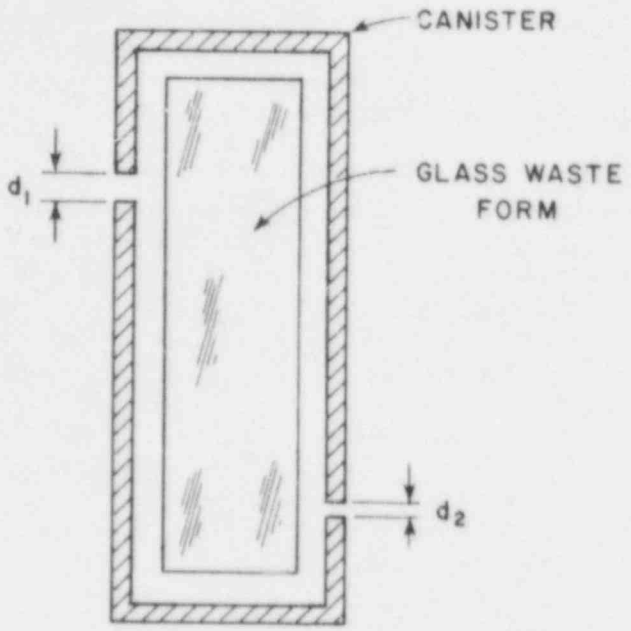

Fig. 4.2.

Model of canister breach in which d_1 and d_2 are gap widths with $d_1 > d_2$. (The gaps are at different hydraulic pressures. An increase in d_1 would provide an increased supply of groundwater for hydration. An increase in d_2 would provide an increased flow-through of groundwater.)

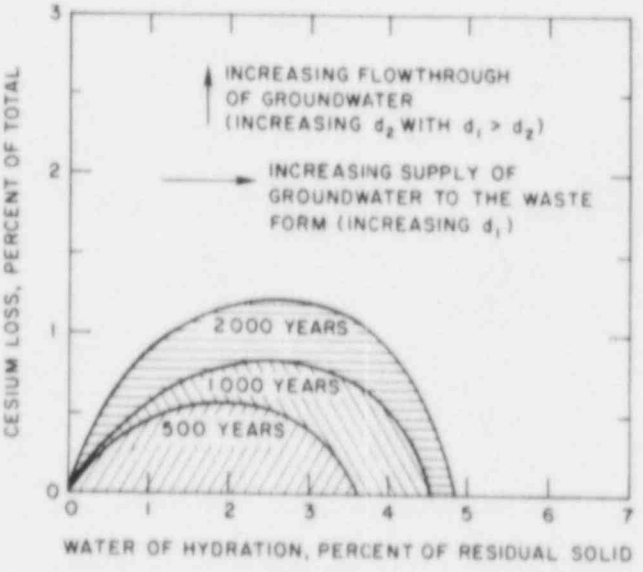

Fig. 4.3.

Hypothetical relationship of cesium loss to water of hydration during aging (see Fig. 4.2 for descriptions of d_1 and d_2)

The point of this discussion is that a great variety of results from aging are possible for repository materials. Different products of aging may exist simultaneously in a repository containing hundreds of waste canisters. The practice in this program was to produce for each material two altered conditions (that could be correlated to aging for 1000 and 2000 yr at specific conditions). The laboratory aging procedures were selected to produce the modifications of waste package behavior that might be found to be significant in terms of nuclide release and migration.

Aging processes evaluated for their applicability to radioactive waste glass are: hydration at elevated temperature, devitrification, radiation damage, and leaching. For basalt, aging processes considered for the selection of a laboratory alteration process were leaching, hydration, and radiation damage. For bentonite in combination with granulated basalt (i.e., backfill), leaching, hydration, and recrystallization were considered for the selection of an alteration process.

4.2.2 Alteration of Waste Glass

Waste glass will age in the hydrous and thermal environments of a waste repository. In the presence of water vapor, the dry waste glass will react to form a hydrous layer on its surface (Bates 1982a, 1982b). This hydrated layer could later be leached by liquid water. Hydration in vapor is, therefore, considered a major aging phenomenon of waste glass and would result, for example, from a breach in the canister during the early thermal period of the repository.

During hydration in the atmosphere, radioactive elements would be released from the glass structure but not detached from the waste form. After hydration in the atmosphere and submersion in water, the radioactive elements could quickly be dissolved. This rapid accumulation in groundwater may have important consequences to migration and, therefore, was of interest to us in this program.

Devitrification is not expected to be an important phenomenon in the aging of waste. At the maximum design temperatures for the repository (temperatures below 500°C), waste glasses are not expected to devitrify (Turcotte 1980). Furthermore, devitrification in the absence of cracking seems to have little effect on the leach rates of the glasses that are candidate waste forms (Wald 1979; Weber 1979). Devitrification may occur during waste processing that precedes storage, however.

Radiation damage, primarily from alpha-recoiling nuclei, is not likely to be an important aging mechanism for 1000-year-old waste, but may be important for older waste. The alpha-recoil damage has no effect initially, when the radiation-damaged areas are isolated and do not overlap to form a connecting network. The consequences of the damage on the chemical stability of the glass after a time (when the integrated alpha-recoil density is high) are an area of controversy (Dran 1980; Hall 1976). The estimates of elapsed time before alpha-recoil damage may be important range from 2000 yr to more than $\sim 10^6$ yr (Dran 1980; Mendel 1976).

Leaching was not selected specifically as an alteration process for glass because dissolution is already an integral part of the laboratory analog experiments. Also, leaching of the waste prior to an experiment would be expected to produce a waste form that is less chemically active than fresh glass; therefore, extensive leaching would not be expected to modify waste form properties in a detrimental way.

Factors that affect the hydration of glass are temperature, water vapor, pressure, glass composition, vapor species other than water, and time. The relation of hydration to time and temperature has been studied for obsidian (Ericson 1977; Ewing 1979; Friedman 1976; Tombrello 1978), reviewed by the NRC (Barkatt 1980), and can be roughly approximated by the relationship,

$$k = Ae^{-E/RT} \tag{4.1}$$

where k is the amount of hydration (μm^2/1000 yr), A is a constant, E is the activation energy of the hydration process (cal/mol), R is the gas constant [cal/(mol·K)], and T is temperature (K).

Using the parabolic rate law derived from considerations of diffusion, the thickness, d, of the hydration layer is given by

$$d = (kt)^{1/2} \tag{4.2}$$

where t is the time in units of 1000 yr. These relationships incorporate (in the values selected for A and E) the effects of water vapor pressure and glass composition, both of which are known to affect the amount of hydration. The influences of water vapor pressure and glass composition on hydration are ignored if A and E are treated as constants for all water pressures and glass compositions. In these studies, water is assumed to be the only important vapor species.

To simulate a repository condition using our present understanding, it is necessary to assume that the above relationships are valid, to ignore the effect of water pressure, and to use data obtained for obsidian. When this is done, the value adopted for A is 1×10^{16} μm^2/1000 yr and for E is 2×10^4 cal/mol (Tombrello 1978). These values are comparable to those obtained from recent measurements of sodium movement in obsidian (White 1983) and obsidian hydration with water (Michels 1983).

Table 4.1 shows data calculated from Eqs. 4.1 and 4.2 as well as data calculated assuming the hydration layer is removed after it reaches a thickness of 20 μm, exposing a new surface, and that the process begins again. If the aging conditions in a repository are assumed to be water vapor at a temperature of 100°C for 1000 yr, the hydrated layer is estimated to attain a thickness of 150 μm. However, this thickness could vary between 318 and 17 μm/1000 yr on the basis of the full range of known values for A and E [A ranging from 1.4×10^{15} to 1.8×10^{16} μm^2/1000 yr and E ranging from 1.92×10^4 to 2.07×10^4 cal/mol, as reported by Friedman (1976)]. Whether these values for waste glasses would fall within these ranges is not known. Given the uncertainty in the thickness of the hydration layer, consideration of a more detailed thermal history for a repository does not appear to be warranted.

To simulate the aging process, hydration was done at a temperature of 340°C. Using Eqs. 4.1 and 4.2, waste glass exposed to vapor at this temperature for 17 days would have a hydration layer thickness of 180 μm, which is near the thickness of 200 μm to which the glass was observed to have been hydrated. One hydrated surface of 200 μm was observed to slough off.

Table 4.1. Calculated hydration layer thicknesses[a]

Temperature (°C)	Total Layer Thickness Formed in 1000 years (μm)	
	From Eqs. 4.1 and 4.2	Assuming Exfoliation[b]
0	0.2	0.2
25	6	6
75	65	200
100	150	1500
125	380	6700
175	1500	1×10^5
225	4000	1×10^8

[a] $A = 1 \times 10^{16}$ $\mu m^2/1000$ yr and $E = 2 \times 10^4$ cal/mol.

[b] That is, the hydration layer is formed to a thickness of 20 μm and sloughed off.

4.2.3 Alteration of Basalt

Recent fracture surfaces of Pomona basalt (similar to the rock surrounding a repository) will age in the hydrous and thermal environments of the waste repository, primarily by reactions with groundwater. Devitrification and radiation damage are not considered factors in the aging of basalt surfaces because (1) it is not likely for a glass to devitrify at temperatures likely to be attained in a repository (Turcotte 1980) and (2) basalt will not be subjected to a significant alpha-recoil dose by the low activities of actinides that will be present in the groundwater streams or sorbed on its surface. (The gamma flux experienced in the near field is probably ineffective in producing structural damage, also.) Radiation from rock surfaces can produce radiolysis of groundwater, which might alter migration, but this would not be considered an aging process.

One way of obtaining aged basalt surfaces is to sample old fissures (Seitz 1981a). This approach has the shortcoming that the length of time and conditions under which the fissures were aged are generally unknown for basalts on the Columbia Plateau. Therefore, this approach was not taken.

The alteration process selected for basalt in this laboratory work is hydration in liquid water at elevated temperature. The laboratory alteration is comparable to aging expected to occur naturally in recent fissures that quickly become saturated with groundwater. A great deal of information on the alteration of Pasco Basin basalts by groundwater, meteoritic water, and humidity is presented in several reports (Ames 1980; Benson 1978, 1979, 1980; Teague 1980). Unfortunately, the specific conditions under which the basalts were altered are not known. As might be expected from the variety of conditions leading to alteration, there are great differences in alteration products from place to place.

The alteration products generally cited in the references are: smectites, illite, clinoptilolite, mordenite, silica (cristobalite, tridymite, opal, chalcedony, quartz), pyrite, gypsum, calcite, apatite, and halloysite.

As a general observation, the groundmass (mostly glass) and pyroxene are seen to alter before plagioclase (Benson 1979, 1980; Teague 1980). Alteration products are very heterogeneous in the flood basalts; some fractures exhibit no alteration products (Benson 1978). Clays in some fractures occur in different-colored layers, with many minerals present (Ames 1980). Different vesicles sometimes record different portions of the alteration sequence. These differences are probably due to differences in environment (groundwater flow, groundwater composition, temperature, etc.) rather than to differences in the age of the flow.

There is a generalized sequence of precipitation observed in vesicles: clay, then clinoptilolite with or without silica, then clay. With vesicles, smectites are observed in the upper portion of the stratigraphic column, and clinoptilolite and silica in the lower portion.

Clinoptilolite is replaced by mordenite at depths greater than 880 m (Benson 1979, 1980); mordenite is among the most siliceous zeolites, and its formation coincides with the advanced stages of silica diagenesis at greater depths. (Because the proposed waste repository is deep, conditions that are expected to produce mordenite were selected for laboratory alteration of basalt.)

Several attempts have been made to model the reactions that have occurred to age basalt surfaces (Benson 1978, 1979, 1980; Deutsch 1982); however, these calculations were limited by a lack of thermodynamic constants and assumption of low ambient temperature (25°C). Also, the models predicted the formation of many phases not observed (Benson 1980; Deutsch 1982). These calculations, therefore, have not been used to plan laboratory alteration procedures for the basalts.

The approach selected for the laboratory modification of basalt surfaces to represent aging is hydrothermal treatment of fresh basalt surfaces. Water formulated to represent the composition of water from the Grande Ronde formation was used as the hydrothermal fluid. To estimate how the laboratory treatments of the basalt relate to long-term aging, the relationship between hydration rim thickness, d, and time, t, expressed in Eq. 4.2 for the waste glass was considered valid for basalt, also. The zero-order dissolution constant, k, is constant at a given temperature.

For the calculation, the zero-order dissolution constants of work by Holloway, cited in Apted (1982), which measured SiO_2 removal from basalt in simulated groundwater, were corrected using an activation energy of 5.3 kcal/mol as suggested by the temperature dependence of data on weight loss from rhyolites (Allnatt 1983; Karkhanis 1982) and SiO_2 removal from basaltic glass and diabase in seawater (Seyfried 1981). This resulted in a calculated hydration rim thickness of 3600 μm for basalt in contact with groundwater at 100°C for 1000 yr. Reaction of the basalt at a temperature of 320°C for 27, 30, and 60 days is calculated to produce alteration rims of 530, 560, and 760 μm, respectively. On the basis of this calculation, the laboratory treatment of basalt would be judged to be comparable to, but not as severe as, a 1000-yr treatment at 100°C (the laboratory alteration producing a 760-μm layer in 60 days rather than the 3600-μm layer expected after 1000 yr of 100°C treatment).

The natural fissured surfaces of the 12-million-year-old Pomona Flow basalt used in this work exhibited ∿0.5- to 1.0-cm-thick alteration rims. This is similar to alteration rims of ∿0.5-cm thickness seen on many other basalts in the Pasco basin, which range in age from ∿12 million yr for flows near the surface to 16.5 million yr for the lower Grande Ronde flows. Present ambient temperatures range from ∿25°C in the surface flows to 58°C in the Umtanum flow (Rockwell Hanford Operations 1982).

On the assumption that an alteration-rim thickness of 1 cm would be developed over the age of the basalt, a rim thickness of ∿90 μm would be expected on initially fresh surfaces experiencing the ambient temperature of 58°C for 1000 yr. This alteration rim is considerably thinner than that seen on many basalt surfaces, suggesting that the alteration had taken place at elevated temperature such as that used experimentally to alter the basalt.

The comparisons of reaction rates at different times and temperatures do not consider the reaction products that are produced. An understanding of reaction products produced by laboratory alteration can be obtained by noting how these altered materials react with groundwater known to exist now in contact with aged basalt.

As stated in Section 3.2.3, the basalt surfaces altered at 320°C reacted very little with groundwater at the 90°C temperature used in the analog experiments. This suggests that the reaction products produced at 320°C are compatible at lower temperatures with the groundwater, as are those on the naturally aged surfaces at the repository site. On this basis, the laboratory alteration could be said to produce, chemically, products similar to those that occur naturally.

4.2.4 Alteration of Bentonite

Bentonite is a hydrous clay formed at low temperature. This clay, combined with granulated basalt, is now under consideration as the backfill for a waste repository in basalt. Aging of the clay in the presence of water and elevated temperature may produce dehydration and recrystallization with some replacement of exchangeable ions by ions from the water.

Heating of the clay in a dry environment may dehydrate the clay, but the clay is not likely to become dry in a basalt environment. Therefore, treatment of the clay in liquid water at elevated temperature was employed as the laboratory process for altering the clay and basalt.

Based on work with a sodium bentonite from Wyoming, MX-80 Volclay (American Colloid Co.), Swedish workers have inferred geologic evidence that the bentonite will retain its desirable adsorption and swelling properties at a 500-m depth in granite (Jacobsson 1978; Pusch 1978). Similarly, no extensive modification of bentonite in basalt is suggested by our current understanding.

Although bentonite may not alter to a nonsmectitic mineral in a basaltic environment, it may be modified to some extent. Temperatures at the interface of the canister and engineered barrier may be as high as 300°C (Taylor

1979). The hydrothermal treatment to which we subjected the bentonite was the same as that selected for the basalt. The treatment did not change the mineralogy of the clay to a perceptible extent, but did change the physical properties (color and agglomeration) to an extent that was readily recognizable. Inasmuch as the bentonite will be subjected to temperatures greater than those to be imposed on basalt in a repository, and the treatment given to the basalt is comparable to that expected to occur with age, the treatment given to the bentonite in this program is considered not to lead to alteration in excess of what might be expected in an actual repository.

Because the temperature of 320°C used in the hydrothermal treatment is not substantially higher than expected in a repository (300°C), we assume that any result seen using laboratory-altered bentonite might have immediate relevance to its performance upon aging.

4.2.5 Compatibility of Altered Surfaces with Groundwaters

The behavior identified in the auxiliary experiments was that the altered basalt surfaces were compatible with the groundwater solution used in the analog experiments. Also noted from the auxiliary experiments was that the surfaces were not compatible with modified groundwater solution (containing $[Na^+]$ of 680 instead of 320 mg/L). The altered basalt surfaces reacted with this modified solution to produce a solution near in composition to that used in the analog experiments. This result suggests that the hydrothermal alteration of basalt and bentonite is specific to one groundwater composition, with the hydrothermal alteration used in this program producing materials compatible with the present groundwater at proposed repository locations.

Because fresh basalt surfaces will be created by construction of the repository, the groundwater and basalt will react to produce a variety of groundwater compositions over time. Therefore, basing repository sorption and solubility parameters on one or a few groundwater compositions can be unsound.

4.3 IMPLICATIONS TO EVALUATIONS OF REPOSITORY PERFORMANCE

The results of this program have direct implications to evaluations of the near- and long-term performance of a repository. Based on the results of the project, we comment here on the issues, both specific and general, that were addressed in the project.

4.3.1 Specific Issues

(1) Do different metal alloys that are proposed for canisters of nuclear waste affect radioelement migration and, hence, potential repository performance?

Metals and their corrosion products may affect migration by reducing, sorbing, or complexing with radioelements that are leached from nuclear waste. Iron has been suggested as a repository component because it may lower the valence state of actinide elements and reduce their ability to migrate (Bolmgren 1981). Alternatively, competition or complexation with metal corrosion products in solution may enhance the mobility of radioelements.

Of the two corrosion-resistant metal alloys, Hastelloy C-276 and Monel-400, which were investigated experimentially, no differences in migration characteristics of uranium, neptunium, or plutonium were detected. Because these alloys are significantly different in composition, this lack of change in migration characteristics suggests that neither alloy affected radioelement migration. Clearly, there is no evidence that these alloys would be detrimental to repository performance. Other metals proposed for a repository, particularly metals with beneficial properties such as iron, which may be chosen to improve performance, could be investigated in future experiments to evaluate their influence on radioelement migration.

(2) Does radiolysis of groundwater solutions affect radioelement migration and, hence, potential repository performance?

The dissolution of plutonium from radioactive waste glass was found in this work to be enhanced, and that of neptunium to be depressed, by ionizing radiation. The species leached in a radiation field were determined to interact with bentonite and basalt to the same extent, within measurement capabilities, as the species leached in the absence of radiation. This observation suggests that no radioelement species produced by radiolysis migrates differently than species formed in the absence of radiation. Hence, the conclusion based on the conditions employed experimentally is that gamma radiation does not enhance the mobility of radioelements, even though it is seen to measurably affect the leaching of plutonium and neptunium.

(3) Does alteration of repository components, such as is expected upon aging of a repository, degrade repository performance or does it improve repository performance as commonly stated?

This is an issue because current regulations specify maximum allowable release rates from a repository for periods of thousands of years (U.S. Nuclear Regulatory Commission 1983). The most significant effects observed in this series of experiments were the greatly enhanced dissolution of plutonium, neptunium, and uranium from hydrated waste and the movement of these leached species through bentonite and basalt that were hydrothermally altered to simulate aging of the repository materials. In contrast, cesium was more strongly bound by the altered materials than by the fresh materials.

The laboratory alterations appear to produce changes that are expected upon aging. The altered basalt is chemically compatible with the groundwater solution as are naturally aged basalt surfaces now at the repository site. The temperature of 320°C used to alter the bentonite is not substantially higher than the maximum temperature of ~300°C suggested for the backfill. Inasmuch as these altered materials represent materials that would evolve upon aging, we conclude that natural aging will increase the potential for uranium, neptunium, and plutonium to migrate from the repository.

Repository performance with aging is not well understood on the basis of results of simple batch tests or from numerical modeling. Repository performance is generally assumed to improve with age because surface areas and ion exchange capacities of rock materials will increase with age. Consistent with this reasoning, cesium has been found to be more strongly bound to hydrated material found in rock fractures or between basalt beds.

In contrast with this thinking are the results for uranium, neptunium, and plutonium from this program, which show their increased mobility in altered materials. These results would suggest that long-term performance of a repository is a major issue that is not adequately addressed by currently employed concepts of radioelement mobility.

(4) What concepts and measurements (solubility products, leach rates, adsorption ratios, etc.) are sufficient to describe radioelement migration in systems with flowing groundwater?

To address this issue comprehensively would require that the conditions explored experimentally be modeled using measurements of radioelement characteristics to predict radioelement migration. Consistency between the observed migration and the model predictions would indicate that the concepts and measurements used in the model are sufficient to describe radioelement migration. Some modeling has been done (Carnahan 1984; Steindler 1984b) and directions for future modeling efforts are clearly apparent.

For the specific case of the leaching of radioactive waste glass, our experience is that measurements made to date are consistent with the leaching observed in the analog experiments. Comparisons were made in this work of the radioelement concentrations seen in these experiments to data from leach tests that were performed with distilled water or water with a single molecular component such as sodium bicarbonate. Inconsistencies between the results reported here and existing leach data could be attributed to differences in water compositions or in leach temperatures rather than to any deficiency in our concepts of leaching phenomena. Suggested by this comparison is that leach data for flowing water conditions should be generated using the range of groundwater compositions and temperatures expected in a repository.

(5) Are experimental programs that are now being undertaken to support repository development properly designed to address the subject of repository performance in the near and long terms?

One observation can be made in this regard from the results of the current program. Groundwater solution in contact with fresh surfaces of basalt was found to alter to a composition of water not presently found at the repository site. Yet, the modified composition of groundwater would be expected within the repository because of the large mass of freshly fractured basalt that would be produced upon mining basalt and crushing the basalt to backfill the repository. Only those solution compositions representative of groundwater at the repository site are considered in current testing programs (Jones 1982), suggesting that the results of such programs would not adequately represent expected repository conditions for considerations of performance.

4.3.2 General Issues

(1) Do laboratory studies economically contribute to our general understanding of repository performance?

Based on the results of this program, studies involving the use of materials and conditions that are reasonably expected in a repository can improve our understanding of repository issues. The experiments gave results in some cases that can be interpreted using results of simpler tests. The experiments highlighted the lack of data and the possible importance of those data in the cases where such comparisons cannot be made. Alternatively, complications of radioelement behavior that preclude making the comparisons are evident in the results of the studies, which can be included in future thinking about repository performance. The experiments were performed at a fraction of the cost of comparable field experiments and have given information about the behavior of radioelements within a well-controlled and accurately specified environment.

(2) Can we identify the interactions between repository components of most importance to repository performance under the conditions of the experiments? By corollary, can we demonstrate that some interactions are not important to issues of repository performance?

The completed experimental program presents a good example of how repository interactions may be ranked in importance to address the licensing efforts to the important issues.

Three interactions investigated experimentally in this program were the effects on radioelement migration of (1) alloys, (2) an ionizing radiation field, and (3) altered repository components. The results clearly indicate that the aging of the repository, as represented by the altered repository components, would most dramatically affect radioelement migration and in a way that would be detrimental to repository performance.

The ionizing radiation field was found to enhance leaching of plutonium, which is consistent with results of simpler leaching tests, but no effects of the radiation field on the mobility of plutonium were detected. Hence, the interaction of the radiation field with radioelements is considered secondary to repository aging in importance as an issue in licensing.

The corrosion-resistant metal alloys proposed for canister construction and used in this program were concluded to have no effect on radioelement migration and, hence, to be of no consequence in this regard to issues of repository performance.

(3) Can we independently evaluate, using laboratory studies, commonly followed practices of repository design with regard to issues of repository performance?

Clearly, the evaluation that repository aging may be detrimental to safety with regard to release of uranium, neptunium, and plutonium differs from the view that radioelement retention will improve with age. This evaluation was made independently of the body of data on cesium adsorption that suggests that radioelement retention improves with age.

Finally, the data from this program can be used to establish methodologies for treating and verifying existing computer codes for predicting radioelement migration. The task to understand the behavior of neptunium in rock fissures consistent with the behavior seen experimentally is presently being undertaken (Carnahan 1984).

5. CONCLUSIONS

In a series of six experiments, the influences of apparatus, ionizing radiation, and hydrothermal alteration of repository materials on the migration of eight radioactive elements in nuclear waste were examined.

The most significant effects observed in this series of experiments were the greatly enhanced dissolution of plutonium, neptunium, and uranium from hydrated waste and the more rapid movement of these leached species through bentonite and basalt that were hydrothermally altered to simulate aging of the repository materials. These results were seen in this work to be independent of whether the basalt was altered in the presence or absence of air (compare results of experiments 4 and 6). Similarly, the indication for barium and europium was that they move more rapidly downstream through altered bentonite and rock than through fresh materials. These observations are contrary to the commonly held idea that radioelement retention will increase with age due to the increased rock surface area and increased ion exchange capacity of aged materials. Inasmuch as the alterations represent changes that may occur upon aging of the repository, the ability of a repository for nuclear waste to isolate certain radioactive elements is concluded from this work to degrade with time due to aging of the repository system. Therefore, the modification of repository behavior with age is a major issue regarding migration in the long term of plutonium, neptunium, and uranium from the repository.

In contrast to the behavior of these elements, cesium was found to move more slowly through hydrothermally altered bentonite and basalt than through fresh materials. This result is consistent with results of batch tests that show a greater sorption of cesium onto altered materials than onto fresh materials. Therefore, cesium would be expected to be immobilized to a greater extent in an aged repository than in a fresh repository.

The dissolution of plutonium from radioactive waste glass was found to be enhanced, and the dissolution of neptunium depressed, by ionizing radiation. The species leached in a radiation field interacted with bentonite and basalt measurably the same as species leached in the absence of radiation. This result suggests that no radioelement species produced by radiolysis migrates differently than species formed in the absence of radiation. Except for the enhanced leaching of plutonium, which may be important to performance in some contexts, the effect of ionizing radiation does not appear to influence radioelement migration in a way detrimental to repository performance.

Migration of the radioactive elements was found in this work not to be measurably changed by the use of either of the alloys, Hastelloy C-276 or Monel-400, as a material of construction for the apparatus. Because these alloys differ substantially in composition, the results indicate that neither alloy affected the chemical properties of dissolved radioelements.

The interactions of solutions representative in composition to groundwaters at the repository site were found to be substantially modified in composition by reaction with fresh surfaces of basalt. These modified solutions have characteristics (pH, element concentrations) unlike the groundwaters presently existing at the repository site. Therefore, sorption and solubility parameters for evaluation of repository performance need to be known for a variety of groundwater compositions, not just the composition of groundwater presently at the undisturbed repository site.

6. RECOMMENDATIONS

The most striking behavior seen in these experiments is that neptunium, uranium, and plutonium moved more rapidly through hydrothermally altered basalt than through freshly fractured basalt. The elements barium and europium also showed this behavior. Although this behavior for neptunium, uranium, and plutonium can be understood in terms of reduction of the radioelements at the basalt surface (Meyer 1984), the behavior is contrary to that predicted from the generally accepted theory that sorption of radioelements increases with the extent of aging of basalt (Barney 1981; Deutsch 1982). This theory was verified in this program for cesium, and is likely due to the increased surface area and cation exchange capacity of the altered basalt. However, the extrapolation in licensing assessments of this behavior of cesium to other radioelements, specifically those radioelements that are sensitive to reduction, is not valid.

The major recommendation from this work is that licensing assessments of a repository in basalt should consider the enhanced mobility of plutonium and neptunium that can now be expected with age. Moreover, greater attention needs to be given, in general, to the consequence of aging of a waste repository.

An additional recommendation is that assumptions used to predict radioelement migration should be checked experimentally. Experiments that measure radioelement movement, such as those described here, give results that can be compared directly with those predicted in models of radioelement migration. The experimental approach is flexible and can be used to investigate many repository configurations in both saturated and unsaturated rock.

7. BIBLIOGRAPHY

Topics were addressed in this program to assist in the design of experiments and to interpret results of experiments in the context of NRC licensing issues. The reports used to present these results and a brief annotation of each report are given in this section.

7.1 PAPERS

M. G. Seitz, "Repository-Analog Experiments of Nuclear Waste Leaching and Migration," International Atomic Energy Agency Symposium on the Migration in the Terrestrial Environment of Long-Lived Radionuclides from the Nuclear Fuel Cycle, IAEA-SM-257, 27-31 July 1981.

The laboratory-analog methodology is described. Experimental design and the goals of such experiments are exemplified using results of previously completed experiments with granite.

G. F. Vandegrift, D. L. Bowers, T. J. Gerding, S. M. Fried, C. K. Wilbur, and M. G. Seitz, "The Interaction of Groundwater and Basalt Fissure Surfaces and Its Effect on the Migration of Actinides," in "Geochemical Behavior of Disposed Radioactive Waste," ACS Symposium Series 246, American Chemical Society, 1983.

This paper describes major compositional changes in groundwater that ensue upon contact with fresh surfaces of basalt. These changes are related to the migration of plutonium, neptunium, and uranium that occurs simultaneously with the major chemical changes.

D. L. Bowers, T. J. Gerding, S. M. Fried, G. F. Vandegrift, and M. G. Seitz, "Analytical Measurements of Actinide Migration in a Laboratory-Simulated Basalt HLW Repository," the 26th ORNL-DOE Conference on Analytical Chemistry in Energy Technology, Knoxville, TN, 10-14 October 1983.

Analytical methods covered include the novel yield monitors used to analyze neptunium and plutonium in solutions from the analog experiments. The leaching procedure used to quantitate the actinide activities on rock surfaces is discussed.

M. G. Seitz, G. F. Vandegrift, D. L. Bowers, and T. J. Gerding, "Effect of Aged Waste Package and Aged Basalt on Radioelement Release," U.S. Nuclear Regulatory Commission, "NRC Nuclear Waste Geochemistry '83," NUREG/CP-0052, 1984.

Evidence is given of the enhanced migration of the actinides plutonium, neptunium, and uranium caused by laboratory alteration of the waste package and basalt. The enhanced leaching of plutonium, the suppressed leaching of neptunium, and no difference in migration of these elements caused by a gamma radiation field are reported. No differences in migration characteristics of radioelements were found upon using different metals that are candidates for waste canisters.

7.2 QUARTERLY REPORTS

M. J. Steindler et al., "Fuel Cycle Programs Quarterly Progress Report, April-June 1981," Section IV, "Fluids in Rocks," Argonne National Laboratory, ANL-81-53, 1982.

> The selection of groundwater analyses for simulation in this program and the formulation of the groundwater composition for experiments are described.

M. J. Steindler et al., "Fuel Cycle Programs Quarterly Progress Report, July-September 1981," Section IV, "Rock-Water Interactions," Argonne National Laboratory, ANL-81-82, 1982.

> The modification of groundwater composition by backfill was investigated. Rationale for selection of, and recommended alteration processes for, waste glass, backfill, and host rock are described.

M. J. Steindler et al., "Fuel Cycle Programs Quarterly Progress Report, October-December 1981," Section IV, "Laboratory Analog Program," Argonne National Laboratory, ANL-82-18, 1982.

> Digital equipment for data acquisition during experimentation is specified. Preparation of basalt cores, assembly of apparatus, and characterization of waste glass are described. Ability of the fissure to maintain groundwater flow (fissure stability) is described. Rock fissure clogging by bentonite is reported.

M. J. Steindler et al., "Fuel Cycle Programs Quarterly Progress Report, January-March 1982," Section IV, "Laboratory Analog Program," Argonne National Laboratory, ANL-82-34, 1982.

> Analyses are given of solution samples from the first experiment. Waste glass characterization is described with microprobe analyses and assessment of X-ray photoelectron spectroscopy for surface analyses of experimental results.

M. J. Steindler et al., "Fuel Cycle Programs Quarterly Progress Report, April-June 1982," Section IV, "Laboratory Analog Program," Argonne National Laboratory, ANL-82-58, 1982.

> Procedures to terminate experiments are specified. Topics covered include a description of fissure surfaces from the first experiment; solution analyses for major constituents; and analyses of neptunium and plutonium, auxiliary experiments, and filtering experiments.

M. J. Steindler et al., "Fuel Cycle Programs Quarterly Progress Report, July-September 1982," Section III, "Laboratory Analog Program," Argonne National Laboratory, ANL-82-78, 1983.

> Topics include the laboratory aging of repository components, experimental data, auxiliary experiments (results of filtering), and determination of anions and Eh in solutions.

M. J. Steindler et al., "Fuel Cycle Programs Quarterly Progress Report, October-December 1982," Section V, "Laboratory Analog Program," Argonne National Laboratory, ANL-83-19, 1983.

> Analyses of plutonium and neptunium in groundwater are provided. Radioactivities of solid phases and rinses and measurements of neptunium distributions on rock fissures are discussed. Analyses of solution for major constituents, pH, and ion equilibria are considered. Comparisons of laboratory analog results of leaching with batch leaching test results are made.

M. J. Steindler, "Fuel Cycle Programs Quarterly Progress Report, January-March 1983," Section III, "Laboratory Analog Program," Argonne National Laboratory, ANL-83-68, 1984.

> A summary of the experimental design is given. Mass balance of neptunium and uranium on basalt, changes in groundwater compositions in analog and auxiliary experiments, and actinide migration mechanisms in rock cores are other topics discussed.

M. J. Steindler, "Fuel Cycle Programs Quarterly Progress Report, April-June 1983," Section III, "Laboratory Analog Program," Argonne National Laboratory, ANL-83-78, 1984.

> Numerical modeling analyses of fissure hydrology observed in analog experiments are described.

M. J. Steindler, "Fuel Cycle Programs Quarterly Progress Report, July-September 1983," Section III, "Laboratory Analog Program," Argonne National Laboratory, ANL-83-88, 1984.

> Auxiliary experiments are concluded. Gamma-ray analyses of solutions and solid samples and secondary mineralization relative to groundwater changes are evaluated.

7.3 STUDENT REPORTS

Jon Dymczyk, "Auxiliary Experiments of the Laboratory Analog Program," Winter-Spring 1982.

> Topics covered are bentonite in groundwater, influence of filtering on groundwater chemical analyses, and autoradiographs of waste glass.

Keith L. Branham, "Auxiliary Experiments of the Laboratory Analog Program," Summer 1982.

> Topics covered are morphology of filtered and suspended bentonite and flow impedance effects of packed bentonite.

Cindy K. Wilbur, "Auxiliary Experiments of the Laboratory Analog Program," Spring 1983.

Major chemical adjustments of groundwater in contact with fresh and aged surfaces of basalt are discussed.

Patrick Hyde, "Auxiliary Experiments of the Laboratory Analog Program," Spring 1983.

The kinetics of groundwater reaction with basalt are discussed.

Roy Wogelius, "Secondary Mineral Phases of Naturally and Artificially Aged Columbia Plateau Basalt," Summer 1983.

Mineralogy of altered and aged basalt surfaces is discussed. Autoradiographs of basalt surfaces are evaluated.

REFERENCES

Ahmad, I., J. Hines, and J. E. Gindler. 1983. "Electron Capture of ^{237}Pu, ^{235}Np, ^{236}Np." Physical Review C 27:2239.

Allnatt, A. R., G. M. Bancroft, W. S. Fyfe, P. W. M. Jacobs, S. N. Karkhanis, P. J. Melling, A. Nishijima, C. S. Vempati, and J. Tait. 1983. "Leaching Behavior and Electrical Conductivity of Natural Rhyolites," Chem. Geol. 38:329-357.

Ames, L. L. 1980. "Hanford Basalt Flow Mineralogy," Battelle Pacific Northwest Laboratory, PNL-2847.

Apps, J., T. Doe, D. Doty, S. Doty, R. Galbraith, A. Kearns, B. Kohrt, J. Lons, A. Monroe, T. N. Narasimhan, P. Nelson, C. R. Wilson, and P. A. Witherspoon. 1979. "Geohydrologic Studies for Nuclear Waste Isolation at the Hanford Reservation: Report of the Lawrence Berkeley Laboratory." Lawrence Berkeley Laboratory, LBL-8764.

Apted, M. J., and J. Meyer. 1982. "Comparison of the Hydrothermal Stability of Simulated Spent Fuel and Borosilicate Glass in a Basaltic Environment." Rockwell-Hanford Operations Report RHO-BW-ST-38P.

Avagadro, A., C. N. Murray, and A. DePlano. 1980. "Transport through Deep Aquifers of Transuranic Nuclides Leached from Vitrified High-Level Wastes." Scientific Basis for Nuclear Waste Management, Vol. 2 (665-671), C. J. M. Northrup (ed.), Plenum Press, NY.

Barney, G. S. 1981. "Radionuclide Reactions with Groundwater and Basalts from Columbia River Basalt Formations." Rockwell Hanford Operations Report RHO-SA-217. (Also conference 8106119-1, Northwest Regional ACS Meeting, Bozeman, MT, 17 June 1981).

Bates, J. K., L. J. Jardine, and M. J. Steindler. 1982a. "Hydration Aging of Nuclear Waste Glass." Science 218:51.

Bates, J. K., L. J. Jardine, and M. J. Steindler. 1982b. "The Hydration Process of Nuclear Waste Glass: An Interim Report," Argonne National Laboratory, ANL-82-11.

Barkatt, A. 1980. "Review of Chemical Stability of Glasses: Dissolution Mechanisms, Test Evaluations, and Applications to Radioactive Waste Fixation." Final Report, NRC Contract No. 04-78-25.

Benson, L. V., et al. 1978. "Basalt Alteration and Basalt-Waste Interaction in the Pasco Basin of Washington State." Lawrence Berkeley Laboratory, LBL-8532.

Benson, L. V., and L. S. Teague. 1979. "A Study of Rock-Water-Nuclear Waste Interactions in the Pasco Basin, Washington." Lawrence Berkeley Laboratory, LBL-9677.

Benson, L. V., C. L. Carnahan, and M. Che. 1980. "A Study of Rock-Water-Nuclear Waste Interactions in the Pasco Basin, Washington, Part II. Preliminary Equilibrium-Step Simulations of Basalt Diagenesis," Lawrence Berkeley Laboratory, LBL-9677.

Bischoff, J. L., and W. E. Seyfried, Jr. 1978. "Hydrothermal Chemistry of Seawater from 25° to 350°C," Am. J. Sci. 278:838-860.

Bolmgren, C. R., et al. 1981. "Engineered Waste Package Conceptual Design: Defense High Level Waste (Form 1), Commercial High Level Waste (Form 1), and Spent Fuel (Form 2), Disposal in Basalt." Draft Westinghouse Report AES-TME-3113.

Bowers, D. L., T. J. Gerding, S. M. Fried, G. F. Vandegrift, and M. G. Seitz. 1983. "Analytical Measurements of Actinide Migration in a Laboratory-Simulated Basalt HLW Repository." The 26th ORNL-DOE Conference on Analytical Chemistry in Energy Technology, Knoxville, TN, 10-14 October.

Bradley, D. J., D. G. Coles, F. N. Hodges, G. L. McVay, and R. E. Westerman. 1983. "Nuclear Waste Package Materials Testing Report: Basaltic and Tuffaceous Environments." Report of the Battelle Pacific Northwest Laboratory, PNL-4452.

Burney, G. A., and R. M. Harbour. 1974. "Radiochemistry of Neptunium." National Academy of Science, NAS-NS-3060, pp. 161-162.

Carnahan, C. L., C. W. Miller, and J. S. Remer. 1984. "Verification and Improvement of Predictive Algorithms for Radionuclide Migration." U.S. Nuclear Regulatory Commission, "NRC Nuclear Waste Geochemistry '83," NUREG/CP-0052.

Charles, R. W., and G. K. Bayhurst. 1983. "Sentinel Gap Basalt Reacted in a Temperature Gradient." Los Alamos National Laboratory, LA-9481-MS.

Coles, D. G., R. W. Mersing, J. Rego, H. C. Weed, and B. W. Buddemeir. 1982. "A Leaching Study of PNL 76-68 Glass Beads Using the LLNL Continuous-Flow Method and the PNL Modified IAEA Method: A Final Report." Lawrence Livermore National Laboratory, UCID-19492, Rev. 1.

Coons, W. E., E. L. Moore, M. J. Smith, and J. D. Kasu. 1980. "The Functions of an Engineered Barrier System for a Nuclear Waste Repository in Basalt." Rockwell Hanford Operations, RHO-BWI-LD-23.

Deutsch, W. J., E. A. Jenne, and K. M. Krupka. 1982. "Solubility Equilibria in Basalt Aquifers: The Columbia Plateau, Eastern Washington, USA." In G. W. Bird and W. S. Fyfe (eds.) "Geochemistry of Radioactive Waste Disposal," Chem. Geol. 36:15-34.

Dran, J. C., M. Maurette, and J. C. Pettit. 1980. "Radioactive Waste Storage Materials: Their α-Recoil Aging." Science 1518-1519.

Duffy, C. J., and A. E. Ogard. 1982. "Uranite Immobilization and Nuclear Waste." Los Alamos National Laboratory, LA-9199-MS.

Edgington, D. N., J. J. Alberts, M. A. Wahlgren, J. O. Karttunen, and C. C. Reeve. 1976. "Plutonium and Americium in Lake Michigan Sediments." In "Transuranium Nuclides in the Environment," International Atomic Energy Agency, Vienna, IAES-SM-199/49.

Ericson, J. E. 1977. "Prehistoric Exchange Systems in California: The Results of Obsidian Dating and Tracing." Thesis, UCLA.

Ewing, R. C., and R. F. Haakes. 1979. "Naturally Occurring Glasses: Analyses for Radioactive Waste Forms." Pacific Northwest Laboratory, PNL-2776.

Friedman, I., and W. Long. 1976. "Hydration Rate of Obsidian." Science 191:347.

Gephart, R. E., R. C. Arnett, R. G. Baca, L. S. Leonhart, and F. A. Spane, Jr. 1979. "Hydrologic Studies within the Columbia Plateau, Washington: An Integration of Current Knowledge." Rockwell Hanford Operations, RHO-BWI-ST-5, Table III-45.

Gerding, T. J., M. G. Seitz, and M. J. Steindler. 1979. "Salvage of Plutonium- and Americium-Contaminated Metals." American Institute of Chemical Engineering Symposium Series No. 191, Volume 75, pp. 118-127.

Guzowski, R. V., and R. M. Cranwell. 1983. "Data Base for Basalt Methodology." Report of the Nuclear Regulatory Commission, NUREG/CR-2739, also SAND 82-1197.

Hall, A. R., J. T. Dalton, B. Hudson, and J. A. C. Marples. 1976. "Development and Radiation Stability of Glasses for Highly Radioactive Wastes." In "Management of Radioactive Wastes from the Nuclear Fuel Cycle," International Atomic Energy Agency, Vienna, Vol. 2, pp. 3-14.

Jacobs, G. K., and M. J. Apted. 1981. "Eh-pH Conditions for Groundwater at the Hanford Site, Washington: Implications for Radionuclide Solubility in a Nuclear Waste Repository Located in Basalt." EOS, Trans. Am. Geophys. Union 62:1065.

Jacobsson, A., et al. 1978. "Egenskaper hos Bentonitbaserate Buffertmaterial (Properties of Bentonite-Based Buffer Material)." Report of the Swedish Nuclear Research Organization, KBS-TR-32.

JCPDS. 1981. "Powder Diffraction File." International Centre for Diffraction Data, Swarthmore, PA.

Jones, T. E. 1982. "Reference Material, Chemistry-Synthetic Groundwater Formulation." Report of the Rockwell Hanford Operations.

Karkhanis, S. N., G. M. Bancroft, W. S. Fyfe, and J. D. Brown. 1982. "Leaching Behavior of Rhyolite Glass." Nature 284:435.

McCarthy, G. J., W. B. White, R. Roy, B. E. Scheetz, S. Komareni, D. K. Smith, and D. M. Roy. 1978. "Interactions Between Nuclear Waste and Surrounding Rock." Nature (London) 273:217-219.

Mendel, J. E., W. A. Ross, F. P. Roberts, R. P. Turcotte, Y. B. Katayama, and J. H. Westsik, Jr. 1976. "Thermal and Radiation Effects on Borosilicate Waste Glasses." In "Management of Radioactive Wastes from the Nuclear Fuel Cycle," International Atomic Energy Agency, Vienna, Vol. 2, pp. 49-61.

Meyer, R. E., W. D. Arnold, and F. I. Case. 1984. "Valence Effects on Sorption." U.S. Nuclear Regulatory Commission, "NRC Nuclear Waste Geochemistry '83," NUREG/CP-0052.

Michels, J. W., I. S. T. Tsong, and C. M. Nelson. 1983. "Obsidian Dating and East African Archeology," 219:361-366.

Moody, J. B. 1982. "Radionuclide Migration/Retardation Research and Development Technology Status Report." U.S. Department of Energy, ONWI-321.

Mysen, B. O., and M. G. Seitz. 1975. "Trace Element Partitioning by Beta Track Mapping: An Experimental Study Using Carbon and Samarium as Examples." J. Geophys. Res. 80(17).

Phillips, S. L., and L. F. Silvester. 1982. "A Data Base for Nuclear Waste Disposal for 10 Up to 300°C." Lawrence Berkeley Laboratory, LBL-14722.

Pusch, R. 1978. "Highly Compacted Na Bentonite as Buffer Substance." Report of the Swedish Nuclear Research Organization, KBS-TR-74.

Rockwell Hanford Operations. 1982. "Rockwell Hanford Operations Site Characterization Report for the Basalt Waste Isolation Project." DOE/RL 82-3.

Rydberg, J. 1981. "Groundwater Chemistry of a Nuclear Waste Repository in Granite Bedrock." Lawrence Livermore National Laboratory, UCRL-53155.

Savage, D., and N. A. Chapman. 1982. "Hydrothermal Behavior of Simulated Waste Glass and Waste-Rock Interactions Under Repository Conditions." In G. W. Bird and W. S. Fyfe (eds.), "Geochemistry of Radioactive Waste Disposal," Chem. Geol. 36:59-86.

Scheetz, B. E., S. Komareni, D. K. Smith, C. A. F. Anderson, S. D. Atkinson, and G. J. McCarthy. 1980. "Hydrothermal Interactions of Simulated Nuclear Waste Glass in the Presence of Basalt." Scientific Basis Nuclear Waste Management, 2, Plenum Press, New York, pp. 207-214.

Scoog, D. A., and D. M. Wester. 1963. "Fundamentals of Analytical Chemistry." Holt, Rinehart, and Winston, New York, p. 772.

Seitz, M. G., P. G. Rickert, S. M. Fried, A. M. Friedman, and M. J. Steindler. 1979a. "Studies of Nuclear-Waste Migration in Geologic Media." Argonne National Laboratory, ANL-79-30.

Seitz, M. G., R. A. Couture, and M. J. Steindler. 1979b. "Leach-Migration Experiments to Determine the Mobility of Radionuclides in Geologic Media." Trans. Am. Nucl. Soc. 32:385.

Seitz, M. G., P. G. Rickert, S. M. Fried, A. M. Friedman, and M. J. Steindler. 1979c. "Migration Properties of Some Nuclear Waste Elements in Geologic Media." Nucl. Technol. 44:284-296.

Seitz, M. G., P. G. Rickert, R. A. Couture, J. Williams, N. Meldgin, S. M. Fried, A. M. Friedman, and M. J. Steindler. 1980. "Studies of Nuclear Waste Migration in Geologic Media, Annual Report, October 1978-September 1979." Argonne National Laboratory, ANL-80-36.

Seitz, M. G., and M. Seliga. 1981a. "A Study of the Migration of Leached Radionuclides in a Natural Fissure of Granite Rock." Jarderna Energie 27:399.

Seitz, M. G., and M. J. Steindler. 1981b. "Influence of Waste Solid on Nuclide Dispersal." In "Alternative Nuclear Waste Forms and Interactions in Geologic Media," 13-15 May 1980, Gatlinburg, TN, CONF-8005107.

Seitz, M. G. 1981c. "Repository-Analog Experiments of Nuclear Waste Leaching and Migration." Proceedings of the International Symposium on the Migration in the Terrestrial Environment of Long-Lived Radionuclides from the Nuclear Fuel Cycle, IAEA-SM-257.

Seitz, M. G., G. F. Vandegrift, D. L. Bowers, and T. J. Gerding. 1984. "Effect of Aged Waste Package and Aged Basalt on Radioelement Release." U.S. Nuclear Regulatory Commission, "NRC Nuclear Waste Geochemistry '83," NUREG/CP-0052.

Seyfried, W. E., Jr., and J. L. Bischoff. 1981. "Experimental Sea Water-Basalt Interaction at 300°C, 500 Bars, Chemical Exchange, Secondary Mineral Formation, and Implications for the Transport of Heavy Metals." Geochim. Cosmochim. Acta 45:135.

Shade, J. W., and D. J. Bradley. 1980. "Initial Waste Package Interactions Tests." Battelle Pacific Northwest Laboratory, Richland, WA, Status Report PNL-3559.

Shade, J. W. 1982. "Release Kinetics and Alteration of Waste Glass in Crystalline Rocks Systems." In G. W. Bird and W. S. Fyfe (eds.), "Geochemistry of Radioactive Waste Disposal," Chem. Geol. 36:103-121.

Soo, P. 1983a. "Review of DOE Waste Package Programs." U.S. Nuclear Regulatory Commission, NUREG/CR-2482.

Soo, P. 1983b. "Review of Waste Package Verification Tests." U.S. Nuclear Regulatory Commission, NUREG/CR-2482.

Steindler, M. J., et al. 1982a. "Fuel Cycle Programs Quarterly Progress Report, April-June 1981." Argonne National Laboratory, ANL-81-53, Section IV.

Steindler, M. J., et al. 1982b. "Fuel Cycle Programs Quarterly Progress Report, July-September 1981." Argonne National Laboratory, ANL-81-82, Section IV.

Steindler, M. J., et al. 1982c. "Fuel Cycle Programs Quarterly Progress Report, October-December 1981." Argonne National Laboratory, ANL-82-18, Section IV.

Steindler, M. J., et al. 1982d. "Fuel Cycle Programs Quarterly Progress Report, January-March 1982." Argonne National Laboratory, ANL-82-34, Section IV.

Steindler, M. J., et al. 1982e. "Fuel Cycle Programs Quarterly Progress Report, April-June 1982." Argonne National Laboratory, ANL-82-58, Section IV.

Steindler, M. J., et al. 1983a. "Fuel Cycle Programs Quarterly Progress Report, July-September 1982." Argonne National Laboratory, ANL-82-78, Section III.

Steindler, M. J., et al. 1983b. "Fuel Cycle Programs Quarterly Progress Report, October-December 1982." Argonne National Laboratory, ANL-83-19, Section V.

Steindler, M. J. 1984a. "Fuel Cycle Programs Quarterly Progress Report, January-March 1983." Argonne National Laboratory, ANL-83-68, Section III.

Steindler, M. J. 1984b. "Fuel Cycle Programs Quarterly Progress Report, April-June 1983." Argonne National Laboratory, ANL-83-78, Section III.

Steindler, M. J. 1984c. "Fuel Cycle Programs Quarterly Progress Report, July-September 1983." Argonne National Laboratory, ANL-83-88, Section III.

Strachen, D. 1982. Personal communication to G. F. Vandegrift, Argonne National Laboratory.

Sudo, T., S. Shimoda, H. Yotsumoto, and A. Aita. 1981. "Electronic Micrographs of Clay Minerals." Elsevier, New York.

Taylor, C. L., et al. 1979. "Borehole Plugging of Man-Made Accesses to a Basalt Repository." Rockwell Hanford Operations, RHO-BWI-C-49.

Teague, L. S. 1980. "Secondary Minerals Found in Cores DS2 A1 and DS2 A2 Taken from the Grande Ronde Basalt Formation, Pasco Basin Washington." Lawrence Berkeley Laboratory, LBL-10387.

Tombrello, T. A. 1978. "Weathering of Natural Glasses." In "High-Level Radioactive Solid Waste Forms," Proc. Conf., Denver, CO, U.S. Nuclear Regulatory Commission, NUREG-CP-0005.

Truesdell, A., and B. F. Jones. 1973. "WATEQ, A Computer Program for Calculating Chemical Equilibria of Natural Waters." Water Resources Division Report No. 73-007, U.S. Geological Survey, p. 73.

Turcotte, R. P., J. W. Wald, and R. P. May. 1980. "Devitrification of Nuclear Waste Glasses." In C. J. Northrup (ed.) "Scientific Basis for Nuclear Waste Management," Vol. 2, Plenum Press.

U.S. Nuclear Regulatory Commission. 1983. "Disposal of High-Level Radioactive Wastes in Geologic Repositories Technical Criteria," 10 CFR 60 Final Rule, Federal Register 48(120), Rules and Regulations, 21 June.

Vandegrift, G. F., D. L. Bowers, T. J. Gerding, S. M. Fried, C. K. Wilbur, and M. G. Seitz. 1983. "The Interaction of Groundwater and Basalt Fissure Surfaces and Its Effect on the Migration of Actinides." In "Geochemical Behavior of Disposed Radioactive Waste," ACS Symposium Series 246, American Chemical Society.

Van Olphen, H., and J. J. Frigiat. 1979. Data Handbook for Clay Materials and Other Non-Metallic Minerals." Pergamon Press, New York.

Wald, J. W., and J. H. Westsik, Jr. 1979. "Devitrification and Leaching Effects in HLW Glass - Comparison of Simulated and Fully Radioactive Waste Glass." Proceedings of the International Symposium on Ceramics in Nuclear Waste Management, CONF-790420, Technical Information Center, Oak Ridge, TN.

Weber, W. J., R. P. Turcotte, L. R. Bunnell, F. P. Roberts, and J. H. Westsik, Jr. 1979. "Radiation Effects in Vitreous and Devitrified Simulated Waste Glass." Proceedings of the International Symposium on Ceramics in Nuclear Waste Management, CONF-790420, Technical Information Center, Oak Ridge, TN.

White, A. F. 1983. "Surface Chemistry and Dissolution Kinetics of Glassy Rocks at 25°C." Geochim. Cosmochim. Acta 47:805-815.

Wollenberg, H. A., D. G. Brookins, L. H. Cohen, S. Flexser, M. Abashian, M. Murphy, and A. E. Williams. 1984. "Uranium, Thorium, and Trace Elements in Geologic Occurrences as Analogues of Nuclear Waste Repository Conditions." U.S. Nuclear Regulatory Commission, "NRC Nuclear Waste Geochemistry '83," NUREG/CP-0052.

APPENDIX A

EQUIPMENT DESCRIPTIONS

METERING PUMPS

Analog Experiment No. 1 - Laboratory Data Control (Milton Roy) Constametric IIG Pump giving flow rates of 0.5 to 600 mL/h at pressures of 0-34 MPa (0-5000 psi). All wetted parts are inert plastic or Hastelloy C-276.

Analog Experiment No. 2 - Varian Model 8500 Syringe Pump giving flow rates of 1.0 to 999 mL/h at pressures of 0-55 MPa (0-8000 psi). All wetted parts are stainless steel or Teflon.

Analog Experiment Nos. 3, 4, 5, and 6 - Laboratory Data Control (Milton Roy) Model CMP2VK Metering Pump giving flow rates of 0.05 to 200 mL/h at pressures from 0-3.4 MPa (0-500 psi). This pump is equipped with Kel-F plumbing.

PRESSURE TRANSDUCERS

Sensotec Model A-5/1503 with a pressure range of 0-34 MPa (0-5000 psi) and Sensotec Model Z/708 with a pressure range of 0-1 MPa (0-150 psi). These transducers were made of stainless steel. Pressure readout instrumentation used was Sensotec Model 450D Digitial Indicator Transducer Strain Gauge Bridge Amplifier System. The output voltages from these instruments were monitored with the data acquisition system.

BENTONITE-WASTE FORM VESSELS

Analog Experiment Nos. 1, 4, and 6 - Hastelloy C-276 body with Hastelloy C-276 gland, 1.32 cm I.D. by 12.7 cm long. Made by Autoclave Engineers, Inc.

Analog Experiment No. 2 - Monel-400 tubing, O.D. of 1.27 cm, I.D. of 1.13 cm, and 16.0 cm long. End fittings were special Swagelock reducing unions of 1/2" O.D. TX 1/2" O.D.T. These were fabricated from one male connector M-200-1-2 and a reducing union M-810-6-4. Each was cut and the 1/2" tube of the M-200-1-2 and the 1/2" tee of M-810-6-4 were joined using electron beam welding.

Analog Experiment Nos. 3 and 5 - Hastelloy C-276 tubing with O.D. of 1.27 cm, I.D. of 1.02 cm, and 13.8 cm long. Each fitting was the same special Swagelock reducing union as in experiment 2, but of Hastelloy C-276 construction.

RECORDERS

Data from Analog Experiment No. 3 were collected on recorders because of computer data acquisition unavailability. Data collected were oven temperature, basalt core confining pressure, flow pressure, and output of a gamma radiation field monitor. The recorders were Schlumberger Model SR-206 Dual Pen Chart Recorders.

OVENS

Hotpack Oven Model 212032, capacity of 270 L, and an ambient-temperature-compensated range of 325°C. Each oven operates at 208 V and uses 4.4 kW. One of the ovens was modified for operation in intense gamma radiation. The solid state controller was removed from this oven and reconnected outside the gamma irradiation facility.

BASALT CORE HOLDER

Holder for axially loading a 6.83-cm-diameter by 15.2-cm-long cylindrical split rock core to pressures of 40 MPa (6000 psi). The cylindrical sleeve is made of Teflon, and wetted parts are made of Hastelloy C-276.

HYDRAULIC PUMPS

Model Enerpac 11-1000. Hand pumps to supply hydraulic pressure to core holders have a range of 0-69 MPa (0-10,000 psi). All wetted parts are made of stainless steel (SS). The pumps are connected to the SS jacket of the holder with 0.16-cm O.D. SS tubing.

PLUMBING

Tubing is Hastelloy C-276 with an I.D. of 1.35 mm and O.D. of 3.2 mm. Monel-400 tubing has an I.D. of 1.75 mm. Fittings are ferruled tube fittings (Speedbite, Swagelock).

Valves are Autoclave Engr. 10V-2072-HC-790-6234, made of Hastelloy C-276, rate to 75 MPa (11,000 psi).

Tees are Autoclave Engr. ST-2220-HC-800-5670, made of Hastelloy C-276; Swagelock M-200-3, made of Monel-400; and Swagelock SS-100-3, made of Type 316 stainless steel.

Elbows are Autoclave Engr. SL-2200-HL-800-5670, made of Hastelloy C-276; and Swagelock M-200-9, made of Monel-400.

Male connectors are Swagelock HC-200-1-2, made of Hastelloy C-276; and SS-100-1-1, made of Type 316 stainless steel.

EQUIPMENT TO CONTROL DISSOLVED GASES IN GROUNDWATER SOLUTIONS

The groundwater reservoir consists of a 2-L Pyrex Erlenmeyer flask fitted with a suction tube (Teflon tubing with a filter) and a glass tube for continous sparging of the groundwater with nitrogen. The nitrogen gas is derived from liquid nitrogen and metered to flow at a rate of $\sim$5 mL/min STP through three 250-mL wash bottles containing 50 mL of water, chromous chloride solution of water, and water, respectively. The water in the first wash bottle saturates the nitrogen with water. The chromous chloride solution in the second wash bottle (Oxsorbent, Manufactured by Burrel Corp.) reacts with oxygen to remove it and any CO_2 that may be present from the gas stream. The water in the third wash bottle prevents carryover of the chromous chloride solution to the groundwater solution.

Distribution for NUREG/CR-3710 (ANL-84-16)

Internal:

J. K. Bates
J. E. Bogner
D. L. Bowers
L. Burris
T. J. Gerding
D. R. Hamrin
W. Harrison
J. E. Harmon
R. B. Keener
J. H. Kittel
M. G. Seitz (24)
M. J. Steindler
N. C. Sturchio
G. F. Vandegrift (3)
ANL Patent Dept.
ANL Contract File
ANL Libraries (3)
TIS Files (6)

External:

NRC, Washington, for distribution per AN (100)
Manager, Chicago Operations Office
Chemical Technology Division Review Committee Members:
S. Baron, Burns and Roe, Inc., Oradell, N. J.
W. N. Delgass, Purdue U.
R. A. Allwes, Pittsburgh Research Center, U. S. Bureau of Mines
F. J. Arsenault, Office of Nuclear Regulatory Research, USNRC
R. Barletta, Brookhaven National Lab.
Battelle Memorial Inst., BPMD Library
Battelle Memorial Inst., Library
Battelle Pacific Northwest Lab., Technical Information Section
M. L. Bell, Rockwell Hanford Operations
J. W. Bennett, Office of Civilian Radioactive Waste Management, USDOE
Bettis Atomic Power Lab., General Manager
Bettis Atomic Power Lab., Library
G. F. Birchard, Office of Nuclear Regulatory Research, USNRC
J. O. Blomeke, Martin Marietta Energy Systems, Inc., Oak Ridge
S. Boggs, Jr., U. Oregon
I. Borg, Lawrence Livermore National Lab.
D. J. Bradley, Battelle Pacific Northwest Lab.
Brookhaven National Lab., Nuclear Waste Management Lib.
T. D. Chikalla, Battelle Pacific Northwest Lab.
D. E. Clark, U. Florida
J. Cleveland, U. S. Geological Survey, Lakewood, Colo.
E. Conti, Office of Nuclear Regulatory Research, USNRC
F. R. Conwell, Woodward-Clyde Consultants, Walnut Creek, Calif.
F. A. Costanzi, Office of Nuclear Regulatory Research, USNRC
J. Crandall, Savannah River Lab.
R. H. Doremus, Rensselaer Polytechnic Inst.
R. D. Dosch, Sandia National Labs., Albuquerque
R. S. Dyer, Office of Radiation Programs, USEPA, Washington
T. Early, Rockwell Hanford Operations
Earth Technology Corp., Long Beach, Calif.
Electric Power Research Inst., Technical Lib., Palo Alto
B. R. Erdal, Los Alamos National Lab.
R. Ewing, U. New Mexico
J. Finucane, Energy Information Administration, USDOE
C. S. Fore, Martin Marietta Energy Systems, Inc., Oak Ridge
D. Fortney, Sandia National Labs., Albuquerque
R. Gates, Shannon & Wilson, Inc., Seattle
A. G. Goff, Oak Ridge National Lab.
R. J. Hall, Battelle Pacific Northwest Lab.

Hanford Engineering Development Lab., Documentation Services
L. Hench, U. Florida
E. J. Hennelly, Savannah River Lab.
G. Holman, Chicago Operations Office, USDOE
B. A. Hudson, Indiana State Board of Health, Indianapolis
T. Hunter, Sandia National Labs., Albuquerque
D. Isherwood, Lawrence Livermore National Lab.
T. C. Johnson, Div. Waste Management, USNRC
K. S. Kim, Office of Nuclear Regulatory Research, USNRC (10)
B. King, Rockwell Hanford Operations
J. Kircher, Battelle Columbus Labs.
M. J. Kniedler, Technical Applications Center, U. S. Air Force, Patrick AFB
D. C. Kocher, Oak Ridge National Lab.
G. A. Kolstad, Office of Energy Research, USDOE
L. W. Lake, U. Texas, Austin
S. Lambert, Sandia National Labs., Albuquerque
E. R. Landa, U. S. Geological Survey, Reston
K. P. Lange, EG&G Idaho, Inc.
Lawrence Livermore National Lab., Technical Information Dept.
S. Livingston, Congressional Information Services, Bethesda
T. P. Longo, Nuclear Waste Policy Act Project Office, USDOE
P. Macedo, Catholic U. of America
J. L. McElroy, Battelle Pacific Northwest Lab.
J. L. Means, Battelle Columbus Labs.
J. E. Mendel, Battelle Pacific Northwest Lab.
M. A. Molecke, Sandia National Labs., Albuquerque
Morgantown Energy Technology Center, Librarian, USDOE
E. J. Nowak, Sandia National Labs., Albuquerque
N. Ortiz, Sandia National Labs., Albuquerque
W. Ott, Office of Nuclear Regulatory Research, USNRC
V. Oversby, Lawrence Livermore National Lab.
G. Pappas, Albuquerque Operations Office, USDOE
M. J. Plodinec, Savannah River Lab.
W. P. Reed, National Bureau of Standards, Washington
Rockwell Hanford Operations, BWIP Library
K. Russell, Massachusetts Inst. Technology
R. Salley, Shannon & Wilson, Inc., St. Louis
Sandia National Labs., Technical Lib., Albuquerque
Savannah River Ecology Lab.
D. G. Schweitzer, Brookhaven National Lab.
M. J. Smith, Rockwell Hanford Operations
R. M. Smith, Rockwell Hanford Operations
P. Soo, Brookhaven National Lab.
D. Stahl, Battelle Columbus Labs.
R. J. Starmer, Div. Waste Management, USNRC
M. Steinberg, Brookhaven National Lab.
K. W. Stephens, The Aerospace Corp., Washington
R. C. Tang, Advisory Committee on Reactor Safeguards, USNRC
Tennessee Valley Authority, Nuclear Systems Group, Chattanooga
G. A. Townes, BE Inc., Barnwell
U. S. Air Force Institute of Technology, Wright-Patterson AFB
U. S. Army Engineers Waterways Experiment Station, Library, Vicksburg
U. S. Army Facility Engineering Support Agency, Commander and Director, Ft. Belvoir

U. S. Army Corps of Engineers, Library, Nashville
U. S. Army Natick R&D Labs., T. G. Martin
U. S. Dept. of Energy, Albuquerque Operations Office, Waste Management and Transportation Development Div.
U. S. Dept. of Energy, Albuquerque Operations Office, National Atomic Museum
U. S. Dept. of Energy, Brookhaven Area Office
U. S. Dept. of Energy, Idaho Operations Office
U. S. Dept. of Energy, Savannah River Operations Office
U. S. Dept. of Energy, Energy Library, Washington (Forrestal Bldg.)
U. S. Dept. of Energy, Energy Library, Washington (Germantown)
U. S. Nuclear Regulatory Commission, Director, Div. Radiation Programs and Earth Sciences
U. S. Nuclear Regulatory Commission, Dep. Dir., Div. Radiation Programs and Earth Sciences
U. S. Nuclear Regulatory Commission, Director, Div. Waste Management
U. S. Nuclear Regulatory Commission, Dep. Dir., Div. Waste Management
U. S. Nuclear Regulatory Commission, Chief, Engineering Br., Div. Waste Management
U. S. Nuclear Regulatory Commission, Document Control Center, Div. Waste Management
U. S. Nuclear Regulatory Commission, Waste Management Subcommittee, Advisory Committee on Reactor Safeguards
C. Wallin, U. Texas, Austin
R. D. Walton, Jr., Office of Defense Waste and Byproducts Management, USDOE
D. F. Weill, Office of Energy Research, USDOE
A. J. Weiss, Brookhaven National Lab.
Westinghouse Electric Corp., Nuclear Energy Systems Lib., Pittsburgh
R. Williams, Electric Power Research Inst., Palo Alto
P. A. Witherspoon, Lawrence Berkeley Lab.
H. Wollenberg, Lawrence Berkeley Lab.
E. L. Zebroski, Electric Power Research Inst., Palo Alto
DOE-TIC (2)

NRC FORM 335 (2 84) NRCM 1102, 3201, 3202

U.S. NUCLEAR REGULATORY COMMISSION

BIBLIOGRAPHIC DATA SHEET

SEE INSTRUCTIONS ON THE REVERSE

1. REPORT NUMBER (Assigned by TIDC add Vol. No., if any)

NUREG/CR-3710
ANL-84-16

2. TITLE AND SUBTITLE

Laboratory Studies of a Breached Nuclear Waste Repository in Basalt

3. LEAVE BLANK

4. DATE REPORT COMPLETED

MONTH: September YEAR: 1984

5. AUTHOR(S)

M. G. Seitz, D. L. Bowers, T. J. Gerding, and G. F. Vandegrift

6. DATE REPORT ISSUED

MONTH: November YEAR: 1984

7. PERFORMING ORGANIZATION NAME AND MAILING ADDRESS (Include Zip Code)

Chemical Technology Division
Argonne National Laboratory
9700 S. Cass Avenue
Argonne, IL 60439

8. PROJECT/TASK/WORK UNIT NUMBER

9. FIN OR GRANT NUMBER

FIN A2230

10. SPONSORING ORGANIZATION NAME AND MAILING ADDRESS (Include Zip Code)

Division of Radiation Programs and Earth Sciences
Office of Nuclear Regulatory Research
U.S. Nuclear Regulatory Commission
Washington, DC 20555

11a. TYPE OF REPORT

Final

b. PERIOD COVERED (Inclusive dates)

12. SUPPLEMENTARY NOTES

13. ABSTRACT (200 words or less)

Experiments are described that combine backfill, radioactive waste, and basalt rock in a single flowing groundwater stream in a manner analogous to a hydraulic breach of a waste repository. The experiments were used to study chemical interactions that would occur if repository components were breached by flowing water.

The result of most significance to issues of repository performance was that uranium, neptunium, and plutonium were found to move more rapidly through repository components that were altered to represent aging than through fresh materials. In contrast, cesium moved slower through altered repository materials, as had been deduced from previous work using batch adsorption tests.

Two other parameters studied experimentally, the metal alloy used in the apparatus and an ionizing radiation field imposed on the experimental apparatus, had little or no measurable effect on radioactive element transport by flowing water.

Inasmuch as the alteration of the repository materials represents aging in an actual repository, we conclude that changes with age will detrimentally affect the ability of a repository to isolate uranium, neptunium, and plutonium. Because these elements have long-lived radioactive isotopes in nuclear waste, the degradation with time is a major issue regarding the performance of a nuclear waste repository in basalt.

14. DOCUMENT ANALYSIS - a. KEYWORDS/DESCRIPTORS

Radioactive Waste
Repository Performance
Radioelement Transport
Bentonite
Aged Basalt
Weathered Basalt
Interactions Testing

b. IDENTIFIERS/OPEN ENDED TERMS

15. AVAILABILITY STATEMENT

Unlimited

16. SECURITY CLASSIFICATION

(This page) Unclassified

(This report) Unclassified

17. NUMBER OF PAGES

18. PRICE